Supporting Information for

Isolation and Study of Ruthenium–Cobalt Oxo Cubanes Bearing a High-Valent, Terminal Ru^{V}–Oxo with Significant Oxyl Radical Character

Jaruwan Amtawong[†], David Balcells[‡], Jarett Wilcoxen[§], Rex C. Handford[†], Naomi Biggins[†], Andy I. Nguyen[†,∥], R. David Britt[§], T. Don Tilley[*,†,∥]

[†]Department of Chemistry, University of California at Berkeley, Berkeley, California 94720-1460, United States

[‡]Hylleraas Centre for Quantum Molecular Sciences, Department of Chemistry, University of Oslo, P.O. Box 1033, Blindern, 0315 Oslo, Norway

[§]Department of Chemistry, University of California, Davis, California 95616, United States

[∥]Chemical Sciences Division, Lawrence Berkeley National Laboratory, Berkeley, California 94720, United States

---

Table of Contents

General Considerations S2

Analytical Methods S2

NMR Spectroscopy S2

Infrared spectroscopy S2

UV-Vis-NIR Spectroscopy S2

Electrochemistry Experiments S2

Synthesis and Characterization S3

EPR Spectroscopy S6

X-ray crystallography S7

Computational Details S15

Supplementary Figures S34

References S57

General Considerations

All reactions and experiments, unless otherwise noted, were performed in a dry nitrogen or argon atmosphere. Cobalt(II) acetate tetrahydrate, pyridine, 4-methoxypyridine, 4-methylpyridine, 4-trifluoromethylpyridine, triphenylphosphine, cyclohexadiene, styrene, benzyl alcohol, isopropyl alcohol, 1,2-diphenylhydrazine, and hydrogen peroxide (30 % in H_2O) were purchased from Sigma-Aldrich. These chemicals were used without further purification. Standard literature procedures were followed to prepare tetrapropylammonium perruthenate,[1] thianthrenium tetrafluoroborate,[2] 2,4,6-tri-*tert*-butylphenoxyl radical,[3] and trityl radical.[4] Solvents were dried with a JC Meyers Phoenix SDS solvent purification system and stored over 3Å molecular sieves prior to use. Dichloromethane-d_2 (CD_2Cl_2) and chloroform-*d* ($CDCl_3$) were degassed with three freeze-pump-thaw cycles and stored under nitrogen over 3Å molecular sieves. Acetonitrile-d_3 (CD_3CN) was dried over CaH_2, degassed with three freeze-pump-thaw cycles, and stored under nitrogen over 3Å molecular sieves. Water was obtained from a Millipore Milli-Q water purification system.

Analytical Methods

Element analyses were performed at the Microanalytical Laboratory at the University of California, Berkeley (UC Berkeley) using a Perkin Elmer 2400 Series II combustion analyzer equipped for determination of %C, %H, and %N. High-resolution electrospray ionization mass spectrometry (HR-ESI-MS) measurements were performed at the Catalysis Center at UC Berkeley. Gas production was measured on an SRI-GC instrument equipped with 6' Hayesep D and 5Å molecular sieve chromatographic columns. Two in-line detectors were used: a TCD for H_2, O_2, and N_2 detection, and a FID equipped with a methanizer for CO, CO_2, and hydrocarbon detection.

NMR Spectroscopy

All ^1H, ^{19}F, and ^{31}P NMR experiments were carried out at the UC Berkeley College of Chemistry NMR facility using Bruker AV-700, AV-600, AV500, AVQ-400, and AVB-400 spectrometers at ambient temperature. ^{19}F NMR spectra were internally referenced to $CFCl_3$. Solution magnetic susceptibilities were determined by ^1H NMR spectroscopy using Evans' method.[5] The shift in chemical shift was measured for dissolved *tetrakis*(trimethylsilyl)silane.

Infrared spectroscopy

Measurements were performed at the UC Berkeley Catalysis center using an A225/Q Platinum ATR accessory with a Bruker Vertex 80 FTIR Spectrometer. The instrument is equipped with a room temperature DLaTGS detector. Spectra were analyzed by the OPUS software (v. 7.2).

UV-Vis-NIR Spectroscopy

UV-Visible-NIR spectrum of compound **1a** was obtained on a Varian Cary 5000 using Cary WinUV software (v. 3.00(339)).

Electrochemistry Experiments

Electrochemical experiments were performed at ambient temperature in a dry nitrogen-filled glovebox using a BASi EC Epsilon potentiostat/galvanostat and a PWR-3 Power Module. A 3 mm diameter glassy carbon electrode was used as the working electrode. The electrode was polished with 0.30 μm alumina slurries, followed by additional 0.05 μm alumina slurries, rinsed with water, and dried *in* vacuo before use. Platinum wire and a $Ag/AgNO_3$ reference electrode (0.1 M $[^nBu_4N][PF_6]$ in acetonitrile) were used as the counter electrode and reference electrode, respectively. Tetrabutylammonium hexafluorophosphate, electrochemical grade, (0.1 M in *ortho*-difluorobenzene) served as the electrolyte. Ferrocene was added at the end of each experiment and the half-potential of $[Cp_2Fc]^{0/+}$

redox couple served as the internal standard to compare with the recorded potentials. *iR* compensation was carried out for each measurement to correct the solution resistance. Concentrations of analyte were 1.0 mM for all experiments. The E° values for the oxidation events reported are the midpoints of the anodic (E_{pa}) and cathodic (E_{pc}) peak potentials, calculated as $E^\circ = (E_{pa} + E_{pc})/2$. The reversibility of the redox events was determined by the peak-to-peak separations ($\Delta E_p = E_{pa} - E_{pc}$) and the ratio of the cathodic peak current to the anodic peak current at multiple scan rates. The peak currents were determined by EC Lab software. For irreversible reduction events, E° values were determined using differential pulse voltammetry.

Synthesis and Characterization

$Ru(O)Co_3(\mu_3\text{-}O)_4(OAc)_4(py)_3$ (1a):

Pyridine (1.7 mL, 21 mmol) was added to a suspension of cobalt(II) acetate tetrahydrate (5.3 g, 21 mmol) in acetonitrile (250 mL). The mixture was stirred vigorously until the solid was partially dissolved, forming a purple solution. Tetrapropylammonium perruthenate (5.0 g, 14 mmol) was then added, and a color change from purple to dark brown was observed. The resulting solution was stirred for 16 h at room temperature to give a dark brown solution and black solid. The solid was collected by vacuum filtration and washed with acetonitrile (100 mL) followed by diethyl ether (50 mL). Dichloromethane (50 mL) was added to dissolve the solid. The solution containing **1a** was separated from an insoluble black solid by vacuum filtration. TLC analysis of the filtrate shows two spots with R_f values of 0.3 and 0 (acetone: dichloromethane; 20:80). The resulting mixture was purified by a wet loaded silica plug (eluting with acetone: dichloromethane; 20:80). Product containing fractions (R_f = 0.3) were combined and concentrated to afford a dark brown solid. X-ray quality crystals of **1a** were obtained by diffusion of *n*-hexane into a saturated dichloromethane solution at room temperature (2.7 g, 45% based on cobalt acetate). ^{1}H NMR spectrum shows somewhat broad and integrable resonances; μ_{eff} = 2.0 μ_B (700.13 MHz, CD_2Cl_2, 22 °C, Evans' method). ^{1}H NMR (700.13 MHz, CD_2Cl_2): δ 10.61 (br s, 2H, py-H), 8.01 (s, 1H, py-H), 7.39 (d, 2H, py-H), 7.12 (t, 2H, py-H), 6.88 (d, 4H, py-H), 6.67 (s, 4H, py-H), 2.65 (s, 6H, OAc-H), 2.62 (s, 6H, OAc-H). IR (ATR, dichloromethane, ν(cm^{-1})): 1608 (w, br), 1531 (s), 1485 (w), 1450 (m), 1416 (s), 1347 (m), 1214 (m), 1071 (m), 853 (s, ν_{Ru-O}), 730 (s), 689 (vs), 652 (s), 629 (s), 594 (w), 569 (m), 539 (m). Anal. Calcd for $C_{23}H_{27}Co_3N_3O_{13}Ru$: C, 33.23; H, 3.27; N, 5.05. Found: C, 33.14; H, 3.57; N, 4.78. HR-MS (ESI): Calcd. for $[RuCo_3O_5(CH_3OO)_4(C_5H_5N)_3]\cdot H^+$: *m/z* = 832.8661. Found: *m/z* = 832.8653.

$Ru(O)Co_3(\mu_3\text{-}O)_4(OAc)_4(4\text{-}CF_3\text{-}py)_3$ (1b):

To a suspension of cobalt(II) acetate tetrahydrate (1.0 g, 4.0 mmol) in acetonitrile (100 mL), 4-trifluoromethylpyridine (0.5 mL, 4.3 mmol) was added. With rapid stirring, tetrapropylammonium perruthenate (0.94 g, 2.7 mmol) was introduced, and the resulting mixture was stirred at room temperature for 16 h to give a dark brown solution and black solid. The solid was collected by vacuum filtration and washed quickly with acetonitrile (30 mL). TLC analysis (acetone: dichloromethane; 20:80) of the solid shows two major spots with R_f values of 0.5 and 0. Dichloromethane (20 mL) was added to dissolve the solid, and the resulting solution is carefully poured onto a silica plug (eluting with acetone: dichloromethane; 20:80). Product containing fractions (R_f = 0.5) are combined and concentrated to afford a dark brown solid. Layering hexanes over a dichloromethane solution of the product at –30 °C afforded X-ray quality crystals of **1b** (0.5 g, 36 % based on cobalt acetate). Magnetic moment (600.13 MHz, CD_2Cl_2, 22 °C, Evans' method): 2.3 μ_B. ^{1}H NMR (600.13 MHz, CD_2Cl_2): δ 10.82 (br s, 2H, py-H), 7.68 (s, 2H, py-H), 7.13 (s, 4H, py-H), 6.98 (br s, 4H, py-H), 2.69 (s, 6H, OAc-H), 2.67 (s, 6H, OAc-H). IR (ATR, dichloromethane, ν(cm^{-1})): 1529 (s, br), 1422 (s), 1348 (w), 1325 (vs, ν_{CF3}), 1185 (s, ν_{CF3}), 1144 (s, ν_{CF3}), 1104 (w), 1087 (s), 1063 (s), 1036 (w), 857 (s, ν_{Ru-O}), 838 (s, ν_{CF3}), 738 (s), 692 (m), 680 (s), 652 (m), 630 (s), 604 (vw), 568 (m), 541 (m). Anal. Calcd for $C_{26}H_{24}Co_3F_9N_3O_{13}Ru$: C, 30.16; H, 2.34; N, 4.06. Found: C,

29.71; H, 2.41; N, 3.77. HR-MS (ESI): Calcd. for $[RuCo_3O_5(CH_3OO)_4(C_6H_4F_3N)_3]\cdot H^+$: *m/z* = 1036.8283. Found: *m/z* = 1036.8181.

$Ru(O)Co_3(\mu_3\text{-}O)_4(OAc)_4(4\text{-}Me\text{-}py)_3$ (1c):

To a suspension of cobalt(II) acetate tetrahydrate (0.2 g, 0.8 mmol) in acetonitrile (10 mL), 4-methylpyridine (0.078 mL, 0.8 mmol) was added. The resulting mixture was stirred vigorously while tetrapropylammonium perruthenate (0.19 g, 0.54 mmol) was added. The solution mixture was stirred for 16 h at room temperature to give a dark brown solution, which was subsequently concentrated *in vacuo* to yield a dark brown solid. TLC analysis (acetone: dichloromethane; 20:80) of the solid reveals two spots with R_f values of 0.5 and 0. The solid was dissolved in dichloromethane (5.0 mL) and purified by a wet loaded silica plug (eluting with acetone: dichloromethane; 20:80). The product was then crystallized with dichloromethane layered with hexanes at –30 °C to afford black crystals of **1c** (0.070 g, 30% based on cobalt acetate). Magnetic moment (600.13 MHz, CD_2Cl_2, 22 °C, Evans' method): 2.3 μ_B. ^{1}H NMR (600.13 MHz, CD_2Cl_2): δ 10.34 (br s, 2H, py-H), 7.23 (s, 2H, py-H), 6.72 (s, 4H, py-H), 6.46 (br s, 4H, py-H), 2.63 (s, 6H, OAc-H), 2.61 (br s, 6H, OAc-H), 2.30 (s, 3H, py-Me), 1.92 (s, 6H, py-Me). IR (ATR, dichloromethane, *ν*(cm^{-1})): 1621 (s), 1576 (s, br), 1559 (s, br), 1541 (s, br), 1504 (s, br), 1415 (vs), 1347 (m), 1253 (w), 1227 (w), 1209 (m), 1070 (w), 1042 (w, br), 1025 (w, br), 853 (s, ν_{Ru-O}), 811 (s, $\nu_{py\text{-}CH3}$), 745 (s), 724 (s), 697 (vs), 653 (m), 629 (vs), 592 (w), 570 (s), 535 (s), 496 (m). Anal. Calcd for $C_{26}H_{33}Co_3N_3O_{13}Ru\cdot 0.3CH_2Cl_2$: C, 35.14; H, 3.77; N, 4.67. Found: C, 35.03; H, 4.14; N, 4.59. HR-MS (ESI): Calcd. for $[RuCo_3O_5(CH_3OO)_4(C_6H_7N)_3]\cdot H^+$: *m/z* = 874.9131. Found: *m/z* = 874.9107.

$Ru(O)Co_3(\mu_3\text{-}O)_4(OAc)_4(4\text{-}OMe\text{-}py)_3$ (1d):

To a suspension of cobalt(II) acetate tetrahydrate (0.2 g, 0.8 mmol) in acetonitrile (10 mL), 4-methoxy pyridine (0.082 mL, 0.8 mmol) was added. Tetrapropylammonium perruthenate (0.19 g, 0.54 mmol) was then added, and the solution mixture was stirred at room temperature for 16 h to give a dark brown solution. Volatile components were removed *in vacuo*. TLC analysis (acetone: dichloromethane; 20:80) of the solid shows two main spots with R_f values of 0.25 and 0. Dichloromethane (5.0 mL) was added to dissolve the solid and the solution was purified by a silica plug (eluting with acetone: dichloromethane; 30:70). Product containing fractions were combined and concentrated *in vacuo*. Vapor diffusion of pentane into a dichloromethane solution of the product at –30 °C gave X-ray quality crystals of **1d** (0.094 g, 38% based on cobalt acetate). Magnetic moment (600.13 MHz CD_2Cl_2, 22 °C, Evans' method): 2.2 μ_B. ^{1}H NMR (400.13 MHz, CD_2Cl_2): δ 10.32 (br s, 2H, py-H), 6.93 (br s, 2H, py-H), 6.44 (br s, 8H, py-H), 3.76 (s, 3H, py-OMe), 3.55 (s, 6H, py-OMe), 2.64 (br s, 12H, OAc-H). IR (ATR, dichloromethane, *ν*(cm^{-1})): 1619 (vs), 1569 (m), 1509 (vs), 1462 (w), 1439 (s, br), 1416 (vs), 1347 (m), 1299 (vs), 1207 (vs), 1062 (s), 1038 (s), 1017 (s), 853 (s, ν_{Ru-O}), 837 (m, $\nu_{py\text{-}OCH3}$), 822 (s, $\nu_{py\text{-}OCH3}$), 653 (s), 629 (vs), 567 (s), 542 (s). Anal. Calcd for $C_{26}H_{33}Co_3N_3O_{16}Ru$: C, 33.89; H, 3.61; N, 4.56. Found: C, 33.56; H, 3.83; N, 4.46. HR-MS (ESI): Calcd. for $[RuCo_3O_5(CH_3OO)_4(C_6H_7NO)_3]\cdot H^+$: *m/z* =922.8961. Found: *m/z* = 922.8978.

$[Ru(MeCN)Co_3(\mu_3\text{-}O)_4(OAc)_4(4\text{-}OMe\text{-}py)_3][BF_4]$ (2-MeCN)

In a nitrogen-filled glovebox, compound **1d** (0.050 g, 0.054 mmol) was dissolved in acetonitrile (3 mL), and then thianthrenium tetrafluoroborate (0.018 g, 0.059 mmol) was added. The reaction mixture was stirred for 10 min at room temperature to give a dark brown solution, which was filtered through a glass wool plug. Layering diethyl ether over the filtrate at –30 °C afforded dark green powder. The supernatant was carefully decanted, and the resulting powder was rinsed with additional diethyl ether (5 mL), which was then removed and combined with the supernatant. The combined solution was concentrated *in vacuo* to yield thianthrene oxide (0.012 g, 90%), which was pure by ^{1}H NMR spectroscopy. Residual volatile components were removed from the green solid *in vacuo* to give **2-MeCN** (0.051 g, 92%). X-ray quality crystals of **2-MeCN** were obtained by vapor diffusion of diethyl ether into an acetonitrile solution of the product at –30 °C. Magnetic moment (500.23 MHz, CD_2Cl_2, 22 °C, Evans' method): 2.8 μ_B. ^{1}H NMR

(500.23 MHz, CD_2Cl_2): δ 27.28 (s), 22.15 (s), 17.52 (s), 15.03 (s), 12.06 (br s), 9.32 (s), 5.35 (s), 1.29 (s). ^{19}F NMR (376 MHz, CD_3CN): δ –151 (BF_4). IR (ATR, dichloromethane, ν(cm^{-1})): 1619 (vs), 1569 (m), 1509 (vs), 1462 (w), 1439 (s, br), 1416 (vs), 1347 (m), 1299 (vs), 1207 (vs), 1098 (s, br, ν_{BF4}), 1062 (s), 1038 (s), 1017 (s), 837 (m, $\nu_{py\text{-}OCH3}$), 822 (s, $\nu_{py\text{-}OCH3}$), 653 (s), 629 (vs), 567 (s), 542 (s). Anal. Calcd for $C_{28}H_{36}BCo_3F_4N_4O_{15}Ru{\cdot}0.5CH_3CN$: C, 33.05; H, 3.59; N, 5.98. Found: C, 33.41; H, 3.40; N, 5.52. HR-MS (ESI): Calcd. for $[Ru(CH_3CN)Co_3O_4(CH_3OO)_4(C_6H_7NO)_3]^+$: *m/z* =946.9216. Found: *m/z* = 946.9301.

$Ru(OC_{18}H_{29}O)Co_3(\mu_3\text{-}O)_4(OAc)_4(py)_3$ (3):

In a nitrogen-filled glovebox, 2,4,6-tri-*tert*-butylphenoxyl radical (0.016 g, 0.061 mmol) in *ortho*-difluorobenzene (2 mL) was added dropwise to a solution of **1a** (0.05 g, 0.06 mmol) in *ortho*-difluorobenzene (3 mL) with vigorous stirring. The reaction mixture was stirred for 1 h at room temperature, and volatile materials were removed *in vacuo* to give a dark brown solid. Vapor diffusion of pentane into a chloroform solution of the product at –30 °C yielded X-ray quality, dark brown crystals of **3** (0.062 g, 95%). Magnetic moment (500.23 MHz, CD_2Cl_2, 22 °C, Evans' method): 3.6 μ_B. ^1H NMR (500.23 MHz, CD_3CN): δ 16.06 (s, 6H, OAc-H), 13.51 (s, 2H, py-H), 6.39 (s, 2H, py-H), 5.96 (s, 6H, OAc-H), 4.33 (s, 2H, py-H), 4.16 (s, 4H, py-H), 2.88 (s, 18H, ^{t}Bu-H), -1.79 (s, 4H, py-H), -2.36 (s, 9H, ^{t}Bu-H), -22.63 (s, 2H, vinyl-H). IR (ATR, solid, ν(cm^{-1})): 2951 (m, br, ν_{H2C-H}), 2867 (m, br), 1654 (m), 1626 (s, $\nu_{C=O}$), 1607 (m), 1525 (vs), 1484 (s), 1401 (vs), 1340 (s), 1264 (w), 1244 (m), 1211 (s), 1154 (m), 1105 (m), 1074 (m), 1048 (s), 1021 (w), 998 (s, $\nu_{C=C}$), 968 (s, $\nu_{C=C}$), 907 (m), 880 (m), 824 (m), 760 (s), 687 (vs), 626 (s), 565 (vs), 540 (s), 450 (m), 413 (w). Anal. Calcd for $C_{41}H_{56}Co_3N_3O_{14}Ru$: C, 45.06; H, 5.17; N, 3.85. Found: C, 44.79; H, 5.25; N, 3.63. HR-MS (ESI): Calcd. for $[Ru(OC_{18}H_{29}O)Co_3O_4(CH_3OO)_4(C_6H_7NO)_3]{\cdot}H^+$: *m/z* =1094.0879. Found: *m/z* = 1094.0963.

$Ru(OC_{19}H_{15})Co_3(\mu_3\text{-}O)_4(OAc)_4(py)_3$ (4):

In a nitrogen-filled glovebox, a solution of Gomberg's dimer (0.088 g, 0.18 mmol) in *ortho*-difluorobenzene (2 mL) was added dropwise to a solution of **1a** (0.05 g, 0.06 mmol) in *ortho*-difluorobenzene (3 mL) with vigorous stirring. The mixture was stirred at room temperature for 1 h to give a dark brown solution, and the volatile components were removed *in* vacuo. Vapor diffusion of pentane into a chloroform solution of the product afforded X-ray quality crystals of **4** (0.06 g, 92%). Magnetic moment (500.23 MHz, CD_2Cl_2, 22 °C, Evans' method): 3.3 μ_B. ^1H NMR (600.13 MHz, CD_2Cl_2): δ 15.09 (s, 6H, OAc-H), 14.32 (s, 2H, py-H), 10.78 (s, 6H, phenyl-H), 7.82 (s, 3H, phenyl-H), 7.33 (s, 6H, phenyl-H), 6.43 (s, 2H, py-H), 6.14 (s, 6H, OAc-H), 5.78 (s, 1H, py-H), 4.31 (s, 2H, py-H), 4.16 (s, 4H, py-H), -1.39 (s, 4H, py-H). IR (ATR, solid, ν(cm^{-1})): 1606 (m), 1523 (s, br), 1505 (s), 1484 (s), 1448 (s), 1403 (vs), 1341 (s), 1265 (m), 1244 (w, br), 1212 (s), 1188 (w, br), 1149 (m), 1101 (w), 1072 (m), 1044 (m, br), 1007 (vs, br), 993 (vs, $\nu_{C=C}$), 937 (w), 917 (w), 896 (m), 840 (w), 781 (s), 757 (vs), 688 (vs), 662 (w), 626 (vs), 589 (w), 561 (vs), 542 (s, br), 528 (s, br), 486 (s), 451 (m). Anal. Calcd for $C_{43}H_{46}Co_3N_3O_{13}Ru$: C, 47.35; H, 4.25; N, 3.85. Found: C, 47.52; H, 4.07; N, 3.69.

$[(py)_3(OAc)_4Co_3(\mu_3\text{-}O)_4Ru]{-}O{-}[RuCo_3(\mu_3\text{-}O)_4(OAc)_4(py)_3]$ (5):

In a nitrogen-filled glovebox, compound **1a** (0.5 g, 0.60 mmol) was dissolved in dichloromethane (15 mL), and triphenylphosphine (0.079 mg, 0.30 mmol) was added. The solution was stirred for 30 min at room temperature to give a reddish-brown solution. The volatile materials were removed in vacuo. In air, the residue was washed with diethyl ether (3 x 10 mL) and dried *in vacuo* to yield a dark brown solid. Column chromatography of the mixture was performed to isolate the species using a silica gel column eluted with a gradient mixture of methanol and dichloromethane (3% to 6% methanol in dichloromethane). Product containing fractions (R_f = 0.2) were combined and volatile components were removed *in vacuo* to afford the title compound as a brown solid. Vapor diffusion of diisopropyl ether into a solution of 1,2-dichloroethane of the product at –30 °C gave X-ray quality, dark brown crystals of **5** (0.13 mg, 28%). Alternatively, **5** can be synthesized in air by dissolving compound **1a** (0.092 g, 0.11

mmol) in 2 mL of water. The solution was stirred for 1 h and the volatile materials were removed *in vacuo*. The resulting solid mixture was purified by the procedures described above to yield the title compound (0.027 g, 30%). ^{1}H NMR (600.13 MHz, CD_3CN) δ 8.66 (td, J = 4.8 Hz, 4H, py-H), 8.12 (td, J = 4.9 Hz, 8H, py-H), 7.59 (tt, J = 2.2 Hz, 2H, py-H), 7.56 (tt, J = 20.0, 1.5 Hz, 4H, py-H), 7.32-7.27 (m, 4H, py-H), 7.08-7.03 (m, 8H, py-H) , 2.12 (s, 12H, OAc-H), 2.09 (s, 12H, OAc-H). IR (ATR, solid, ν(cm^{-1})): 1607 (m), 1527 (vs, br), 1484 (s), 1445 (s), 1409 (vs), 1339 (s), 1244 (w), 1215 (m), 1205 (m), 1158 (m), 1075 (m), 1041 (m, br), 980 (vw), 940 (w), 870 (vw), 789 (m, $\nu_{Ru–O–Ru}$), 771 (m), 758 (m), 690 (vs), 651 (m, br), 644 (m, br), 620 (vs), 587 (m), 563 (vs), 536 (s, br), 463 (m), 453 (m), 415 (w). Anal. Calcd for $C_{46}H_{54}Co_6N_6O_{25}Ru_2$: C, 33.55; H, 3.31; N, 5.10. Found: C, 33.35; H, 3.43; N, 4.78. HR-MS (ESI): Calcd. for $[Ru_2Co_6O_9(OAc)_8(py)_6]\cdot H^+$: *m/z* =1648.7295. Found: *m/z* = 1648.7836.

EPR Spectroscopy

X-Band CW EPR Measurements:

Samples for X-band (~9.4 GHz) EPR spectroscopy were measured at the CalEPR center at the University of California, Davis (UC Davis). Continuous wave (CW) spectra were collected using a Bruker Instruments EleXsys-II E500 CW EPR spectrometer (Bruker Corporation, Billerica, MA) equipped with an Oxford Instruments ESR900 liquid helium cryostat and an Oxford Instruments ITC503 temperature and gas-flow controller. Samples were measured under non-saturating slow-passage conditions using a Super-High Q resonator (ER 4122SHQE). Unless otherwise stated, typical acquisition conditions were as follows: T = 20 K; 9.3858 GHz microwave frequency; 5G modulation amplitude; 1 μW microwave power.

Pulse EPR and ENDOR Measurements:

All Q-band (34 GHz) pulse EPR studies were carried out at the UC Davis CalEPR center, using a Bruker EleXsys E580 pulse EPR spectrometer equipped with an Oxford-CF935 liquid helium cryostat and an ITC-503 temperature controller. Q-band pulse EPR and Davies electron nuclear double resonance (ENDOR) spectroscopy were performed using the same E580 EPR spectrometer along with a 1 kW ENI RF amplifier and an R.A. Isaacson-designed cylindrical TE011 resonator[6] adapted for pulse EPR in an Oxford Instruments CF935 cryostat. Two-pulse electron spin echo field swept (2PFS) EPR spectrum was collected using the pulse sequence π/2-τ-π-τ-echo, stepping the field after each point. Davies ENDOR spectra were acquired using the pulse sequence π−tRF−πRF−tRF−π/ 2−τ−π−echo, where πRF is the RF pulse length and tRF is a fixed delay separating MW and RF pulses.[7] Typical collection conditions were as follows: T = 6 K, 34.164 GHz microwave frequency, 12.1 mW microwave power, 96 *n*s inversion (π) pulse, τ = 500 *n*s, RF pulse length = 5 μs. To avoid saturation of the ENDOR transitions, data were collected using stochastic RF frequency jumping.[8] Spectral simulations were performed using the EasySpin 4.0 toolbox in Matlab.[9]

ENDOR Notes:

In principle, the hyperfine-coupled cobalt centers should give rise to two peaks that are centered at the Larmor frequency of ^{59}Co (υ_L = 12.8 MHz at 1270 mT) and split by the magnitude of the HFI. The absence of an observed partner peak at lower frequency (~0-5 MHz) can be attributed to the decreased sensitivity at low frequencies of the EPR probe in addition to hyperfine enhancement which will increase the intensity of the higher field peak at the expense of the lower field peak (Figure SEPR1).[5]

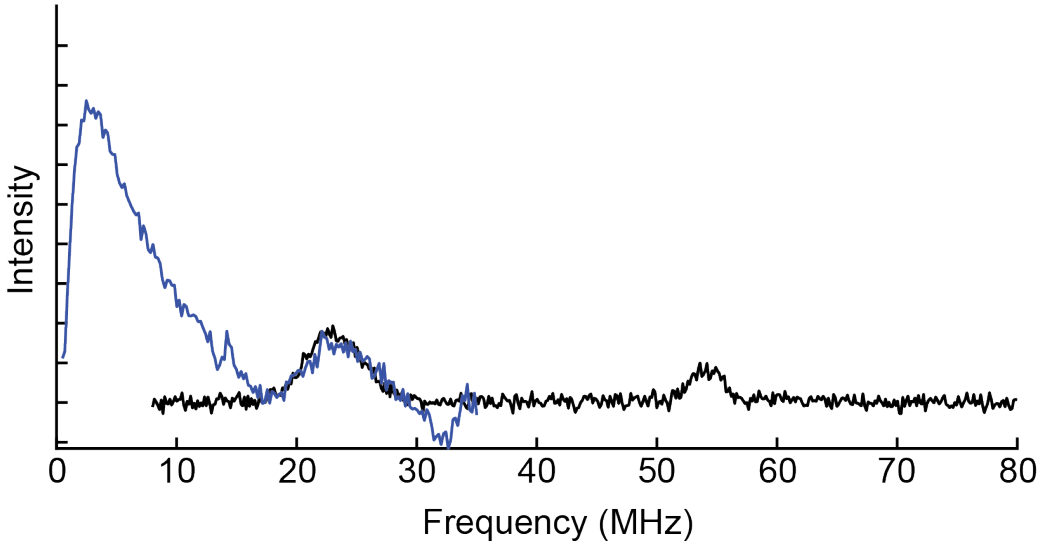

Figure SEPR1. Q-band Davies ENDOR of **1a** collected at 1270mT showing the data collected using a low field (Blue, 0-35 MHz) and high field (Black, 8-80 MHz) radio frequency amplifier. Due to a combination of poor matching of the radio frequency and ENDOR resonator, weak coupling of pyridine nitrogen at the ^{14}N Lamour (3.9 MHz at 1270 mT), and hyperfine enhancement effects, the expected low field peak between ~0-5 MHz of the ^{59}CO was not observed.

X-ray crystallography

X-ray diffraction data for compound **1a** were collected at Beamline 11.3.1 (synchrotron radiation λ = 0.7749 Å) and data for **1b**, **1d**, **2-MeCN**, **3**, **4**, and **5** were collected at Beamline 12.2.1 (synchrotron radiation λ = 0.7288 Å) at the Advanced Light Source, Lawrence Berkeley National Laboratory using a Bruker AXS D8 diffractometer equipped with a Bruker PHOTON II detector. The crystals were cooled to 100 K using an Oxford Cryosystems Cryostream 700 Plus for data collection. Raw data were integrated and corrected for Lorentz and polarization effects using Bruker AXS SAINT software.[10] Data for **1a** were corrected for absorption using TWINABS.[11] Absorption corrections for **1b**, **1d**, **2-MeCN**, **3**, **4**, and **5** were applied using SADABS.[12] The structures were solved using intrinsic phasing with SHELXT[13] and refined using SHELXL[14] operated in the OLEX2 interface.[15] Thermal parameters were refined anisotropically for all non-hydrogen atoms. All hydrogen atoms were placed in ideal positions and refined using a riding model.

Refinement details for Ru(O)Co$_3$(μ_3-O)$_4$(OAc)$_4$(py)$_3$ (1a):

The crystal was found to be a two-component twin based on analysis of its diffraction pattern, and CELL_NOW[16] was used to determine the orientation matrices. The diffraction pattern was indexed to two domains that were found to be related by a 180° rotation about the reciprocal axis [0 0 1]. TWINABS was used to produce a merged HKLF4 file for structure solution and initial refinement and an HKLF5 file for final structure refinement. The HKLF5 file contained all the reflections that involved in domain 2. TWINABS determined the twin fraction to be 48:52. Atomic displacement parameter restraints (RIGU and SIMU) were used on the disordered dichloromethane solvent molecules to obtain a stable refinement. Distance restraints (DFIX) were used for the C–Cl (1.729 Å) and Cl···Cl (2.874 Å) distances in some of the dichloromethane solvent molecules.

Table SC1. Summary of crystallographic data for 1a

Empirical formula	$C_{48.97}H_{59.94}Cl_{5.94}Co_6N_6O_{26}Ru_2$
Formula weight	1915.02
Temperature	100 K
Wavelength	0.7749 Å
Crystal system	Monoclinic
Space group	$P2_1/c$
Unit cell dimensions	a = 15.1378(8) Å α = 90° b = 19.5659(9) Å β = 96.458(3)° c = 23.2044(11) Å γ = 90°
Volume	6829.2(6) $Å^3$
Z	4
Density (calculated)	1.863 g/cm^3
Absorption coefficient	2.658 mm^{-1}
F(000)	3819
Crystal size	0.084 x 0.056 x 0.042 mm
Theta range for data collection	1.476 to 36.210°
Index ranges	$-23 \le h \le 22$, $0 \le k \le 29$, $0 \le l \le 35$
Reflections collected	25396
Independent reflections	25396 [R(int) = 0.1629]
Absorption correction	Multi-scan
Data / restraints / parameters	25396 / 126 / 931
Goodness-of-fit on F^2	1.078
Final R indices [I>2sigma(I)]	$R1$ = 0.0870, w$R2$ = 0.1932
Final R indices (all data)	$R1$ = 0.1173, w$R2$ = 0.2117
Largest diff. peak and hole	2.195 and -1.791 e/Å

Refinement details for $Ru(O)Co_3(\mu_3\text{-}O)_4(OAc)_4(4\text{-}CF_3\text{-}py)_3$ (1b):

The structure was refined as a two-component inversion twin.

Table SC2. Summary of crystallographic data for 1b.

Empirical formula	$C_{27}H_{26}Cl_2Co_3F_9N_3O_{13}Ru$
Formula weight	1120.27
Temperature	100 K
Wavelength	0.7288 Å
Crystal system	Orthorhombic
Space group	$P2_12_12_1$
Unit cell dimensions	a = 13.6937(5) Å α = 90° b = 15.5925(5) Å β = 90° c = 217.7445(6) Å γ = 90°
Volume	3788.8(2) $Å^3$
Z	4
Density (calculated)	1.964 g/cm^3
Absorption coefficient	2.054 mm^{-1}
F(000)	2212
Crystal size	0.1 × 0.1 × 0.02 mm
Theta range for data collection	3.566 to 60.062
Index ranges	$-18 \le h \le 18$, $-21 \le k \le 21$, $-23 \le l \le 24$
Reflections collected	64502
Independent reflections	10279 [R_{int} = 0.0720]
Absorption correction	Multi-scan
Data / restraints / parameters	10279/0/528
Goodness-of-fit on F^2	1.094
Final R indices [I>2sigma(I)]	$R1$ = 0.0442, w$R2$ = 0.1040
Final R indices (all data)	$R1$ = 0.0582, w$R2$ = 0.1126
Largest diff. peak and hole	1.04 and -1.04 e/Å

Refinement details for $Ru(O)Co_3(\mu_3\text{-}O)_4(OAc)_4(4\text{-}OMe\text{-}py)_3$ (1d):

The structure was refined as a two-component inversion twin. One of the two dichloromethane solvent molecules was disordered over two positions, which were modeled at 50:50 occupancies. RIGU restraints were applied to the disordered dichloromethane molecule to obtain reasonable atomic displacement parameters.

Table SC3. Summary of crystallographic data for 1d.

Empirical formula	$C_{28}H_{37}Cl_4Co_3N_3O_{16}Ru$
Formula weight	1091.26
Temperature	100 K
Wavelength	0.7288 Å
Crystal system	Orthorhombic
Space group	$P2_12_12_1$
Unit cell dimensions	a = 11.3063(6) Å α = 90° b = 15.5087(8) Å β = 90° c = 21.9831(11) Å γ = 90°
Volume	3854.6(3) $Å^3$
Z	4
Density (calculated)	1.880 g/cm^3
Absorption coefficient	2.130 mm^{-1}
F(000)	2188
Crystal size	0.2 × 0.1 × 0.02 mm
Theta range for data collection	3.296 to 55.06
Index ranges	-14 ≤ h ≤ 14, -19 ≤ k ≤ 19, -27 ≤ l ≤ 27
Reflections collected	57578
Independent reflections	8226 [R_{int} = 0.0512]
Absorption correction	Multi-scan
Data / restraints / parameters	8226/15/513
Goodness-of-fit on F^2	1.081
Final R indices [I>2sigma(I)]	$R1$ = 0.0507, w$R2$ = 0.1468
Final R indices (all data)	$R1$ = 0.0586, w$R2$ = 0.1573
Largest diff. peak and hole	1.12 and -1.48 e/Å

Refinement details for [Ru(MeCN)Co_3(μ_3-O)$_4$(OAc)$_4$(4-OMe-py)$_3$][BF_4] (2-MeCN):

One of the uncoordinated acetonitrile solvent molecules was disordered over two positions, which were modeled at 50:50 occupancies.

Table SC4. Summary of crystallographic data for 2-MeCN.

Empirical formula	$C_{35}H_{46.5}BCo_3F_4N_{7.5}O_{15}Ru$
Formula weight	1176.96
Temperature	100 K
Wavelength	0.7288 Å
Crystal system	Monoclinic
Space group	$P2_1/n$
Unit cell dimensions	a = 15.6166(10) Å α = 90° b = 14.8708(10) Å β = 99.329(3)° c = 20.7444(13) Å γ = 90°
Volume	4753.8(5) Å^3
Z	4
Density (calculated)	1.644 g/cm^3
Absorption coefficient	1.516 mm^{-1}
F(000)	2380
Crystal size	0.2 × 0.2 × 0.05 mm
Theta range for data collection	3.902 to 52.354
Index ranges	-18 ≤ h ≤ 18, -17 ≤ k ≤ 17, -25 ≤ l ≤ 25
Reflections collected	41669
Independent reflections	8498 [R_{int} = 0.0680]
Absorption correction	Multi-scan
Data / restraints / parameters	8498/0/625
Goodness-of-fit on F^2	1.153
Final R indices [I>2sigma(I)]	$R1$ = 0.1001, w$R2$ = 0.1958
Final R indices (all data)	$R1$ = 0.1399, w$R2$ = 0.2201
Largest diff. peak and hole	2.68 and -1.45 e/Å

Refinement details for $Ru(OC_{18}H_{29}O)Co_3(\mu_3\text{-}O)_4(OAc)_4(py)_3$ (3):

Atomic displacement parameter restraints (RIGU and SIMU) were used on the disordered chloroform and pentane solvent molecules to obtain a stable refinement. Without these restraints, anisotropic refinement resulted in several atoms with very enlarged or elongated thermal ellipsoids, or non-positive definite atoms. Distance restraints (DFIX) were used for the C–Cl (1.76 Å) and 1,3-Cl···Cl (2.89 Å) distances in some of the chloroform solvent molecules. Distance restraints were also used for the C–C (1.54 Å) and 1,3-C···C (2.54 Å) distances in the disordered pentane molecule.

Table SC5. Summary of crystallographic data for 3

Empirical formula	$C_{46.38}H_{63.91}Cl_{10.72}Co_3N_3O_{14}Ru$
Formula weight	1545.14
Temperature	100 K
Wavelength	0.7288 Å
Crystal system	Monoclinic
Space group	$P2_1/c$
Unit cell dimensions	a = 10.097(2) Å α = 90° b = 21.476(5) Å β = 93.105(4)° c = 29.661(7) Å γ = 90°
Volume	6422(3) $Å^3$
Z	4
Density (calculated)	1.598 g/cm^3
Absorption coefficient	1.589 mm^{-1}
F(000)	3129
Crystal size	0.06 x 0.06 x 0.03 mm
Theta range for data collection	1.713 to 29.132°
Index ranges	-13 ≤ h ≤ 13, -28 ≤ k ≤ 28, -39 ≤ l ≤ 39
Reflections collected	105836
Independent reflections	15952 [R(int) = 0.0629]
Absorption correction	Multi-scan
Data / restraints / parameters	15952 / 118 / 799
Goodness-of-fit on F^2	1.075
Final R indices [I>2sigma(I)]	$R1$ = 0.0476, w$R2$ = 0.1160
Final R indices (all data)	$R1$ = 0.0574, w$R2$ = 0.1215
Largest diff. peak and hole	1.363 and -0.917 e/Å

Refinement details for $Ru(OC_{19}H_{15})Co_3(\mu_3\text{-}O)_4(OAc)_4(py)_3$ (4):

The structure was refined as a two-component inversion twin. Distance restraints were used for the C–Cl distances in some of the dichloromethane solvent molecules. RIGU restraints were applied to some of the disordered chloroform molecules and one of the pyridine rings to obtain a stable refinement.

Table SC6. Summary of crystallographic data for 4

Empirical formula	$C_{45}H_{46}Cl_9Co_3N_3O_{13}Ru$
Formula weight	1433.76
Temperature	100 K
Wavelength	0.7288 Å
Crystal system	Orthorhombic
Space group	$P2_12_12_1$
Unit cell dimensions	a = 13.6058(7) Å α = 90° b = 20.0678(10) Å β = 90° c = 26.2552(13) Å γ = 90°
Volume	7168.7(6) $Å^3$
Z	4
Density (calculated)	1.328 g/cm^3
Absorption coefficient	1.353 mm^{-1}
F(000)	2876
Crystal size	0.15 x 0.15 x 0.03 mm
Theta range for data collection	3.458 to 52.346°
Index ranges	-16 ≤ h ≤ 16, -24 ≤ k ≤ 24, -31 ≤ l ≤ 31
Reflections collected	91497
Independent reflections	13260 [R(int) = 0.1062]
Absorption correction	Multi-scan
Data / restraints / parameters	13260 /150/744
Goodness-of-fit on F^2	1.024
Final R indices [I>2sigma(I)]	$R1$ = 0.0895, w$R2$ = 0.2541
Final R indices (all data)	$R1$ = 0.1129, w$R2$ = 2777
Largest diff. peak and hole	1.16 and -0.89 e/Å

Refinement details for [(py)$_3$(OAc)$_4$Co$_3$(μ_3-O)$_4$Ru]–O–[RuCo$_3$(μ_3-O)$_4$(OAc)$_4$(py)$_3$] (5):

Atomic displacement parameter restraints (RIGU and SIMU) were used on the disordered dichloroethane solvent molecules to obtain a stable refinement. Distance restraints (DFIX) were used for the C–Cl (1.74 Å), C–C (1.58 Å) and 1,3-C···Cl (2.725 Å) distances in some of the dichloroethane solvent molecules. A linear free variable (SUMP) was used on the three-component dichloroethane disorder to restrain the sum of the occupation factors to unity. Despite the restraints used to model the disorder, a level A alert was still reported by checkCIF. A response addressing this alert has been included in the CIF and can be read in the reports generated by checkCIF.

Table SC7. Summary of crystallographic data for 5

Empirical formula	$C_{54}H_{70}Cl_8Co_6N_6O_{25}Ru_2$
Formula weight	2042.47
Temperature	100 K
Wavelength	0.7288 Å
Crystal system	Monoclinic
Space group	$P2_1/c$
Unit cell dimensions	a = 21.308(5) Å α = 90° b = 14.505(3) Å β = 93.693(4)°. c = 24.145(5) Å γ = 90°
Volume	7447(3) Å^3
Z	4
Density (calculated)	1.822 g/cm^3
Absorption coefficient	2.190 mm^{-1}
F(000)	4088
Crystal size	0.046 x 0.034 x 0.024 mm
Theta range for data collection	1.680 to 30.959°
Index ranges	-30<=h<=30, -20<=k<=20, -34<=l<=34
Reflections collected	133143
Independent reflections	21916 [R(int) = 0.0637]
Absorption correction	Multi-scan
Max. and min. transmission	0.7461 and 0.6466
Data / restraints / parameters	21916 / 348 / 1040
Goodness-of-fit on F^2	1.101
Final R indices [I>2sigma(I)]	R1 = 0.0584, wR2 = 0.1198
Final R indices (all data)	R1 = 0.0854, wR2 = 0.1309
Largest diff. peak and hole	1.352 and -1.076 e/Å

Computational Details

Unrestricted DFT calculations were performed with the hybrid *meta*-GGA TPSSh functional,[17] as implemented in the Gaussian09 program.[18] The double-ζ def2SVP and triple-ζ def2TZVP basis sets[19] were used for geometry optimization and single-point energy refinement, respectively. This level of theory was benchmarked in a previous work.[20] Geometries were fully optimized without any geometry or symmetry constraint. Vibrational frequencies were computed analytically to confirm the energy minimum nature of the stationary points (*i.e.*, all frequencies were real numbers) and corrected with a scaling factor of 0.959.[21] Free energies were obtained by adding the thermodynamic energies determined with the def2SVP basis set (ZPE, thermal and entropy) to the potential energy determined with the def2TZVP basis set. Dispersion was included in the geometry optimizations and energy refinements by using Grimme's GD3 model.[22] The stability of the electron densities was verified by means of test calculations relaxing orbital constraints.[23] The pruned (99,590) grid was used to increase numerical accuracy in the calculation of two-electron integrals and to avoid spurious imaginary frequencies. Geometry optimizations were carried out in either gas phase, when comparing to experimental results obtained in the solid state (X-ray structures and IR frequencies), or with implicit solvation, when comparing to experimental results obtained in solution (redox potentials and UV-Vis spectra). Solvent effects were modeled by means of the CPCM continuum model.[24] UV-Vis spectra were simulated with TD-DFT(ωB97xd/def2TZVP) calculations.[25] Spin densities were obtained from natural population analysis with the NBO6 method and software.[26]

Geometry optimization of the $Ru(O)Co_3(\mu_3\text{-}O)_4(OAc)_4(py)_3$ (1a)

The DFT geometry optimization of complex **1a** yielded a doublet $Ru^{V}(S=½)Co^{III}_3(S=0)$ ground state, in which the singly-occupied molecular orbital (SOMO) is the antibonding combination of the Ru(d_{xz}) and κ^1-O(p_x) orbitals. In line with the nature of the SOMO, **1a** has oxyl character, with 93% of the spin density (ρ) delocalized over the Ru ($\rho = 0.55\alpha$) and O ($\rho = 0.38\alpha$) atoms of the Ru-κ^1-oxo moiety. In the quartet state, this moiety also concentrates most of the spin density (85%; $\rho = 2.56/3.00\alpha$). However, the doublet is 6.5 kcal mol^{-1} more stable than the quartet. Further, the fully optimized geometry of the doublet state was in better agreement with the X-ray crystal structure, with low root-mean-square and maximum-deviations of 0.014 and 0.042 Å, respectively, over all metal-ligand bond distances. These deviations were clearly higher in the quartet state (*i.e.* 0.027 and 0.067 Å, respectively). Alternative configurations combining low- and high-spin Ru^{IV} (S = 0 and 1) and Ru^{V} (S = 1/2 and 3/2) centers with Co^{IV} (S = ½) and Co^{III} (S = 1) centers, respectively (*e.g.* $Ru^{IV}(S=0)Co^{IV}(S=1/2)\ Co^{III}_2(S=0)$), were also explored by splitting the initial guess of the density into fragments with different local charge and spin multiplicity. These calculations did not yield low-energy states with high-spin cobalt centers. The sextet spin state was also optimized, converging into a high-spin ferromagnetic-coupled state with the $O^{-I}(S=1/2)Ru^{IV}(S=1)Co^{III}_2(S=0)$ configuration. However, this was a high-energy state with an energy of 26.2 kcal mol^{-1} relative to the doublet. In summary, the DFT calculations were consistent with a doublet ground state with the $Ru^{V}(S=½)Co^{III}_3(S=0)$ configuration.

Gas phase DFT-optimized Cartesian coordinates (Å) and free energies (G, in hartrees) of 1a

1a, S = 1/2 | G = – 6279.13906734

Ru	5.46227700	10.78803900	7.45427100
Co	4.38056400	8.35094600	6.44608700
Co	6.37991400	8.25975000	8.40264600
Co	3.83713600	8.95069800	9.03132500
O	6.13657600	9.00381500	6.68314600
O	5.51885000	9.78035000	9.12006800
O	4.68052500	7.56692900	8.10492300
O	2.56327100	7.66344500	6.47005200

O	3.75129500	9.86013000	7.39073500
O	5.22603200	11.21587500	5.40015400
O	4.18023200	9.29331800	4.76698100
O	7.53997800	11.10939300	7.65956900
O	8.10450100	9.11446900	8.60489100
O	6.36144200	7.49383800	10.18875000
O	2.12724100	8.12868500	8.66248000
O	5.24930300	12.44007900	7.75040900
N	4.98812300	6.79824000	5.49573400
O	4.20239100	8.03789100	10.69452700
N	3.01562400	10.45593100	9.93161500
N	7.24698500	6.69363900	7.70766700
C	4.61112000	10.47304100	4.57955100
C	1.83312800	7.69015300	7.50787400
C	8.23610600	6.82614500	6.81004400
H	8.43838100	7.84839100	6.48997900
C	5.85697400	6.93794800	4.48223500
H	6.21034600	7.95470900	4.31092800
C	8.58229000	4.44684200	6.78462400
H	9.11147600	3.56170300	6.42381800
C	6.89003500	5.47677400	8.14676800
H	6.06078800	5.46356700	8.85414300
C	8.33820600	10.30188800	8.22016900
C	5.34125400	7.53498800	10.94289100
C	4.51273300	5.58533900	5.81780500
H	3.83467900	5.56516900	6.67112300
C	4.34181900	11.07384700	3.21489800
H	3.37649700	11.60353200	3.25851100
H	4.26935900	10.28447300	2.45526400
H	5.12242900	11.80207200	2.95939600
C	3.58882500	10.97959900	11.02674900
H	4.47815000	10.45957500	11.38332100
C	8.93192200	5.72004700	6.32547400
H	9.73071800	5.86132400	5.59550400
C	7.54118500	4.32463300	7.70938800
H	7.22780000	3.34984600	8.08687200
C	6.27273700	5.84487200	3.72457000
H	6.97970700	5.99173600	2.90633800
C	5.77426900	4.57681600	4.03702200
H	6.08010300	3.70187400	3.45855600
C	0.42209900	7.16348000	7.33764900
H	-0.21515500	7.99056200	6.98454700
H	0.02793000	6.80335400	8.29657100
H	0.40127200	6.37156900	6.57738200
C	9.73713200	10.82341800	8.47893500
H	10.45937000	9.99639600	8.48452500
H	9.74727900	11.29877900	9.47302500
H	10.00529700	11.58114500	7.73146100
C	4.88184000	4.44602900	5.10493200
H	4.47625300	3.47407200	5.39075900
C	5.51702000	6.93586600	12.32405400
H	6.21501200	6.08905000	12.28335100
H	4.54753000	6.63049500	12.73781300
H	5.95557200	7.70418700	12.98134600
C	3.07909300	12.12189800	11.64116300
H	3.57134700	12.52443800	12.52789800
C	1.93654400	11.04204400	9.38900000
H	1.55428800	10.57063700	8.48354400
C	1.36968800	12.18608400	9.94663700

H	0.49502800	12.64011200	9.47819700
C	1.94932500	12.73581900	11.09332600
H	1.53164300	13.63650100	11.54923800

1a, *S* = 3/2 | G = – 6279.12872748

Ru	5.45745800	10.74471600	7.45585700
Co	4.37550600	8.32114300	6.45258000
Co	6.37075700	8.22905000	8.40259000
Co	3.83573700	8.90894600	9.03015300
O	6.13802700	8.93888100	6.67574800
O	5.52766300	9.74419400	9.12614300
O	4.67822900	7.52451400	8.10309300
O	2.55012400	7.64345400	6.46956200
O	3.74123300	9.82603300	7.38037100
O	5.13124000	11.29295900	5.49076400
O	4.20080100	9.33537000	4.78490000
O	7.45407200	11.18467900	7.75738400
O	8.08769500	9.15592500	8.58177900
O	6.36158600	7.47137900	10.19680900
O	2.12753300	8.09964300	8.66541800
O	4.87586200	12.27744800	8.12548100
N	4.97279100	6.77273800	5.48231600
O	4.19932800	8.00843300	10.69161600
N	3.03194200	10.43300100	9.91489700
N	7.25751700	6.66467700	7.71815200
C	4.58847200	10.52697900	4.62510500
C	1.82424500	7.66880400	7.50960400
C	8.24478500	6.80131100	6.81916200
H	8.44511500	7.82526800	6.50329100
C	5.85047400	6.91760100	4.47725800
H	6.20168600	7.93627500	4.31256100
C	8.59017600	4.42211300	6.77946700
H	9.11788100	3.53873800	6.41218700
C	6.90146400	5.44531200	8.15102700
H	6.07390800	5.42803600	8.86048500
C	8.29496100	10.35495900	8.24224200
C	5.34013000	7.51240400	10.94810000
C	4.50066700	5.55693300	5.79812300
H	3.81425900	5.53167600	6.64469800
C	4.36581400	11.14946000	3.26429900
H	3.49365800	11.81909000	3.33104500
H	4.16825400	10.37531200	2.51256200
H	5.23486200	11.76125100	2.98576700
C	3.62873200	10.97640800	10.98636300
H	4.50729600	10.44575000	11.35287600
C	8.94053400	5.69792100	6.32806400
H	9.73919100	5.84287900	5.59859900
C	7.55025000	4.29506300	7.70497700
H	7.23626600	3.31811800	8.07638500
C	6.27825500	5.82770400	3.72149600
H	6.99119400	5.97897800	2.90920900
C	5.78492700	4.55642800	4.02917100
H	6.10180300	3.68350200	3.45357800
C	0.40895500	7.15268700	7.34623100
H	-0.22337000	7.98449100	6.99546000
H	0.01618000	6.79596700	8.30693600
H	0.37930700	6.36056700	6.58642100

C	9.68976900	10.90097000	8.45552000
H	10.40902900	10.08286100	8.58560100
H	9.68079200	11.52101700	9.36603200
H	9.97180900	11.54818800	7.61378000
C	4.88343000	4.41983300	5.08877600
H	4.48158600	3.44520500	5.37083800
C	5.51066600	6.92508900	12.33451000
H	6.22323300	6.09005200	12.30701000
H	4.54181000	6.60644900	12.73969500
H	5.92752300	7.70567100	12.99151100
C	3.15804900	12.15343300	11.56409300
H	3.66990500	12.57176300	12.43218200
C	1.97181600	11.03532400	9.35539900
H	1.57357700	10.55022100	8.46458400
C	1.44358200	12.21408400	9.87617900
H	0.58351800	12.68090900	9.39359200
C	2.04542700	12.78333500	11.00098000
H	1.65974900	13.71272800	11.42655400

1a, *S* = 5/2 | G = – 6279.09733282

Ru	5.40972400	10.80237900	7.45600600
Co	4.42021500	8.27227800	6.49878900
Co	6.40712300	8.32348500	8.47849200
Co	3.85163400	9.00103900	9.08662300
O	6.13238400	8.97085500	6.72200500
O	5.53785700	9.84650200	9.15736400
O	4.71511500	7.59112600	8.19934600
O	2.56913700	7.55278100	6.61544400
O	3.67444700	9.96019400	7.45998700
O	5.11923800	11.30157900	5.48060100
O	4.26362100	9.30438300	4.79693100
O	7.43151700	11.24657100	7.70882900
O	8.10356600	9.26986000	8.62052900
O	6.41854300	7.59374100	10.26853500
O	2.16003200	8.14014900	8.78025900
O	4.89186600	12.36474200	8.08925500
N	4.93548500	6.58726500	5.27567200
O	4.25083200	8.11512300	10.75712200
N	3.03982200	10.50003900	9.98773400
N	7.26550300	6.73051700	7.78740600
C	4.63620700	10.49523800	4.61357800
C	1.86419800	7.60429500	7.66861900
C	8.39789300	6.81015900	7.07100100
H	8.81544100	7.81126200	6.96552800
C	6.06868400	6.69515100	4.56776800
H	6.58651100	7.65297000	4.66794400
C	8.37527400	4.43700300	6.68630400
H	8.80922400	3.53485200	6.24886600
C	6.66692100	5.54181600	7.96943800
H	5.73296900	5.57659300	8.53286600
C	8.28640700	10.46043000	8.22815000
C	5.39482900	7.63036300	11.01774100
C	4.23289500	5.44733700	5.24008500
H	3.31599300	5.44844100	5.83358100
C	4.46130600	11.07363600	3.22629600
H	3.52399800	11.65263900	3.21203400
H	4.39435400	10.27109400	2.48104600

H	5.28591700	11.76194700	2.99734800
C	3.64454000	11.05048500	11.05101100
H	4.54626600	10.54291900	11.39265900
C	8.98934200	5.68010200	6.50911800
H	9.91202500	5.78191200	5.93518400
C	7.19252300	4.36970100	7.42757100
H	6.67379800	3.42265300	7.58467100
C	6.55035300	5.64659000	3.78273200
H	7.47822800	5.76682700	3.22062800
C	5.82524200	4.45182500	3.74128000
H	6.17517000	3.61135300	3.13668000
C	0.51253000	6.92090300	7.60370600
H	0.08354600	7.02674700	6.59826600
H	-0.16320800	7.32877900	8.36603900
H	0.65725100	5.84673200	7.80479200
C	9.67344000	11.03730700	8.41115400
H	10.39321800	10.24983300	8.66637100
H	9.63560800	11.77595900	9.22711100
H	9.97676600	11.56908500	7.49827400
C	4.64431800	4.34925200	4.48285200
H	4.04669700	3.43569500	4.47415100
C	5.57196300	7.05205000	12.40702200
H	6.25298700	6.19116100	12.37285600
H	4.60102700	6.77147700	12.83426600
H	6.03250800	7.82244600	13.04650700
C	3.15159800	12.20777500	11.65021300
H	3.67074400	12.63401900	12.51005200
C	1.94929500	11.07363200	9.45632700
H	1.54956100	10.58584300	8.56795100
C	1.39687100	12.22951200	10.00285900
H	0.51097100	12.67301600	9.54567400
C	2.00685200	12.80713900	11.11916200
H	1.60199200	13.71973500	11.56293700

IR and UV-vis-NIR analysis of compound 1a

The IR and UV–vis–NIR spectra of **1a** were investigated by means of DFT and TD-DFT calculations, respectively. In agreement with the experiments, the analytic calculation of the frequencies showed that the stretching of the terminal Ru^{V}–oxo bond is IR-active (IR intensity = 141 km mol^{-1}), with a predicted frequency of 904 cm^{-1}. The UV–vis–NIR spectrum of **1a** was simulated with the aim of understanding the nature of the weak absorption observed at *ca.* 1000 nm. The closest absorption predicted by the TD-DFT calculations, at λ = 1007 nm, has the SOMO – 3 → LUMO + 4 excitation as main component (Figure SCD1). This excitation can be classified as a CT transition between two cobalt centers across a μ–oxo ligand, due to the Co(*d*)–O(*p*)–Co(*d*) nature of the molecular orbitals involved. In line with experimental spectrum, and owing to its *d-d* character, this transition has a very small intensity, with a predicted oscillator strength f < 0.0001.

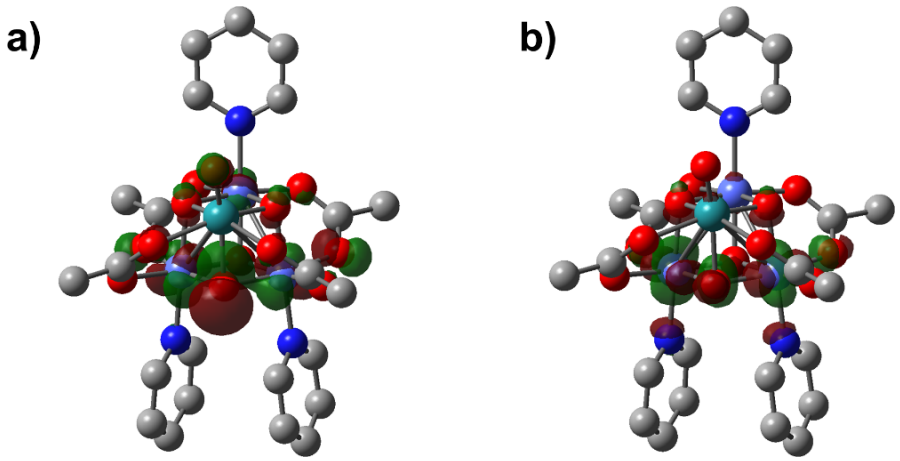

Figure SCD1. **a)** SOMO – 3 and **b)** LUMO + 4 orbitals of **1a** (0.05 isovalue) from TD-DFT calculations (doublet ground state).

Analysis for oxidation of 1a–d

The geometry of the oxidized species **1a**$^{+}$ was fully optimized in fluorobenzene (used as solvent model of *ortho*-difluorobenzene), converging into a closed-shell singlet ground state with S = 0 at all atomic centers. The triplet state also yielded an energy minimum, though it was 3.9 kcal mol^{-1} less stable than the singlet state. In the triplet state, the spin density is mostly delocalized over Ru ($\rho = 0.98\alpha$) and the terminal and μ–oxo ligands ($\Sigma\rho = 0.76\alpha$), with negligible contributions from the Co centers ($\rho < 0.04\alpha$). Other electronic configurations were also explored for **1a**$^{+}$, including triplet and quintet states combining low-spin and high-spin Ru^{V} (S = 1/2 and 3/2), Ru^{VI} (S = 0 and 1), Co^{III} (S = 0 and 1) and Co^{IV} (S = 1/2) centers, but none of these yielded a state with an energy lower than that of the singlet. The geometry of the reduced form (**1a**$^{-}$) was also fully optimized in fluorobenzene (used as solvent model of *ortho*-difluorobenzene), which did not alter to any significant extent (*e.g.* ρ(Ru:O) = 0.56:0.36 *vs.* 0.55:0.38 in gas phase). Considering the ground states of both **1a** (doublet) and **1a**$^{+}$ (singlet), the calculations predicted an oxidation potential of 0.41 V vs. Fc/Fc^{+}, with a small deviation of 120 mV relative to the experimental value (0.53 V). In conclusion, these data and the nature of the SOMO of **1a** (Figure 8a), are consistent with the oxidation of the [Ru^{V}Co$^{III}_3$] core in **1a** to [Ru^{VI}Co$^{III}_3$] in **1a**$^{+}$.

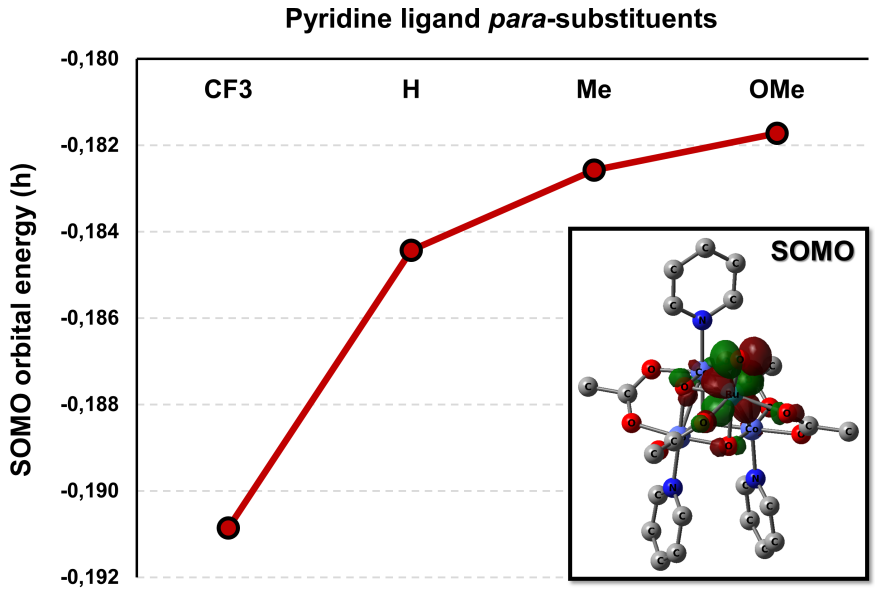

Figure SCD2. SOMO energy dependence on the nature of the *para*-substituents of the pyridine ligands.

DFT/CPCM-optimized Cartesian coordinates (Å) and free energies (G, in hartrees) of 1a and $1a^+$

1a, *S* = 1/2 | G = – 6279.24409415

Ru	5.48105800	10.79148900	7.43513400
Co	4.38506400	8.37250600	6.43927500
Co	6.38855200	8.28042500	8.39777800
Co	3.84358100	8.97794100	9.02743400
O	6.14617100	9.02442500	6.67353000
O	5.52709700	9.81564300	9.11424000
O	4.68825100	7.59878800	8.09879300
O	2.56232500	7.71000800	6.46157900
O	3.75845600	9.89623000	7.38592700
O	5.26243800	11.21571600	5.36707300
O	4.17327400	9.31369600	4.75713000
O	7.57341900	11.10754100	7.61838100
O	8.11667600	9.13343300	8.61064700
O	6.37442900	7.53844000	10.19013800
O	2.14598200	8.13210700	8.66420900
O	5.30704300	12.46285100	7.69359200
N	4.98488600	6.81144800	5.49634400
O	4.20359800	8.04194400	10.67692900
N	2.99899400	10.45972500	9.94956300
N	7.24736400	6.70561000	7.70958100
C	4.63700300	10.47614500	4.54544100
C	1.83729700	7.70966100	7.50520700
C	8.24083000	6.82417000	6.81272200
H	8.46397800	7.84029900	6.48859100
C	5.85958600	6.93724900	4.48426100
H	6.22075000	7.94801300	4.29699100
C	8.55512300	4.44089000	6.78772400
H	9.07068400	3.54913500	6.42513100
C	6.87475900	5.49163400	8.14829600
H	6.04426000	5.48070900	8.85360300
C	8.37317500	10.30330100	8.19021000
C	5.34796600	7.55361200	10.93919300
C	4.50436400	5.60151500	5.82801500
H	3.82245900	5.58351800	6.67770400
C	4.39953900	11.05635000	3.16849800
H	3.42563800	11.57211100	3.17487200
H	4.36141000	10.25608600	2.41805100
H	5.17824700	11.78898700	2.92128800
C	3.55385900	10.96899100	11.06275300
H	4.45050100	10.46107900	11.41875400
C	8.92252100	5.70949300	6.32921500
H	9.72172300	5.84109800	5.59859300
C	7.51183600	4.33188500	7.71183900
H	7.18300700	3.36192800	8.08726800
C	6.27674900	5.83533900	3.74123700
H	6.99055400	5.97215000	2.92784200
C	5.77361400	4.57183800	4.06521200
H	6.08316800	3.68991800	3.50050500
C	0.43076200	7.17797600	7.34093200
H	-0.21986300	8.01413400	7.03712300
H	0.05784300	6.77612900	8.29159000
H	0.40082300	6.41413000	6.55334200
C	9.78285300	10.80510900	8.41419800
H	10.49290300	9.96805000	8.39780300
H	9.82716200	11.27746100	9.40891500

H	10.04665700	11.55798100	7.66065300
C	4.87420500	4.45450400	5.12897700
H	4.46634600	3.48718300	5.42533100
C	5.51870800	6.94956100	12.31545500
H	6.24409900	6.12632900	12.28208200
H	4.55357800	6.60596400	12.70847700
H	5.91325800	7.72886300	12.98753600
C	3.01306000	12.08136800	11.70506100
H	3.48911600	12.46928300	12.60670900
C	1.90349900	11.03177900	9.42104500
H	1.52555800	10.57311100	8.50717700
C	1.30591400	12.14578100	10.00674100
H	0.41764900	12.58515400	9.55072000
C	1.86875900	12.68039800	11.16952700
H	1.42455500	13.55497900	11.64951100

Fc^+, *S* = 1/2 | G = – 1650.75747262

Fe	-0.07630700	2.01912400	1.72045100
C	-1.73370300	2.39422300	2.87829400
C	-1.71571900	3.23995900	1.71832900
C	-1.80328500	1.03825700	2.42983200
H	-1.69077100	2.72420400	3.91489900
C	-1.77080300	2.39472700	0.56249100
H	-1.66428800	4.32741400	1.71611200
C	-1.82863400	1.04195900	1.00725600
H	-1.79021200	0.15350100	3.06451900
H	-1.74213900	2.72462700	-0.47472400
H	-1.82630300	0.16034700	0.36794600
C	1.62048600	2.39330700	0.56560500
C	1.56347600	3.23939600	1.72073900
C	1.67708200	1.04083700	1.01147300
H	1.59395200	2.72246900	-0.47190100
C	1.57901100	2.39448700	2.88133700
H	1.51240400	4.32686600	1.71763900
C	1.64901900	1.03818900	2.43399400
H	1.67571200	0.15875700	0.37280600
H	1.53415200	2.72521800	3.91762400
H	1.63441700	0.15390000	3.06930100

$1a^+$, *S* = 0 | G = – 6279.04840754

Ru	5.46669900	10.81609800	7.41885700
Co	4.40950500	8.38039000	6.43275500
Co	6.39811100	8.25907700	8.40171700
Co	3.83371500	8.98637100	9.00217800
O	6.16474200	9.04728600	6.70170700
O	5.51911200	9.80789100	9.03817000
O	4.68937900	7.60667300	8.08595300
O	2.60087900	7.73193500	6.43867500
O	3.76596400	9.95948800	7.36998100
O	5.26492000	11.16938900	5.43881900
O	4.18552900	9.30941200	4.74796000
O	7.55723800	11.05892300	7.48054700
O	8.10937100	9.14390400	8.58974000
O	6.35765500	7.55003800	10.18685600
O	2.15931800	8.14802000	8.63681100

O	5.44414800	12.39688800	7.90971900
N	5.00868300	6.82762200	5.51313100
O	4.17796000	8.05419300	10.63061200
N	2.98592100	10.45808200	9.94088500
N	7.24928300	6.68296500	7.73350200
C	4.62226000	10.47397800	4.56776700
C	1.86189600	7.72045300	7.47444500
C	8.24372800	6.78960900	6.83466000
H	8.47141900	7.79835600	6.49134800
C	5.88353900	6.95109600	4.49893200
H	6.24834000	7.95789500	4.29959300
C	8.55912300	4.40691200	6.85082000
H	9.07618300	3.51013300	6.50387400
C	6.87701500	5.47577800	8.19469900
H	6.04821900	5.47028800	8.90143700
C	8.36668300	10.27739900	8.09306000
C	5.31688700	7.55984500	10.91740800
C	4.52490100	5.62061300	5.85509000
H	3.84264500	5.60387900	6.70369100
C	4.39596800	11.14497300	3.24239100
H	3.51092000	11.79429500	3.33646700
H	4.20710500	10.39079400	2.46924500
H	5.25690500	11.77371600	2.98194400
C	3.55224500	10.96679000	11.04969300
H	4.46151200	10.47339400	11.39391600
C	8.92511900	5.66758000	6.37016800
H	9.72441300	5.78861800	5.63824200
C	7.51641400	4.31138700	7.77690800
H	7.18962200	3.34806700	8.17000300
C	6.29861600	5.84412300	3.76426800
H	7.01128500	5.97692400	2.94966900
C	5.79522200	4.58321100	4.09723700
H	6.10415100	3.69805600	3.53786600
C	0.46731000	7.17518300	7.29745100
H	-0.18145300	8.00037000	6.96200900
H	0.08243600	6.79230900	8.25050200
H	0.46108000	6.39504900	6.52596500
C	9.77550800	10.79636200	8.23744100
H	10.47333500	9.96134300	8.37416400
H	9.81165500	11.44199200	9.12940500
H	10.04899700	11.40208200	7.36419200
C	4.89646500	4.47163700	5.16183900
H	4.48771800	3.50694600	5.46431200
C	5.45432100	6.95156000	12.29057800
H	6.17220200	6.12203900	12.26503200
H	4.47792500	6.61828500	12.66253800
H	5.84512200	7.72635400	12.96971300
C	3.00297700	12.06413400	11.70901800
H	3.48783800	12.45250100	12.60545000
C	1.86837500	11.01165000	9.43722500
H	1.47229700	10.55167700	8.53182700
C	1.26298800	12.10986300	10.04286800
H	0.35721400	12.53410900	9.60803700
C	1.83855000	12.64593100	11.19853900
H	1.38737700	13.50811400	11.69367600

Fc, *S* = 0 | G = – 1650.93814144

Fe	-0.07631500	2.01946800	1.72018100
C	-1.70275600	2.39580000	2.87815700
C	-1.70187900	3.23876700	1.71907200
C	-1.70211700	1.03290500	2.43465900
H	-1.68634200	2.73232400	3.91413200
C	-1.70044900	2.39683400	0.55924000
H	-1.68417800	4.32802400	1.71956500
C	-1.70066300	1.03354200	1.00152000
H	-1.68581600	0.15133800	3.07454800
H	-1.68191900	2.73429600	-0.47639600
H	-1.68308200	0.15254500	0.36087900
C	1.55015400	2.39586600	0.56226500
C	1.54928000	3.23872000	1.72143000
C	1.54947300	1.03293000	1.00563100
H	1.53380000	2.73249100	-0.47367900
C	1.54781000	2.39667500	2.88118000
H	1.53164000	4.32797800	1.72104200
C	1.54799600	1.03342800	2.43876800
H	1.53319400	0.15142500	0.36565600
H	1.52930200	2.73403700	3.91684800
H	1.53041400	0.15237000	3.07932400

1b (CF_3), *S* = ½ | G = –7290.80448607

Ru	5.48311900	10.79373200	7.43613300
Co	4.38266800	8.37749000	6.43502500
Co	6.38297600	8.27748700	8.40051200
Co	3.83935200	8.97645900	9.02153700
O	6.14575700	9.02089300	6.67543700
O	5.52415500	9.81027200	9.11292300
O	4.68198400	7.59739900	8.09402100
O	2.56200600	7.71433800	6.45308600
O	3.75945100	9.89694900	7.38156100
O	5.26926900	11.21916000	5.37235500
O	4.18049400	9.31915500	4.75572500
O	7.57116800	11.10276700	7.62522200
O	8.11059200	9.12499400	8.61269500
O	6.36243600	7.53220100	10.18932300
O	2.14082600	8.13911300	8.65414700
O	5.30659900	12.46203400	7.70248400
N	4.98461100	6.82145200	5.48888000
O	4.19294900	8.04405700	10.67191100
N	3.00027600	10.46108400	9.94067700
N	7.23785100	6.69964800	7.71708000
C	4.64530500	10.48251100	4.54700000
C	1.83362800	7.71497100	7.49496300
C	8.23501700	6.81373600	6.82351000
H	8.47542800	7.82843400	6.50853600
C	5.87804200	6.95265300	4.49566600
H	6.23873500	7.96398300	4.31254500
C	8.50028100	4.43089500	6.77003300
C	6.84594700	5.48911200	8.14446700
H	6.01382200	5.48121000	8.84745100
C	8.36958800	10.29657900	8.19621300
C	5.33510400	7.55175000	10.93786100
C	4.50255600	5.61020500	5.81353100
H	3.80327600	5.58735100	6.64838400

C	4.41190700	11.06443600	3.17108100
H	3.43465300	11.57376900	3.17418400
H	4.38214200	10.26556700	2.41884200
H	5.18749700	11.80220000	2.92995600
C	3.56631600	10.97538700	11.04550900
H	4.46653900	10.47192100	11.39738600
C	8.89672000	5.69636600	6.32427100
H	9.69143000	5.81659500	5.58782300
C	7.45977000	4.32197100	7.69522700
H	7.11576100	3.35049900	8.04892800
C	6.32481700	5.85326600	3.76680500
H	7.06178900	5.98307700	2.97484200
C	5.82456700	4.59047000	4.09246500
C	0.42831800	7.18317800	7.32836800
H	-0.22128100	8.01912800	7.02191800
H	0.05364000	6.78269000	8.27880000
H	0.40047800	6.41860200	6.54152600
C	9.77859900	10.79601300	8.42367500
H	10.48706900	9.95767200	8.41383600
H	9.81890000	11.27270000	9.41646100
H	10.04623200	11.54540400	7.66810000
C	4.89739800	4.46315200	5.13217400
H	4.50204000	3.49048700	5.42528700
C	5.50138200	6.94975300	12.31460500
H	6.22945800	6.12890300	12.28529000
H	4.53534300	6.60413800	12.70339900
H	5.89030300	7.73146900	12.98713800
C	3.03536800	12.09139500	11.68562500
H	3.51936300	12.49315700	12.57602100
C	1.90402300	11.03086400	9.41497400
H	1.51838600	10.57109300	8.50536600
C	1.30996000	12.14842200	9.99623100
H	0.42332000	12.59500400	9.54674800
C	1.88587100	12.68237100	11.15150700
C	1.26148000	13.87031000	11.84626700
C	9.20954500	3.20093900	6.25229000
C	6.26579600	3.36380700	3.32809700
F	2.19851800	14.70365600	12.33413000
F	0.50123700	13.47483400	12.88772900
F	0.47201600	14.57767500	11.01993600
F	10.41055100	3.04789500	6.84398700
F	9.43055700	3.29051200	4.92623100
F	8.50435800	2.08003900	6.47600500
F	7.41374800	3.57235900	2.66277900
F	6.45374000	2.31743700	4.15578400
F	5.33709600	2.99265000	2.42500600

1b^{+} (CF_3), *S* = 0 | G = –7290.60269774

Ru	5.46337900	10.82337400	7.41181300
Co	4.40368600	8.37793100	6.43197100
Co	6.39863100	8.26605700	8.39860900
Co	3.83650400	8.98652600	9.00037300
O	6.15912800	9.04584400	6.69693000
O	5.52092700	9.81176600	9.03140100
O	4.69044000	7.60696100	8.08641600
O	2.59802300	7.72502700	6.44428100
O	3.76684100	9.95437800	7.36536500
O	5.25779200	11.16339900	5.43435400

O	4.18041900	9.30096300	4.74685800
O	7.54787000	11.06369100	7.46679000
O	8.10767100	9.15174500	8.57730600
O	6.36285500	7.55732000	10.18293800
O	2.16144600	8.15059500	8.64134400
O	5.43426900	12.40145600	7.90620300
N	5.00312500	6.82431800	5.51354200
O	4.18482300	8.06355200	10.63115400
N	2.98900100	10.46067000	9.93791400
N	7.25274000	6.68804700	7.73436800
C	4.61440600	10.46653100	4.56429100
C	1.86061200	7.71696700	7.48170400
C	8.24475100	6.79223600	6.83500500
H	8.48439400	7.79962200	6.49681900
C	5.89241800	6.94836700	4.51192100
H	6.25791200	7.95465700	4.31274600
C	8.52402200	4.41156200	6.82330000
C	6.87047100	5.48191700	8.19071200
H	6.04478900	5.47747600	8.90061400
C	8.36138700	10.28583400	8.07958600
C	5.32450100	7.56967900	10.91752900
C	4.51743600	5.61917700	5.85281100
H	3.82200800	5.60010500	6.69025200
C	4.38525600	11.13560300	3.23929100
H	3.49098200	11.77254400	3.33126500
H	4.20858600	10.37937000	2.46526800
H	5.23876000	11.77576700	2.98272100
C	3.56351300	10.97526600	11.03920000
H	4.47704000	10.48848900	11.38020600
C	8.91049900	5.66807000	6.35275400
H	9.70198600	5.77731000	5.61217400
C	7.48927200	4.31351900	7.75953200
H	7.15065300	3.34843200	8.13676100
C	6.32928700	5.84222700	3.79225800
H	7.06268900	5.96806600	2.99577000
C	5.82564200	4.58217100	4.13198800
C	0.46702100	7.16918700	7.31092000
H	-0.18408500	7.99301600	6.97667400
H	0.08664300	6.78731100	8.26611100
H	0.45944900	6.38809800	6.54050300
C	9.76772900	10.80999200	8.22048000
H	10.46823000	9.97801800	8.36135600
H	9.80100700	11.46036500	9.10910000
H	10.03831800	11.41237000	7.34407700
C	4.90603500	4.46584600	5.17600800
H	4.50803800	3.49708200	5.47600000
C	5.46547000	6.96672200	12.29187400
H	6.18560000	6.13919700	12.26799300
H	4.49039100	6.63256200	12.66631300
H	5.85530900	7.74532000	12.96721500
C	3.02113600	12.07512700	11.69641700
H	3.51271700	12.47832300	12.58188800
C	1.86913100	11.00896500	9.43785700
H	1.46678600	10.54737200	8.53648900
C	1.26416000	12.10939000	10.03915600
H	0.35909400	12.53891300	9.61041700
C	1.85118200	12.64685100	11.18678800
C	1.21785800	13.82203300	11.90012800
C	9.21063700	3.15408700	6.33479600

C	6.28396200	3.36220900	3.36200300
F	0.49560100	13.40573600	12.95741400
F	0.39470100	14.51006200	11.09250200
F	2.15158000	14.67174400	12.36196500
F	8.30760000	2.19956600	6.04070000
F	9.94557700	3.37983700	5.23550000
F	10.02796200	2.65418400	7.27918000
F	5.97878800	2.22373400	4.00202100
F	7.61715600	3.38835900	3.17441500
F	5.70951200	3.31663100	2.14669800

1c (Me), *S* = ½ | G = –6397.18751928

Ru	5.46952100	10.79285700	7.43788500
Co	4.37834300	8.37247200	6.44324000
Co	6.38714500	8.28537200	8.39973400
Co	3.84043200	8.97590000	9.03362700
O	6.13862000	9.02932700	6.67505000
O	5.52188900	9.81911200	9.11721200
O	4.68802900	7.59961400	8.10268800
O	2.55877000	7.70110200	6.47004100
O	3.74889200	9.89462300	7.39277000
O	5.24535200	11.21842700	5.36927900
O	4.15787000	9.31480500	4.76172900
O	7.56294100	11.11484100	7.61523500
O	8.11501100	9.14219500	8.60584900
O	6.37893600	7.54637800	10.19398600
O	2.14511400	8.12277800	8.67346500
O	5.29344800	12.46457200	7.69617500
N	4.98421800	6.81676800	5.49784600
O	4.20656000	8.04082500	10.68309400
N	2.99403700	10.45443900	9.95722000
N	7.24458500	6.71037900	7.71291700
C	4.61902300	10.47791800	4.54926400
C	1.83680400	7.69714500	7.51563600
C	8.22277000	6.81710500	6.80020900
H	8.45501100	7.83064700	6.47376300
C	5.85817300	6.94252400	4.48423100
H	6.20175900	7.95638400	4.28156900
C	8.51166300	4.41457700	6.73102600
C	6.87430700	5.49403500	8.14952300
H	6.05742400	5.48153500	8.87046500
C	8.36683800	10.31210300	8.18336500
C	5.35357700	7.55870000	10.94441800
C	4.53256100	5.59936500	5.83686000
H	3.84811900	5.57061000	6.68444000
C	4.37678500	11.05816500	3.17286800
H	3.40214700	11.57250900	3.18179700
H	4.33782900	10.25801700	2.42229400
H	5.15371800	11.79199900	2.92351600
C	3.54713800	10.97208000	11.06731200
H	4.44511700	10.46895900	11.42700200
C	8.87586900	5.69715400	6.29312800
H	9.65615300	5.83009200	5.54146700
C	7.48591100	4.33435700	7.68879200
H	7.14518500	3.36701500	8.06299600
C	6.30516200	5.84129000	3.76434600
H	7.02520400	5.98865800	2.95712900
C	5.84789800	4.55379100	4.09439800

C	0.43318800	7.15577100	7.35531800
H	-0.22371200	7.98652500	7.05017800
H	0.06451100	6.75398900	8.30768700
H	0.40695600	6.38942600	6.56997000
C	9.77672500	10.81738600	8.40022700
H	10.48840700	9.98168700	8.38447700
H	9.82400000	11.29408100	9.39274900
H	10.03640300	11.56774700	7.64269000
C	4.93774800	4.45363900	5.15795900
H	4.55421100	3.48216600	5.47531900
C	5.52914600	6.95917000	12.32233100
H	6.26612700	6.14617600	12.29284500
H	4.56770400	6.60271400	12.71312800
H	5.90991900	7.74526200	12.99449300
C	3.00629700	12.08330000	11.70613300
H	3.48786500	12.46797100	12.60729900
C	1.89498700	11.02718800	9.43808200
H	1.50727400	10.56758000	8.52864800
C	1.30067400	12.14004100	10.02448400
H	0.40654000	12.57004500	9.56890300
C	1.85501100	12.69972700	11.18743400
C	1.26490000	13.92495300	11.83033600
H	1.75849900	14.82876100	11.43414900
H	0.18998200	14.01197300	11.61726200
H	1.41595000	13.91691100	12.91952500
C	9.17863100	3.17467400	6.20120300
H	9.81766800	2.72209700	6.97748800
H	8.42831600	2.42070000	5.91732000
H	9.80585500	3.39594900	5.32665200
C	6.31754600	3.34344000	3.33474600
H	5.83810600	3.30758400	2.34218800
H	7.40511700	3.38230900	3.17028200
H	6.07191000	2.41338900	3.86584100

1c^{+}(Me), *S* = 0 | G = –6396.99355111

Ru	5.45237900	10.81518100	7.42036200
Co	4.40069700	8.38009200	6.43708600
Co	6.39572400	8.26296500	8.40256400
Co	3.82921700	8.98342500	9.00874900
O	6.15530300	9.05180600	6.70216800
O	5.51233700	9.80978800	9.04013700
O	4.68779800	7.60653900	8.08982000
O	2.59581100	7.72144700	6.44806200
O	3.75262000	9.95713200	7.37754800
O	5.24383500	11.17196300	5.43988800
O	4.16644900	9.30949700	4.75297200
O	7.54449600	11.06655500	7.47683600
O	8.10631600	9.15228400	8.58294300
O	6.36216000	7.55696800	10.18926800
O	2.15702200	8.13771800	8.64697900
O	5.42821900	12.39715900	7.90924800
N	5.00670300	6.83374000	5.51494400
O	4.18109100	8.05190900	10.63681900
N	2.98138600	10.45184400	9.94820500
N	7.24494500	6.68737200	7.73521400
C	4.60013400	10.47490900	4.57128100
C	1.86006000	7.70651600	7.48598100
C	8.22551700	6.78197400	6.82194900

H	8.46195500	7.78797500	6.47595800
C	5.88135400	6.95778500	4.49942100
H	6.22868900	7.96772700	4.28567300
C	8.51916200	4.37902100	6.79728500
C	6.87510200	5.47744400	8.19407400
H	6.05860800	5.47040600	8.91492100
C	8.35831400	10.28627700	8.08470300
C	5.32286600	7.56372500	10.92182800
C	4.55122400	5.61899900	5.86279600
H	3.86584900	5.59089900	6.70880300
C	4.36763500	11.14492300	3.24619000
H	3.48218100	11.79327000	3.34311000
H	4.17677700	10.39014600	2.47410300
H	5.22674700	11.77460200	2.98191900
C	3.54722800	10.96974500	11.05333500
H	4.45762200	10.48053300	11.40086200
C	8.88059400	5.65481600	6.33645500
H	9.66264600	5.77762200	5.58540200
C	7.49101600	4.31313400	7.75420400
H	7.15259700	3.35256200	8.14656700
C	6.32570100	5.85247300	3.78697500
H	7.04420300	5.99688200	2.97838400
C	5.86736300	4.56650600	4.12397400
C	0.46870200	7.15096900	7.31314500
H	-0.18648900	7.97006100	6.97530600
H	0.08782900	6.76891700	8.26815000
H	0.46685500	6.36772100	6.54474300
C	9.76711000	10.80827100	8.22187800
H	10.46673900	9.97551000	8.36299100
H	9.80477300	11.46124900	9.10840400
H	10.03748800	11.40765800	7.34322000
C	4.95716900	4.47217600	5.18830400
H	4.57091500	3.50373700	5.51024400
C	5.46587400	6.95952400	12.29650500
H	6.20165700	6.14578700	12.27660300
H	4.49453900	6.60557400	12.66287900
H	5.83426200	7.74361400	12.97753800
C	2.99976000	12.06683200	11.70824200
H	3.49170700	12.45200100	12.60321200
C	1.86078500	11.00690300	9.45436500
H	1.45409800	10.54552800	8.55423100
C	1.26039200	12.10529600	10.05992900
H	0.34925400	12.52029500	9.62535700
C	1.82789600	12.66730600	11.21554300
C	1.23026700	13.87554700	11.88033000
H	1.35592900	13.83206300	12.97182300
H	1.74285700	14.78570900	11.52514900
H	0.16218400	13.97799600	11.64367200
C	9.19236700	3.13296700	6.29405700
H	9.82294400	3.33950200	5.41875000
H	9.82858700	2.70033800	7.08376600
H	8.44582200	2.37051300	6.02391700
C	6.33796400	3.35383600	3.37159900
H	5.89991700	3.34351900	2.35982300
H	7.43199700	3.37095300	3.25229300
H	6.04920000	2.42458500	3.88089900

1d (OMe), *S* = ½ | G = –6622.90538685

Ru	5.51142000	10.80828800	7.49354400
Co	4.40014900	8.41907300	6.45355100
Co	6.39000600	8.27400200	8.43807900
Co	3.84499400	8.99210700	9.04953000
O	6.16615300	9.04673000	6.71701000
O	5.53808500	9.81166600	9.15989300
O	4.68587200	7.61857500	8.10937600
O	2.58029300	7.75052200	6.45838500
O	3.78069700	9.93273600	7.42208000
O	5.29936200	11.27529700	5.43223100
O	4.18353700	9.39976800	4.79217200
O	7.60990400	11.09242900	7.68267000
O	8.13211600	9.09891700	8.64932700
O	6.35492000	7.53535200	10.23347300
O	2.14615400	8.15753300	8.66110900
O	5.36443700	12.47822700	7.78179400
N	5.00600300	6.87247600	5.48215200
O	4.17960200	8.03940900	10.69546400
N	3.00273500	10.46846400	9.98157900
N	7.22848000	6.68130600	7.74748200
C	4.65458100	10.56310400	4.60214000
C	1.84979100	7.73826800	7.49750300
C	8.03959000	6.76974000	6.68298900
H	8.17223000	7.77299400	6.27691600
C	5.74084000	6.99646700	4.35842100
H	5.94410100	8.01554100	4.03362700
C	8.37925700	4.38938900	6.65305600
C	6.99344100	5.47176300	8.29526900
H	6.32468200	5.46202200	9.15450200
C	8.40240800	10.26702600	8.23522000
C	5.32085000	7.55387700	10.97217800
C	4.72030500	5.64677900	5.94518700
H	4.14170700	5.61886300	6.86905800
C	4.40605800	11.18242300	3.24405700
H	3.50932000	11.81915700	3.31387200
H	4.22684000	10.40451200	2.49119300
H	5.25346000	11.81847600	2.95616100
C	3.55684300	10.98306100	11.08991800
H	4.45723800	10.48107400	11.44556300
C	8.63866200	5.65669900	6.10231300
H	9.26471000	5.79235900	5.22194400
C	7.55520100	4.31133300	7.79194100
H	7.33827400	3.34234300	8.24152100
C	6.22125900	5.89860500	3.66626400
H	6.82713900	6.02304400	2.76873900
C	5.95316700	4.60799000	4.16092400
C	0.44831800	7.19569600	7.32057100
H	-0.20115000	8.02064900	6.98532700
H	0.06021300	6.81181500	8.27250100
H	0.43682300	6.41464300	6.54929600
C	9.82407400	10.74263600	8.44489200
H	10.52114300	9.89658200	8.38359600
H	9.89781400	11.17805900	9.45459200
H	10.08308300	11.51715500	7.71197600
C	5.16693100	4.48682900	5.32009800
H	4.92167800	3.52170900	5.76004400
C	5.47512400	6.95803700	12.35435400

H	6.25823400	6.18917000	12.35646800
H	4.51943900	6.54531000	12.70244700
H	5.77598000	7.76272200	13.04485000
C	3.03243100	12.09184400	11.74658600
H	3.52952200	12.46190600	12.64199500
C	1.90114700	11.05107600	9.46648600
H	1.51057400	10.59864400	8.55490800
C	1.30884800	12.15696200	10.05105000
H	0.41860500	12.61340700	9.61792500
C	1.87737900	12.70037200	11.22052900
O	6.49714400	3.57813500	3.49181100
O	8.84038900	3.22908900	6.15798500
O	1.26809100	13.77218700	11.74681800
C	6.28145500	2.24843300	3.97282800
H	5.20851300	1.99965000	3.97136800
H	6.81328400	1.59099900	3.27582800
H	6.69858800	2.13087300	4.98542300
C	1.80888300	14.36973100	12.92619100
H	1.15286100	15.21593300	13.15980000
H	1.80598900	13.65631200	13.76601200
H	2.83371300	14.73364100	12.74894100
C	9.64596900	3.25188400	4.97593600
H	9.89548100	2.20548200	4.76693900
H	9.08025800	3.67440900	4.13051300
H	10.57039400	3.82728900	5.14121200

1d^{+} (OMe), *S* = 0 | G = –6622.71205221

Ru	5.49453400	10.83562700	7.46618200
Co	4.41969800	8.42881800	6.44504600
Co	6.40369800	8.26070200	8.42905800
Co	3.84013800	9.00553900	9.02271000
O	6.18028900	9.07471400	6.73263400
O	5.53432900	9.81063400	9.07312600
O	4.69078100	7.63136200	8.09345700
O	2.61597200	7.77017500	6.44135500
O	3.78378600	9.99804900	7.40458800
O	5.29192900	11.22614100	5.49130900
O	4.18224800	9.39308300	4.77981100
O	7.59158400	11.05914100	7.53004800
O	8.12857500	9.12140500	8.60912900
O	6.35144100	7.55435000	10.21602300
O	2.16425400	8.17565500	8.64013000
O	5.49435300	12.41039600	7.97973000
N	5.02330800	6.89213800	5.49810600
O	4.16941800	8.05750900	10.64639200
N	2.99922100	10.47097600	9.97064000
N	7.23112700	6.67104800	7.75533200
C	4.62707600	10.55740900	4.61700000
C	1.87520500	7.74901900	7.47521900
C	8.06794500	6.74820000	6.70825000
H	8.22941900	7.74616500	6.30019600
C	5.78719100	7.01655700	4.39147000
H	6.02009000	8.03190000	4.07628600
C	8.37775500	4.36352000	6.69346500
C	6.96782100	5.46527200	8.30328800
H	6.27998600	5.46210600	9.14680900
C	8.39603000	10.25564100	8.12036300
C	5.30623800	7.56509200	10.94065400

C	4.70319700	5.66768900	5.94694500
H	4.09708600	5.63771000	6.85210300
C	4.38537900	11.25853600	3.30988800
H	3.52640500	11.93592900	3.44033500
H	4.15034400	10.52548000	2.52920500
H	5.25943300	11.86331300	3.03603800
C	3.56511500	10.98434000	11.07560500
H	4.47649600	10.49447500	11.42010000
C	8.66636300	5.62747000	6.14605500
H	9.31584100	5.75402800	5.28164500
C	7.52669500	4.29913300	7.81483600
H	7.28846800	3.33473500	8.26297300
C	6.26549200	5.91649500	3.70535900
H	6.89438900	6.03891100	2.82386700
C	5.96705000	4.62532600	4.18510900
C	0.48544400	7.19219400	7.29176100
H	-0.16525900	8.00737700	6.93634900
H	0.09274400	6.81995900	8.24579500
H	0.49299200	6.40075000	6.53171700
C	9.81567300	10.75026200	8.25126100
H	10.50363300	9.90127000	8.34653800
H	9.88050700	11.36499200	9.16325800
H	10.08081300	11.37992200	7.39257500
C	5.14788300	4.50858000	5.32348000
H	4.87299300	3.54470500	5.74802700
C	5.43433500	6.96034100	12.31672000
H	6.20715300	6.18174900	12.31992300
H	4.46833100	6.56027800	12.64896800
H	5.73921700	7.75803100	13.01322600
C	3.03539100	12.07867300	11.74840700
H	3.54171300	12.44815300	12.63866700
C	1.87619000	11.03771900	9.48055500
H	1.46702400	10.58455800	8.57762000
C	1.27902900	12.12882500	10.08395300
H	0.37219600	12.57139000	9.67181800
C	1.86063900	12.67407600	11.24765400
O	6.51343600	3.59665000	3.52770200
O	8.83143900	3.20031300	6.21234000
O	1.24680100	13.72872500	11.78983600
C	6.26675400	2.26161000	3.98726000
H	5.19115500	2.02997800	3.95182000
H	6.80972500	1.60738000	3.29657000
H	6.65512600	2.12910200	5.00903600
C	1.79143200	14.32891200	12.96952600
H	1.12223200	15.16083700	13.21484800
H	1.80916500	13.60812800	13.80211800
H	2.80672200	14.71176100	12.78042000
C	9.67244300	3.20322700	5.05190000
H	9.90540900	2.15127800	4.85411600
H	9.13843700	3.63487400	4.19101200
H	10.60199200	3.76056500	5.24483300

NBO6 analysis

The role of the $[Co_3O_4]$ subcluster in the stabilization of the oxidized RuO dopant moiety was also investigated in the DFT calculations. Natural bond orbital (NBO) analysis was carried out in the neutral $[Ru^{V}O]$ (**1a**) and oxidized $[Ru^{VI}O]^{+}$ (**1a**$^{+}$) forms, including the calculations of the stabilization energy (SE) from second-order perturbation analysis, which quantifies the strength of the donor-acceptor

interactions. The strongest interactions involved π-electron donation from the *p* orbitals of the bridging-oxos to the *d* orbitals of ruthenium. These interactions were divided in two groups, *cis*-π and *trans*-π, depending on the orientation of the donor μ-O(*p*) orbitals relative to the Ru–O bond axis. The calculation of the natural localized molecular orbitals (NLMOs) yielded two *cis*-π interactions, one for each *cis*-μ-O ligand (shown for **1a**$^+$ in Figure SCD3). Both interactions were strong, as shown by their large SE values; *e.g.* 88.0 and 100.3 kcal mol^{-1} in **1a**$^+$ (Table S8). Two *trans* interactions were also found, each one corresponding to a different *p* orbital of the *trans*-μ-O ligand. These interactions were weaker than the *cis*, yet significant (SE = 28.5 and 74.7 kcal mol^{-1} in **1a**$^+$) and, interestingly, they had relevant contributions from Co *d* orbitals. These *cis* and *trans* interactions were observed both in **1a** and **1a**$^+$, though they were clearly stronger in the latter, with an overall increase of the SEs of 68.0 kcal mol^{-1}. In summary, NBO analysis showed that, despite the spin densities suggesting a redox-innocent character of the [Co_3O_4] subcluster, it stabilizes the Ru^{V}O dopant moiety of **1a** by strong $\pi(p\rightarrow d)$ donation, facilitating the further oxidation of the system to **1a**$^+$.

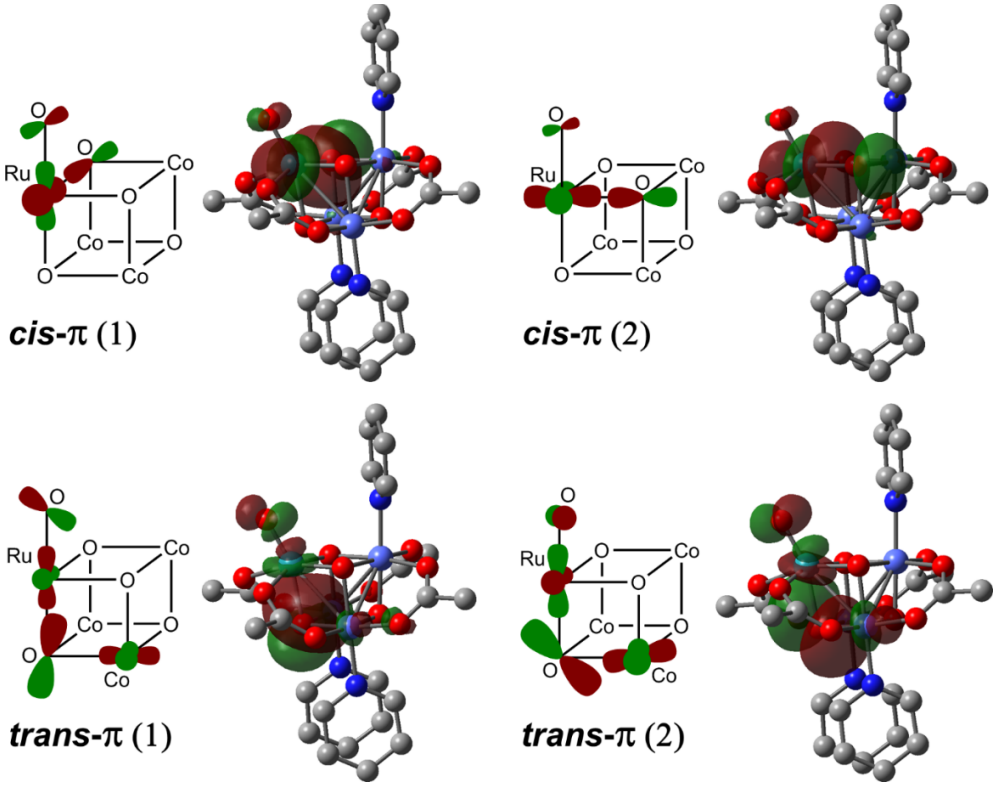

Figure SCD3. Selected NLMOs (natural localized molecular orbitals) associated with the covalent interactions between the [Co_3O_4] (donor) and RuO (acceptor) moieties. Orbitals were plotted for **1a**$^+$, with a surface isovalue of 0.02.

Table SCD1. Stabilization energies (SE, in kcal mol^{-1}) from NBO second-order perturbation analysis of the $\pi(p\rightarrow d)$ donor-acceptor interactions, with donation in either *cis* (*cis*-π) or *trans* (*trans*-π) to the Ru–O bond.

	cis-π (1)	*cis*-π (2)	*trans*-π (1)	*trans*-π (2)
1a	71.8	72.0	76.4	3.3
1a$^+$	100.3	88.0	74.7	28.5

Supplementary Figures

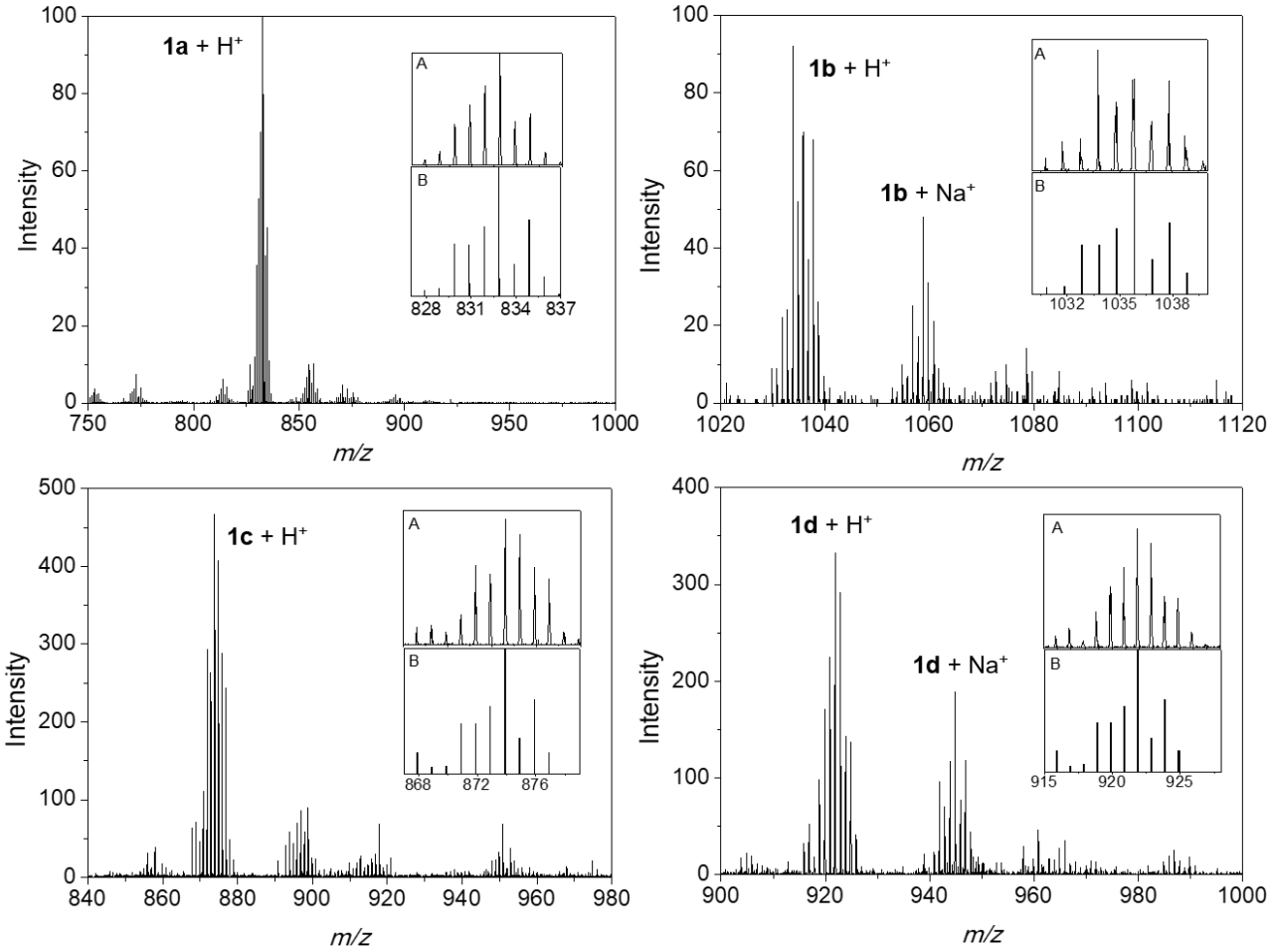

Figure S1. HR-ESI-MS spectra of **1a**–**d** dissolved in acetonitrile (inset: A is the enlarged spectrum of $[Ru(O)Co_3(\mu_3\text{-}O)_4(OAc)_4(4\text{-}R\text{-}py)_3]\cdot H^+$, and B is the simulated spectrum).

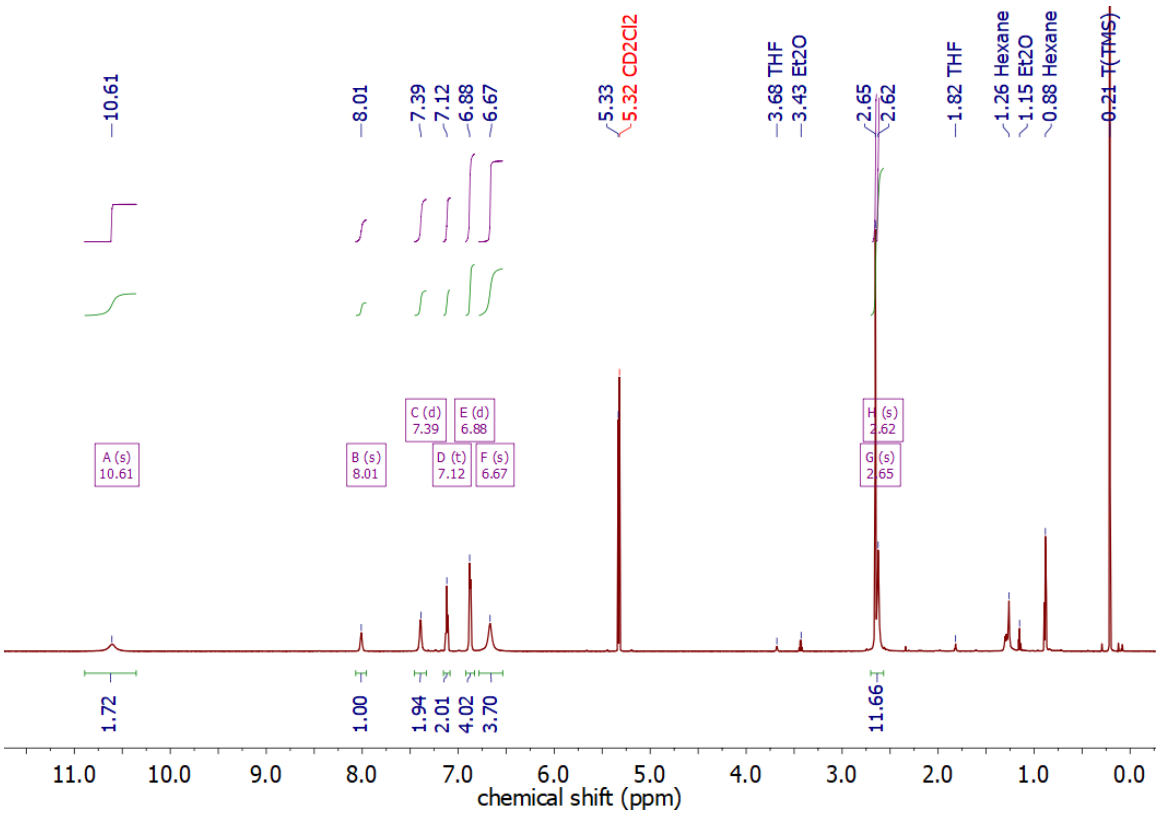

Figure S2. ^{1}H NMR spectrum of compound **1a** in CD_2Cl_2.

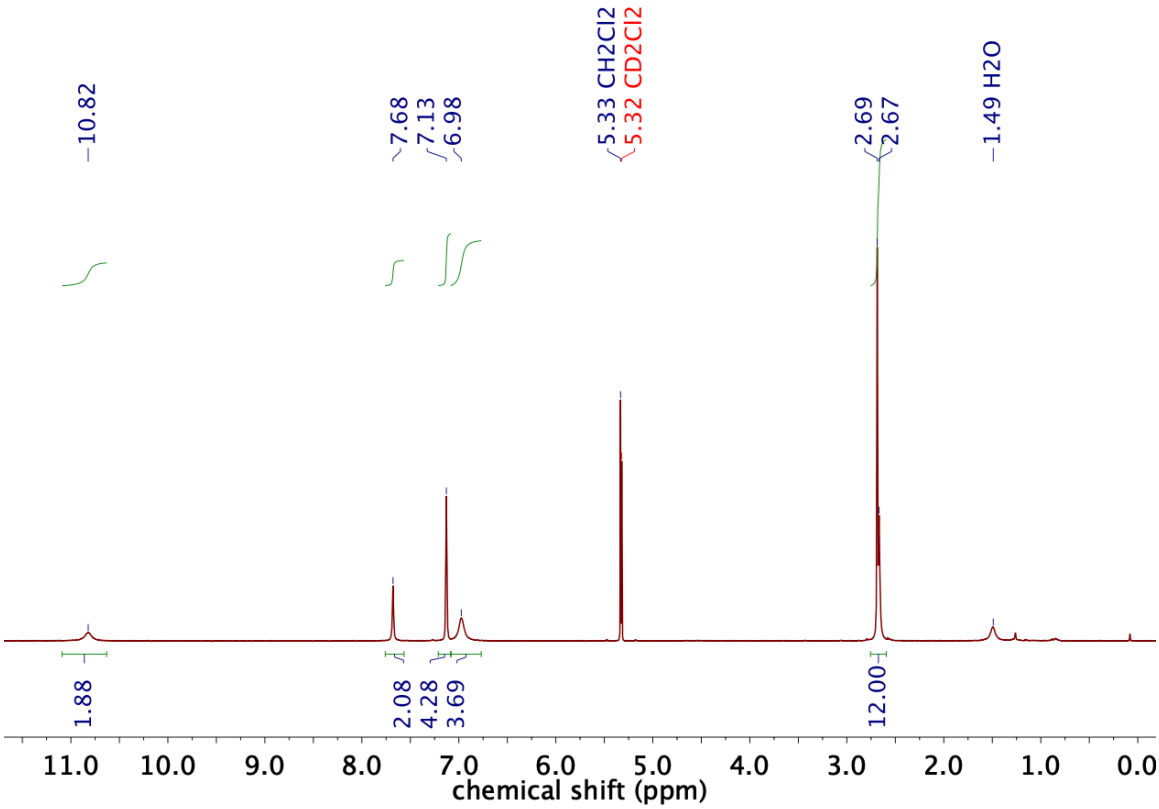

Figure S3. ^{1}H NMR spectrum of compound **1b** in CD_2Cl_2.

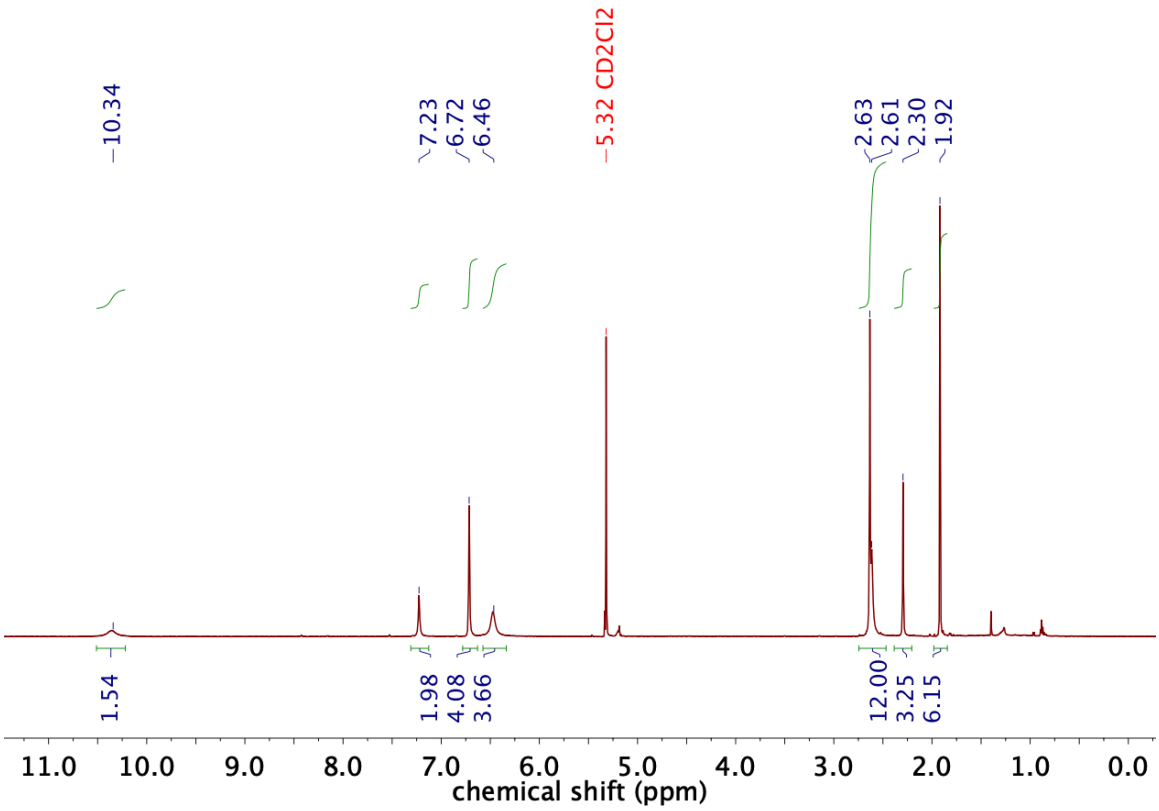

Figure S4. ^{1}H NMR spectrum of compound **1c** in CD_2Cl_2.

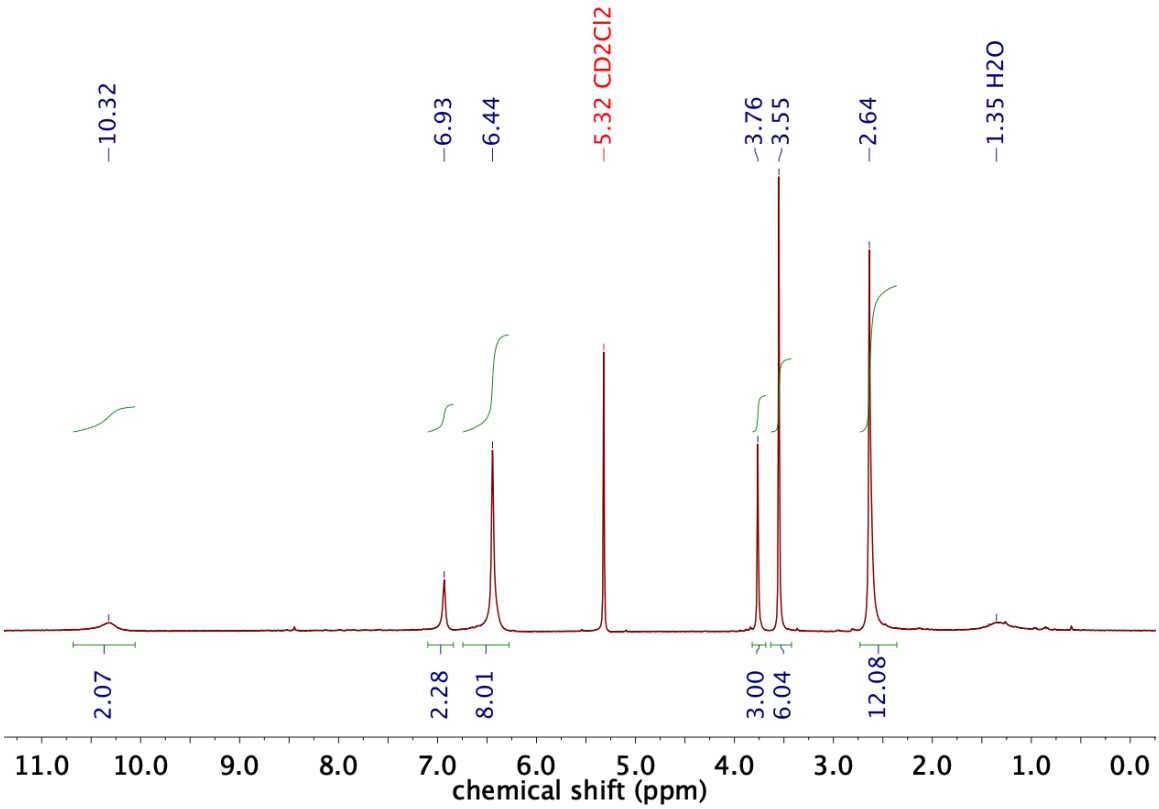

Figure S5. ^{1}H NMR spectrum of compound **1d** in CD_2Cl_2.

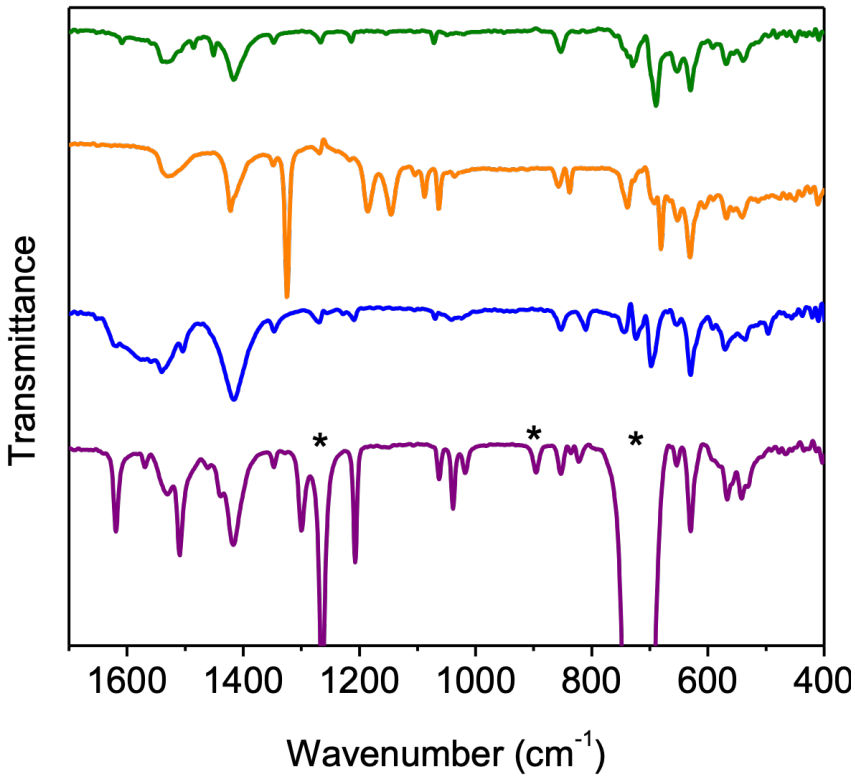

Figure S6. Solution-state IR spectra of **1a**–**d** in dichloromethane. The asterisks (*) indicate vibrational wavenumbers associated with dichloromethane.

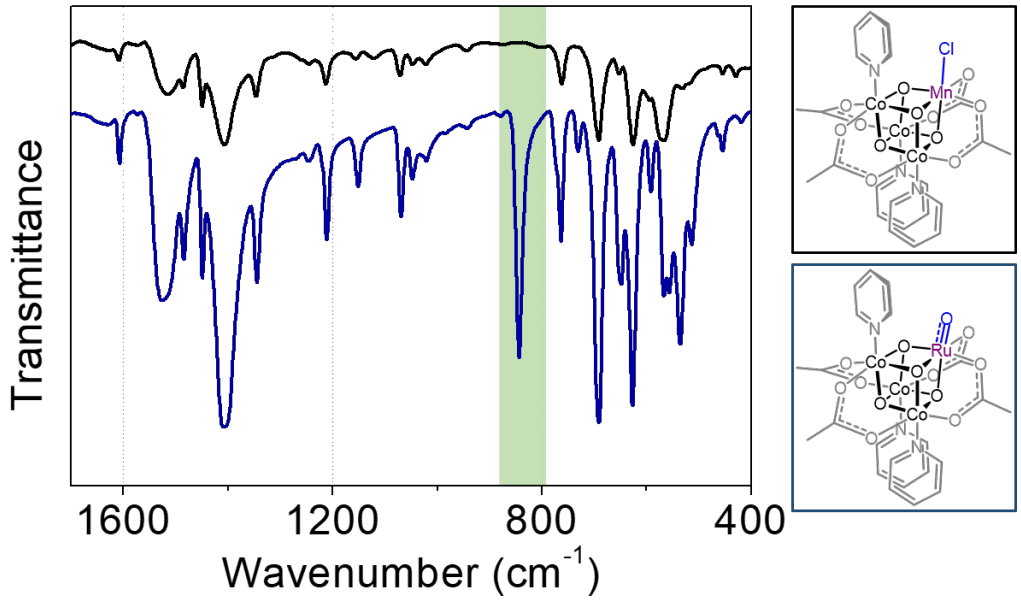

Figure S7. Solid-state IR spectra of compound $Mn(Cl)Co_3(\mu_3\text{-}O)_4(OAc)_4(py)_3$ cubane (black) *vs.* **1a** (blue). There is a notable absence of the 853 cm^{-1} band (ν_{Ru-O}) in the spectrum of the $[MnCo_3O_4]$ cubane (highlighted in green).

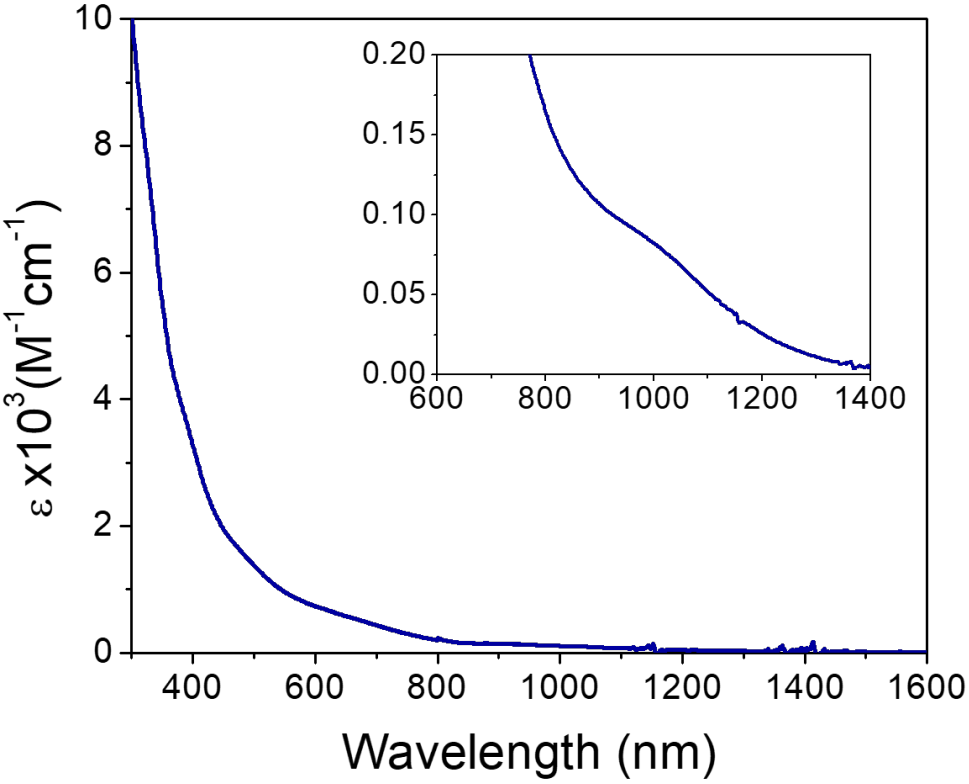

Figure S8. UV-vis-NIR spectrum of **1a** in dichloromethane at room temperature (inset: the enlarged curve for absorption at ~1000 nm). There are five broad absorption bands at around 330 (ε = ~7500 M^{-1} cm^{-1}), 400 (ε = ~3300 M^{-1} cm^{-1}), 480 (ε = ~1600 M^{-1} cm^{-1}), 650 (ε = ~400 M^{-1} cm^{-1}) and 1000 (ε = ~80 M^{-1} cm^{-1}) nm. Bands analogous to the 330 and 650 nm absorptions are observed for $Co_4(\mu_3\text{-}O)_4(OAc)_4L_4$ cubane complexes at similar ε values.[27] The highest energy absorption is assigned to a charge-transfer transition between Co and μ_3-O ligands, while the band at ~650 nm is attributed to a ligand field $^1A_1 \longrightarrow {}^1T_1$ or $^1A_1 \longrightarrow {}^1T_2$ transition for the Co^{III} centers.[27] Bands at 400 and 480 nm may be associated with charge-transfer transitions between dπ(Ru) and pπ(μ_3-O) orbitals. Additionally, a very weak absorption at ~1000 nm is tentatively assigned to a CT transition within the cluster. The assignment of this CT band is discussed in the computational section.

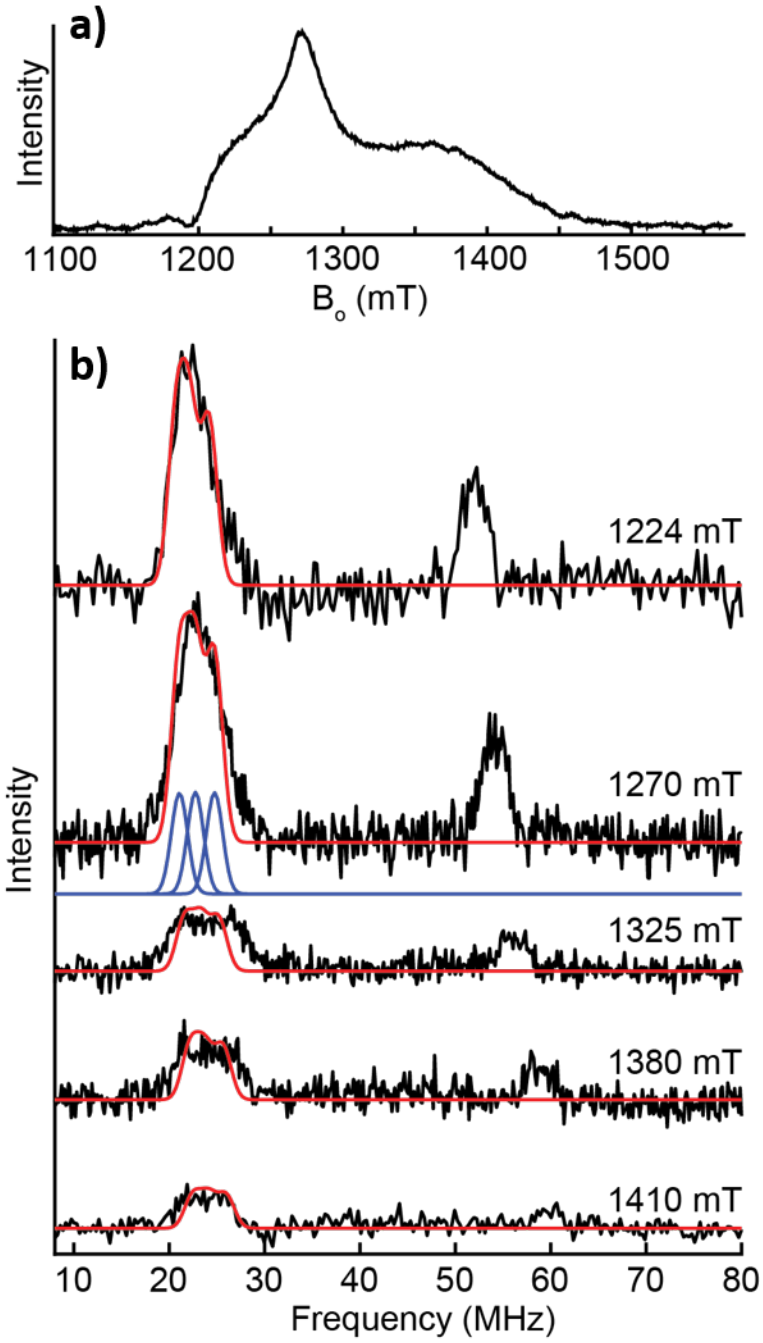

Figure S9. a) Q-Band (34.1 GHz) two-pulse electron spin echo field swept (2PFS) spectrum of **1a**. **b**) Field dependent Q-band Davies ENDOR of **1a** collected at the following field positions: 1224, 1270, 1325, 1380, and 1410 mT. The data in black is simulated in red using three isotropic hyperfine values of 17, 20, and 24 MHz. These hyperfine couplings are similar to those observed in the $MnCo_3(\mu_3\text{-}O)_4(OAc)_5(py)_3$ cubane previously described.[28] The additional feature that moves to higher frequency with increasing field (at 54 MHz at 1270 mT) is assigned to weak contributions from nearby protons. All ENDOR spectra have been normalized to the number of scans, the variation of intensity at each field position is reflected by the overall echo intensity, seen in the top panel.

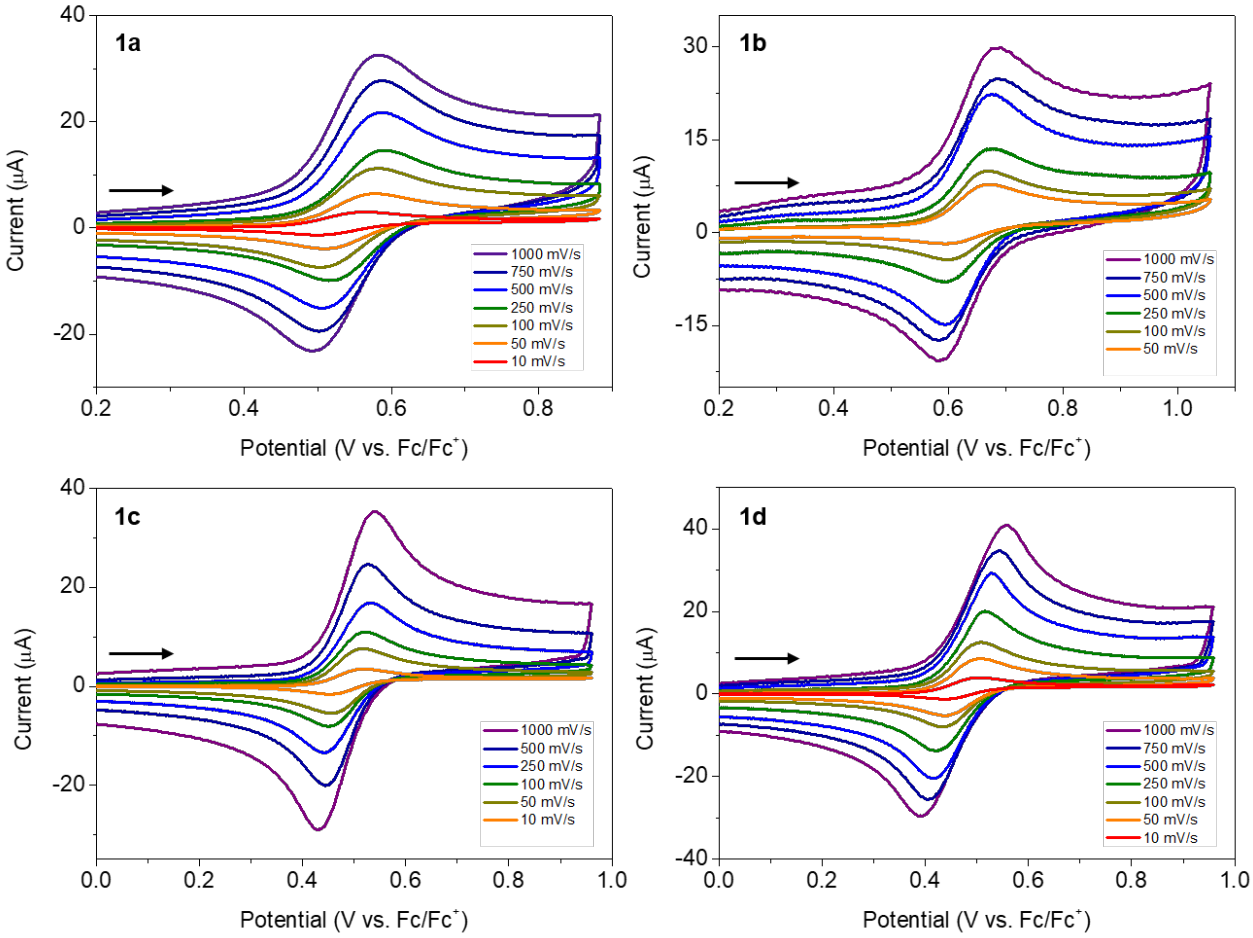

Figure S10. Cyclic voltammograms recorded at multiple scan rates of **1a**–**d** (1.0 mM) in *ortho*-difluorobenzene with $[^{n}Bu_4N][PF_6]$ (0.1 M) as a supporting electrolyte. The arrows indicate the scanning direction.

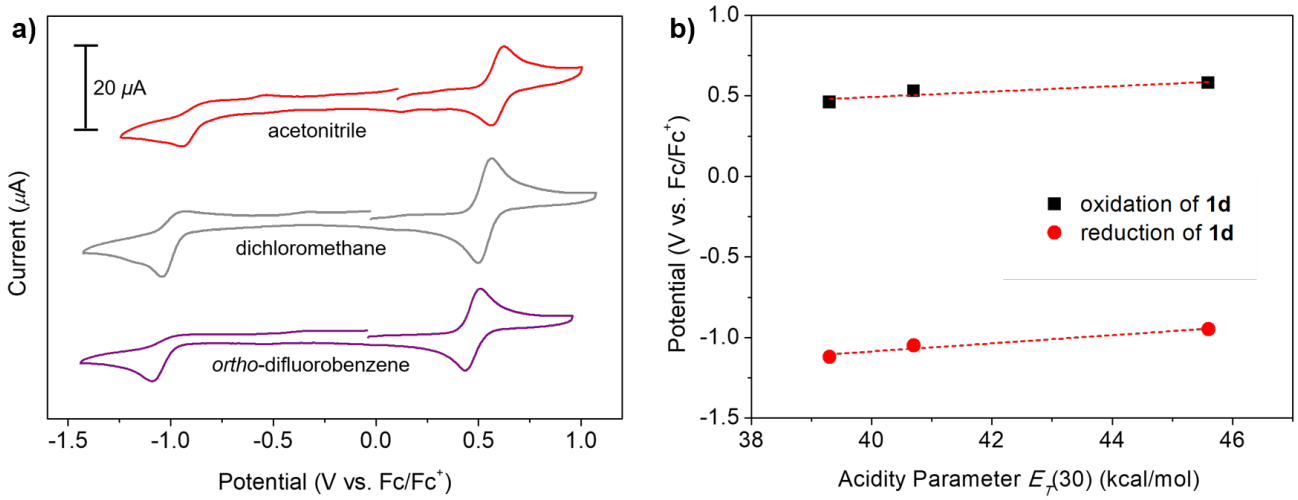

Figure S11. a) Cyclic voltammograms of **1d** in *ortho*-difluorobenzene (purple), dichloromethane (grey), and acetonitrile (red) (v = 100 mV/s, 0.1 M [^{n}Bu$_4$N]PF$_6$ electrolyte). Oxidation potentials are 0.46, 0.53, and 0.58 V vs. Fc/Fc$^+$ and reduction potentials are –1.12, –1.05, and –0.95 V vs. Fc/Fc$^+$ for *ortho*-difluorobenzene, dichloromethane, and acetonitrile, respectively. **b)** Plot of redox potentials of **1d** vs. Dimroth-Reichardt parameter E_T(30) (kcal/mol) of solvents[29] with linear regression (R^2 = 0.8438 for oxidation and R^2 = 0.9570 for reduction). Among the reported empirical solvent parameters,[30,31] the acidity (electrophilicity) parameter E_T(30) is the only one that shows a linear relationship with the redox potentials: more electrophilic solvents shift the potentials more positively. This correlation suggests an increase stabilization of the reduced cubane with increasing electrophilicity of the solvent, but an opposite effect for the oxidation. Note that the empirical parameters of fluorobenzene were used for linear regression analyses when there are no reports for *ortho*-difluorobenzene.

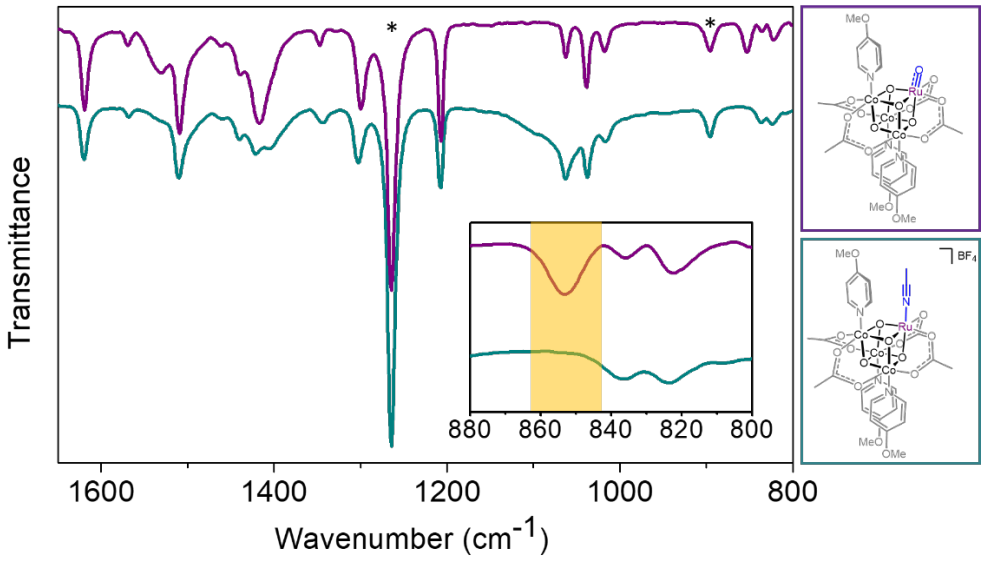

Figure S12. Solution-sate IR spectra of compound **1d** (purple) *vs.* **2-MeCN** (green) in dichloromethane. The inset indicates the absence of the 853 cm^{-1} band (ν_{Ru-O}) in the spectrum of **2-MeCN** (highlighted in yellow). The asterisks (*) indicate vibrational wavenumbers associated with dichloromethane.

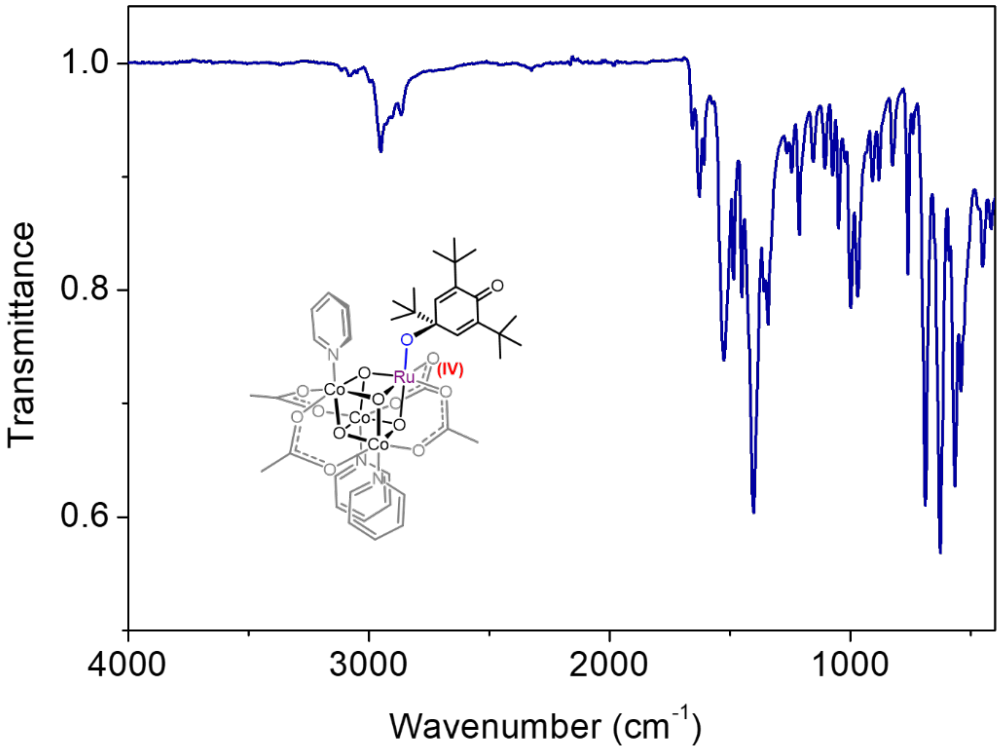

Figure S13. Solid-state IR spectrum of compound **3**.

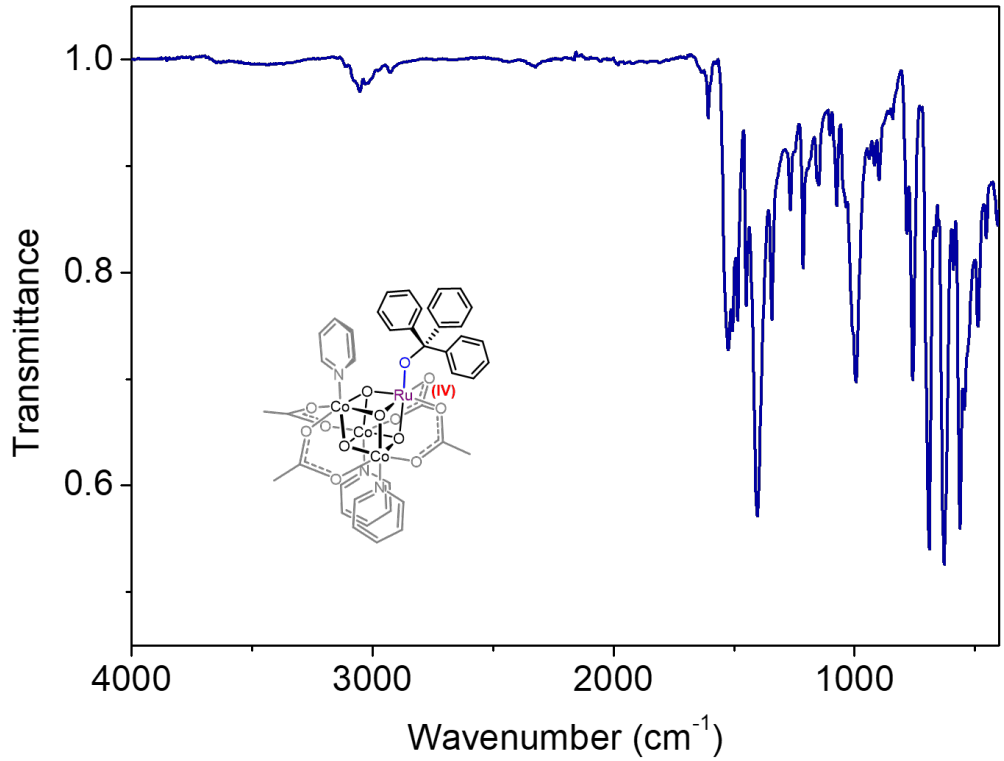

Figure S14. Solid-state IR spectrum of compound **4**.

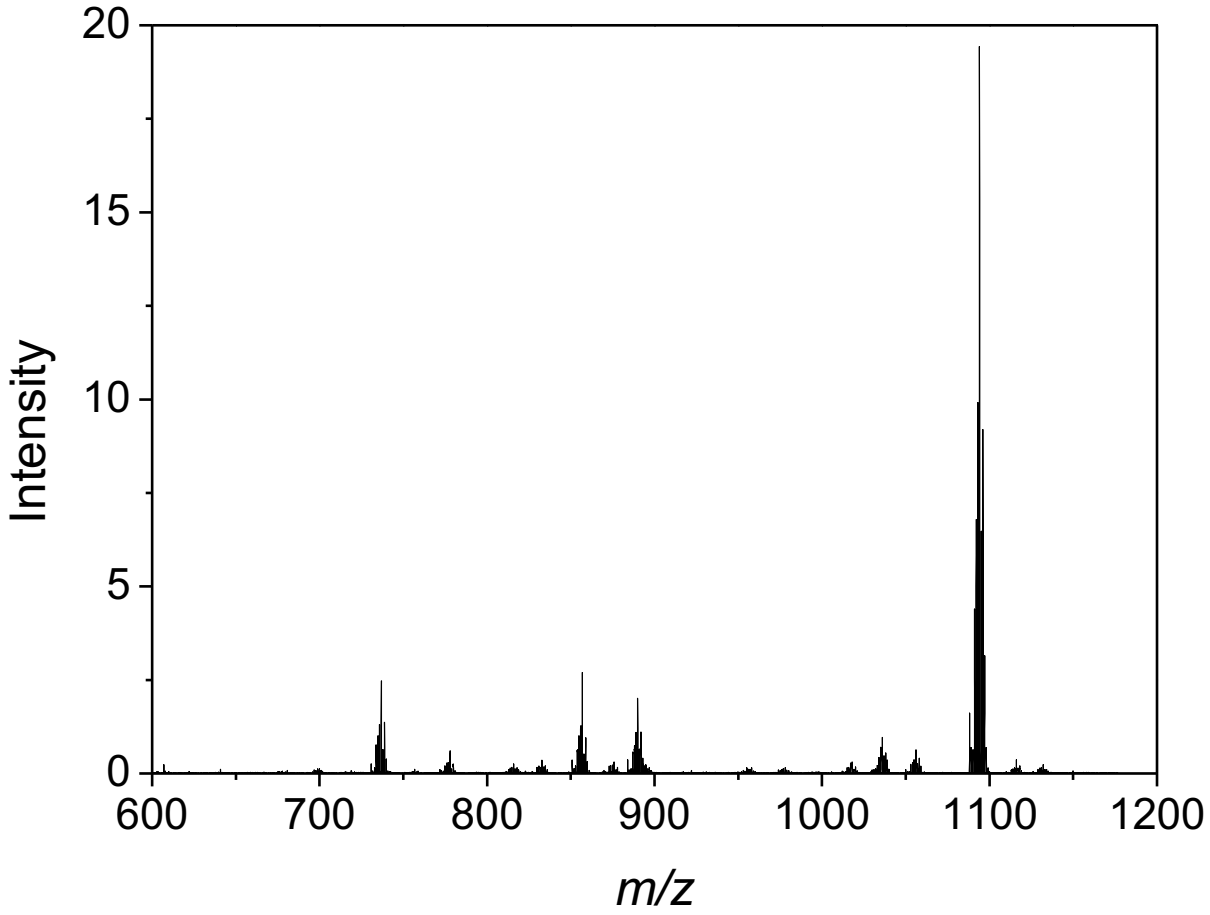

Figure S15. ESI Spectrum of the reaction mixture between **1a** and 2,4,6-tri-*tert*-butylphenol. An aliquot was taken from the reaction mixture and diluted with acetonitrile for ESI measurement.

Table S1. Major products from the reaction of compound **1a** and 2,4,6-tri-*tert*-butylphenol identified by HR-ESI-MS in acetonitrile

Found *m/z*	Theoretical *m/z*	Assignment
1094.0961	1094.0879	$[Ru(OC_{18}H_{29}O)Co_3(\mu_3\text{-}O)_4(OAc)_4(py)_3]\cdot H^+$, compound **3**
895.9534	895.9134	$[Ru(py)Co_3(\mu_3\text{-}O)_4(OAc)_4(py)_3]\cdot H^+$
857.8990	857.8978	$[Ru(MeCN)Co_3(\mu_3\text{-}O)_4(OAc)_4(py)_3]\cdot H^+$
736.8242	737.8290	$[RuCo_3(\mu_3\text{-}O)_4(OAc)_4(py)_2]\cdot H^+$

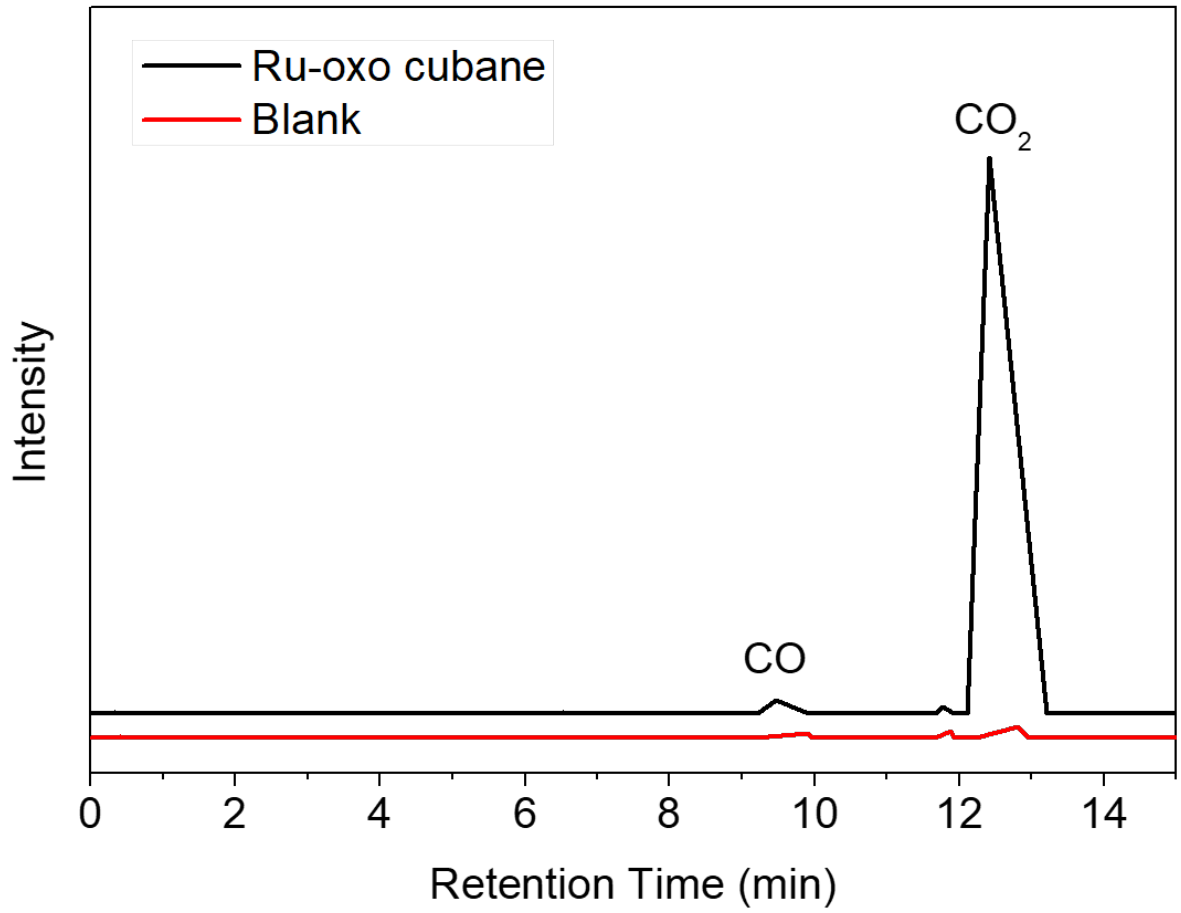

Figure S16. GC traces (FID channel) show an exclusive formation of CO_2 from the reaction of **1a** with degassed water after 1 h (black). The blank sample (red) contained only degassed water. The measurements were made under an inert atmosphere of argon.

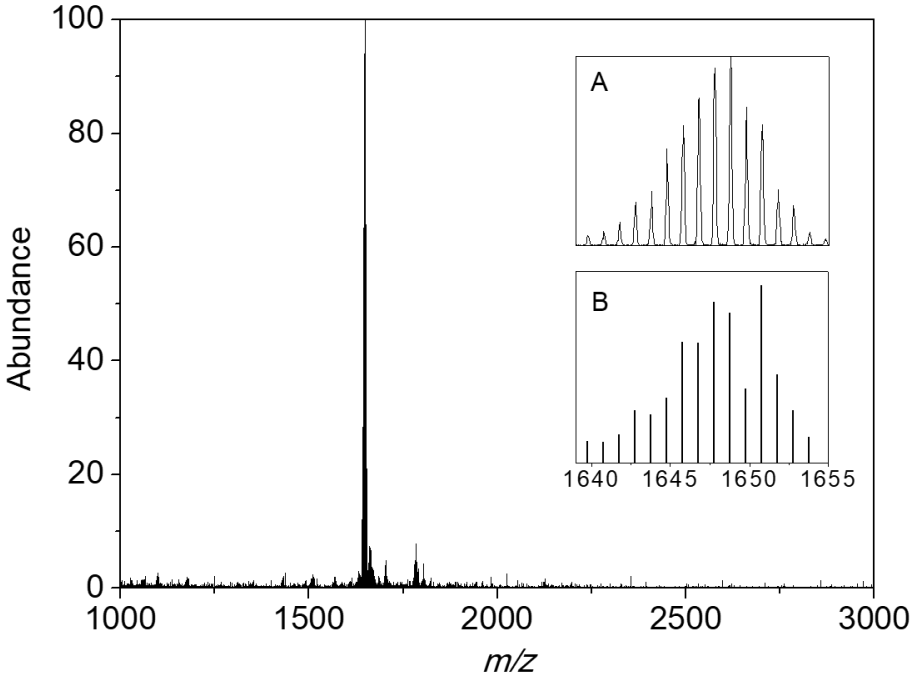

Figure S17. ESI spectrum of compound **5** in acetonitrile (inset: A is the enlarged spectrum of $[(py)_3(OAc)_4Co_3(\mu_3\text{-}O)_4Ru]\text{–}O\text{–}[RuCo_3(\mu_3\text{-}O)_4(OAc)_4(py)_3]\cdot H^+$ ion and B is the simulated spectrum).

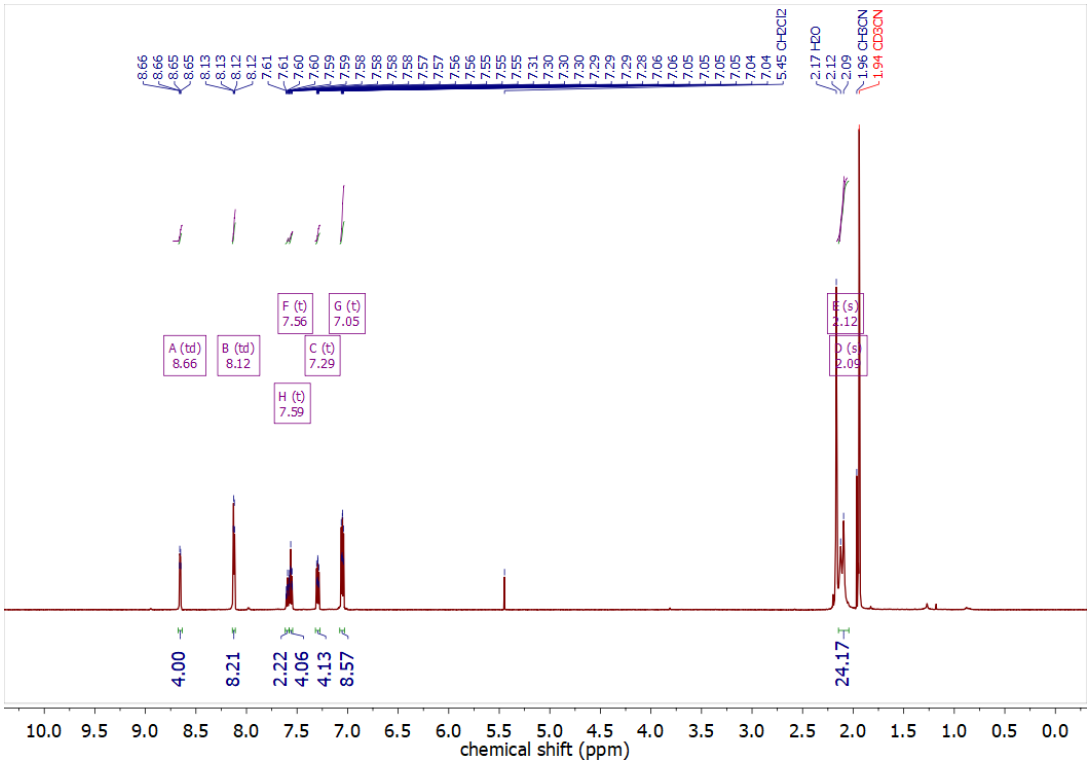

Figure S18. ^{1}H NMR spectrum of compound **5** in CD_3CN.

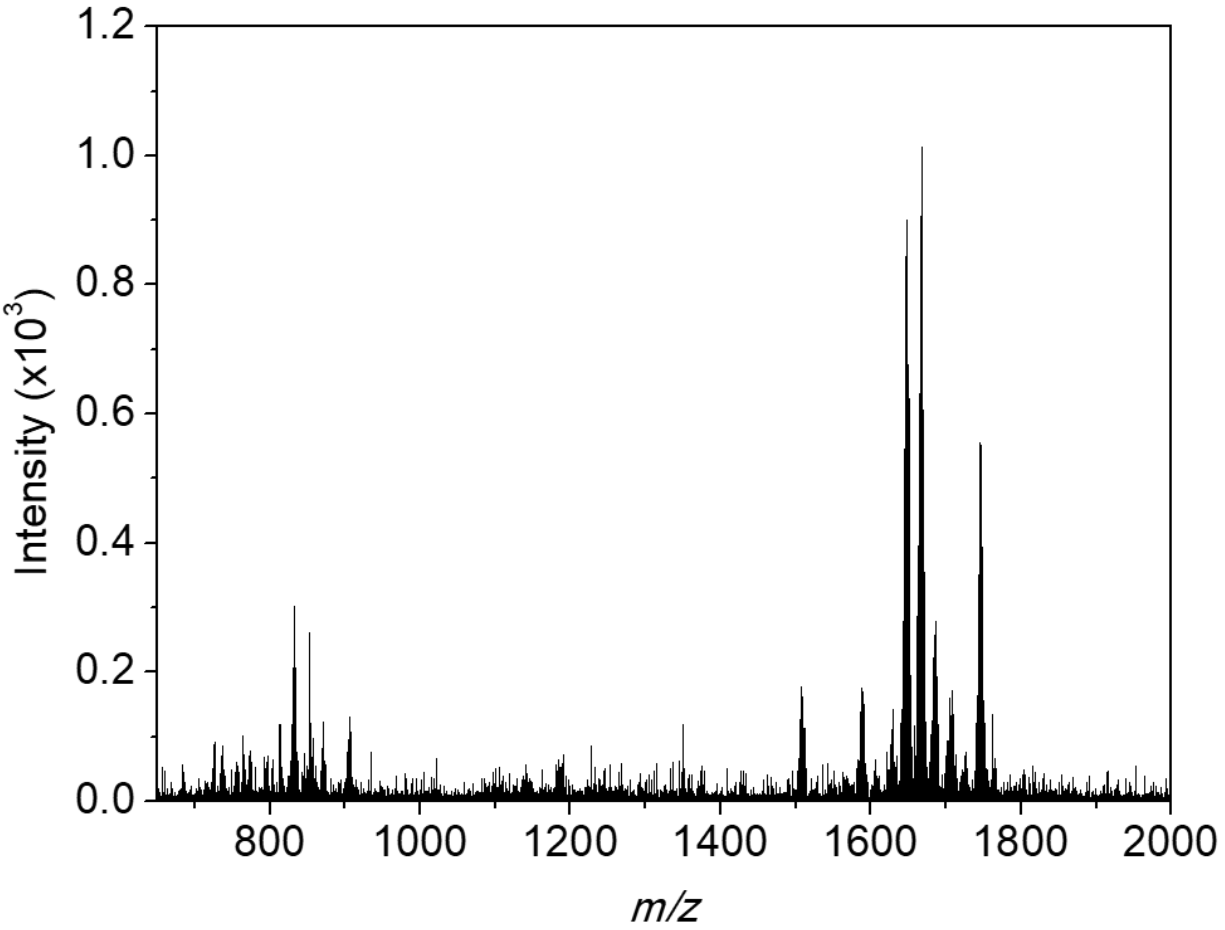

Figure S19. ESI spectrum of reaction mixture between compound **1a** and water. After 1 h of stirring, the volatile materials were removed, and the residue was dissolved in acetonitrile for ESI measurement.

Table S2. Major products from reaction of compound **1a** and water identified by HR-ESI-MS in acetonitrile

Found *m/z*	Theoretical *m/z*	Assignment
1746.7911	1746.7901	$[RuCo_3(\mu_3\text{-}O)_4(OAc)_4(py)_3 + Ru(py)Co_3(\mu_3\text{-}O)_4(OAc)_4(py)_3 + (H_2O)_2]^+$
1667.7493	1667.7479	$[[RuCo_3(\mu_3\text{-}O)_4(OAc)_4(py)_3]_2 + (H_2O)_2]^+$
1648.7354	1648.7295	$[(py)_3(OAc)_4Co_3(\mu_3\text{-}O)_4Ru]\text{–}O\text{–}[RuCo_3(\mu_3\text{-}O)_4(OAc)_4(py)_3]\cdot H^+$, compound **5**
852.9490	852.94229	$[Co_4(\mu_3\text{-}O)_4(OAc)_4(py)_4]\cdot H^+$
832.8531	832.86615	$[Ru(O)Co_3(\mu_3\text{-}O)_4(OAc)_4(py)_3]\cdot H^+$, compound **1a**

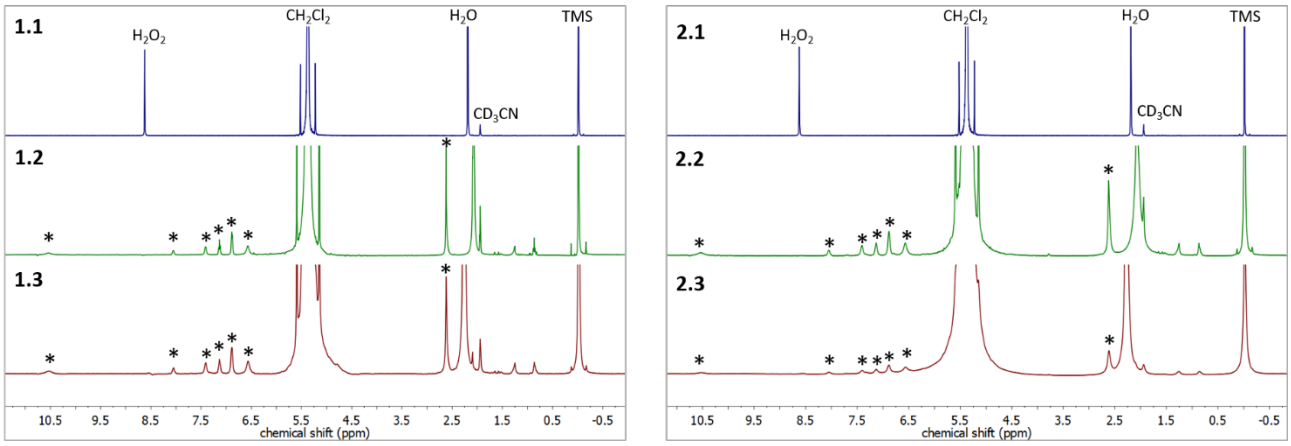

Figure S20. ^{1}H NMR spectra acquired at ambient temperature monitoring the reaction between **1a** and water (**1.1**–**1.3**) and the reaction between **1a** and H_2O_2 (**2.1**–**2.3**). All normalized to an internal standard, tetramethylsilane (TMS). Spectra **1.1** and **2.1** serve as a reference for expected chemical shifts. The asterisks (*) indicate resonances of compound **1a**.

Table S3. Observations of the reaction between **1a** and water

Spectrum	Stoichiometry and content	Details
1.1	H_2O_2 solution in H_2O (5 μL, 90 μmol H_2O_2) + CH_2Cl_2 (0.3 mL) + CD_3CN (0.2 mL) + TMS (5 μL)	H_2O_2 resonance observed at 8.62 ppm
1.2	**1a** (6 mg, 7.2 μmol) + H_2O (3.2 μL) + CH_2Cl_2 (0.3 mL) + CD_3CN (0.2 mL) + TMS (5 μL)	No H_2O_2 observed and decomposition of **1a** (≤ 5%)
1.3	**1a** (6 mg, 7.2 μmol) + H_2O (8.2 μL) + CH_2Cl_2 (0.3 mL) + CD_3CN (0.2 mL) + TMS (5 μL)	No H_2O_2 observed and decomposition of **1a** (≤ 5%)

Table S4. Observations of the reaction between **1a** and H_2O_2

Spectrum	Stoichiometry and content	Details
2.1	H_2O_2 solution in H_2O (5 μL, 90 μmol H_2O_2) + CH_2Cl_2 (0.3 mL) + CD_3CN (0.2 mL) + TMS (5 μL)	H_2O_2 resonance observed at 8.62 ppm
2.2	**1a** (6 mg, 7.2 μmol) + H_2O_2 solution in H_2O (3.2 μL, 57.6 μmol H_2O_2) + CH_2Cl_2 (0.3 mL) + CD_3CN (0.2 mL) + TMS (5 μL)	Rapid consumption of H_2O_2 and decomposition of **1a** (≤ 20%)
2.3	**1a** (6 mg, 7.2 μmol) + H_2O_2 solution in H_2O (8.2 μL, 148 μmol H_2O_2) + CH_2Cl_2 (0.3 mL) + CD_3CN (0.2 mL) + TMS (5 μL)	H_2O_2 was rapidly consumed along with rapid gas evolution and decomposition of **1a** (peak broadening impeded quantification)

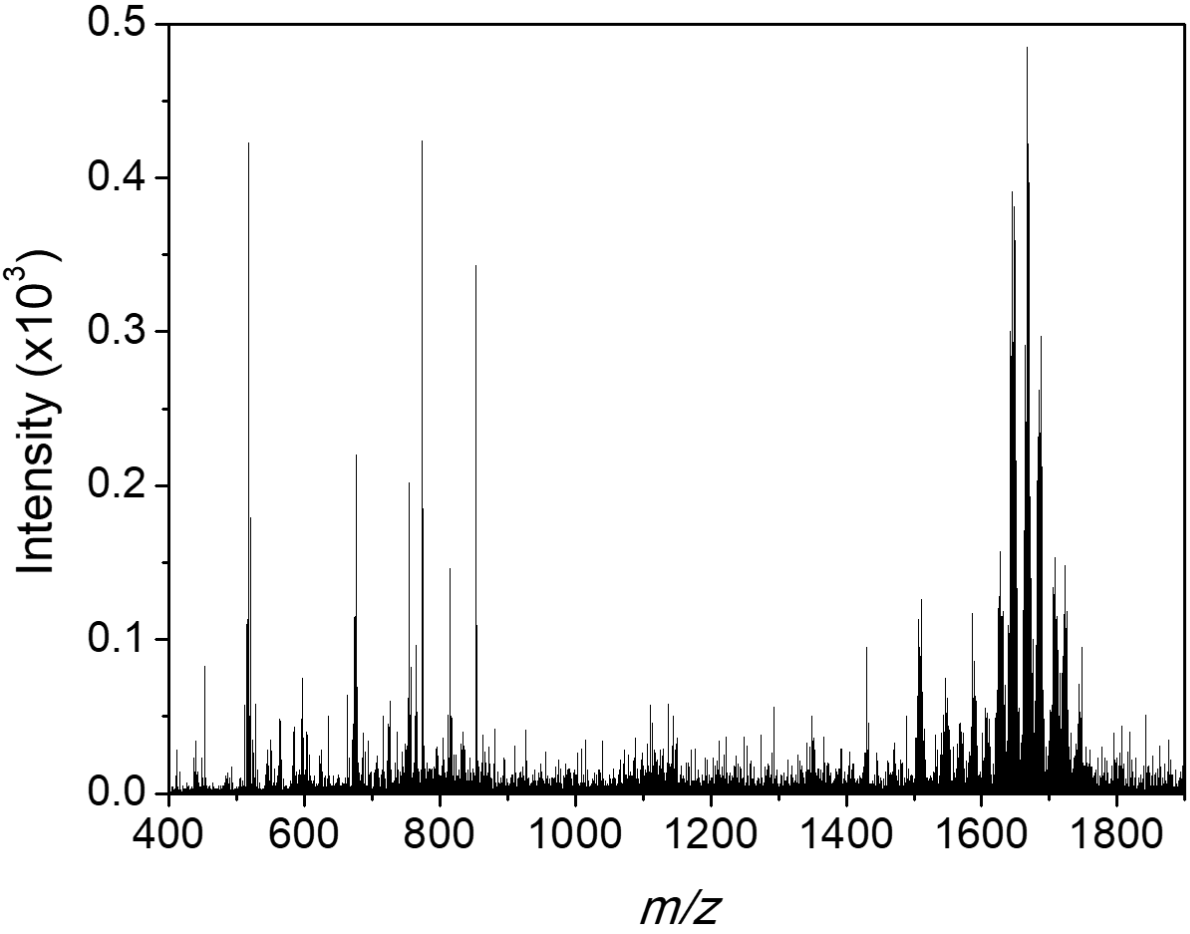

Figure S21. ESI spectrum of the reaction mixture of **1a** and H_2O_2 in acetonitrile. An aliquot was taken from the reaction mixture described in **Table S4** (spectrum **2.3**) and diluted with acetonitrile for ESI measurement.

Table S5. Major products from reaction of **1a** and H_2O_2 identified by HR-ESI-MS in acetonitrile.

Found *m/z*	Theoretical *m/z*	Assignment
1685.7860	1685.7585	$[[RuCo_3(\mu_3\text{-}O)_4(OAc)_4(py)_3]_2 + (H_2O)_3]^+$
1667.7622	1667.7479	$[[RuCo_3(\mu_3\text{-}O)_4(OAc)_4(py)_3]_2 + (H_2O)_2]^+$
1648.6907	1648.7295	$[(py)_3(OAc)_4Co_3(\mu_3\text{-}O)_4Ru]\text{–}O\text{–}[RuCo_3(\mu_3\text{-}O)_4(OAc)_4(py)_3]\cdot H^+$, compound **5**
852.9465	852.9423	$[Co_4(\mu_3\text{-}O)_4(OAc)_4(py)_4]\cdot H^+$
733.9048	773.9001	$[Co_4(\mu_3\text{-}O)_4(OAc)_4(py)_3]\cdot H^+$
675.9441	675.9352	$[Ru(O)Co_2(\mu_3\text{-}O)_4(OAc)(py)_4]\cdot H^+$
517.8535	517.8508	$[Ru(O)Co_2(\mu_3\text{-}O)_4(OAc)(py)_2]\cdot H^+$

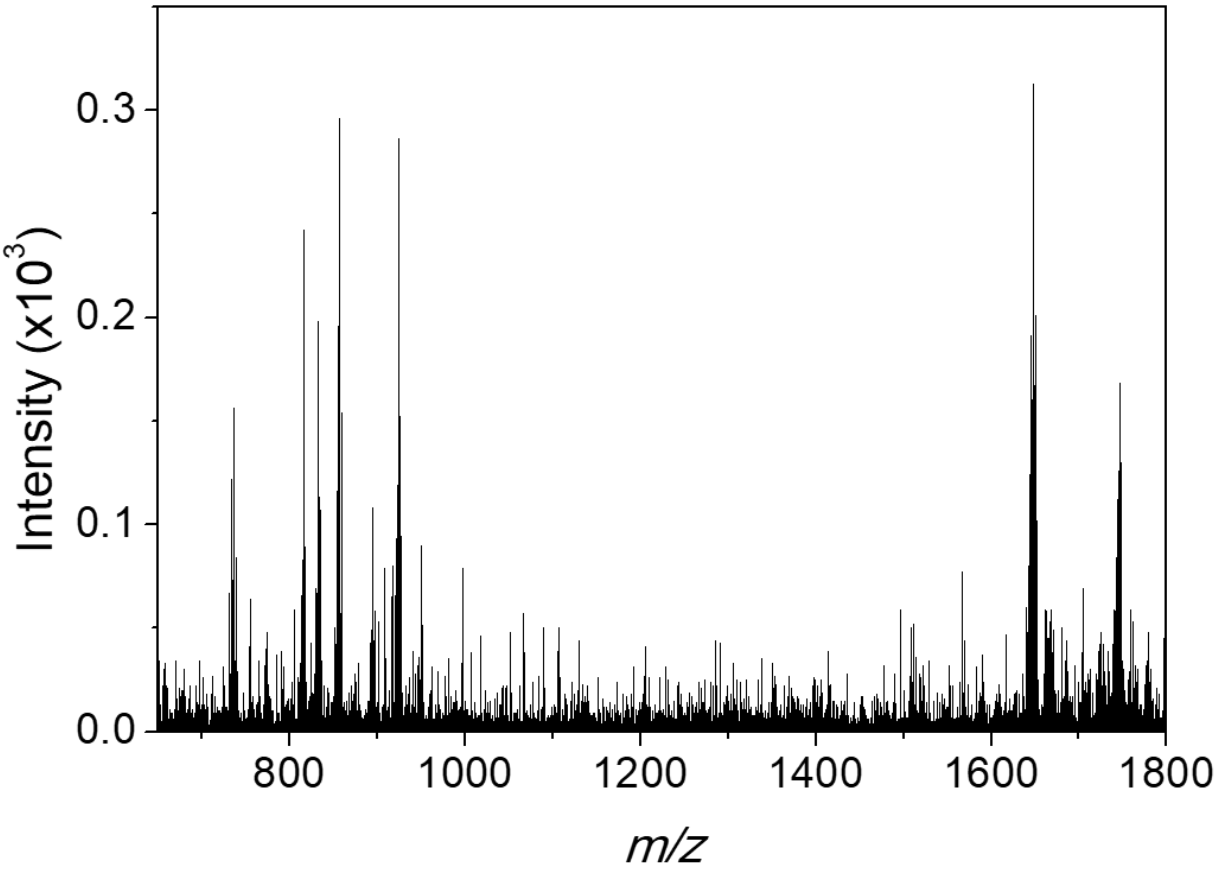

Figure S22. ESI spectrum of reaction mixture between compound **1a** and benzyl alcohol in acetonitrile. An aliquot was taken from the reaction mixture and diluted with acetonitrile for ESI measurement.

Table S6. Products from reaction of compound **1a** and benzyl alcohol identified by HR-ESI-MS in acetonitrile

Found *m/z*	Theoretical *m/z*	Assignment
1746.6112	1746.7901	$[RuCo_3(\mu_3\text{-}O)_4(OAc)_4(py)_3$ + $Ru(py)Co_3(\mu_3\text{-}O)_4(OAc)_4(py)_3 + (H_2O)_2]^+$
1648.5445	1648.7295	$[(py)_3(OAc)_4Co_3(\mu_3\text{-}O)_4Ru]\text{–}O\text{–}[RuCo_3(\mu_3\text{-}O)_4(OAc)_4(py)_3]\cdot H^+$, compound **5**
922.8149	922.9131	$[RuCo_3(\mu_3\text{-}O)_4(OAc)_4(py)_3 + C_7H_6O]\cdot H^+$
857.7869	857.8978	$[Ru(MeCN)Co_3(\mu_3\text{-}O)_4(OAc)_4(py)_3]\cdot H^+$
832.7860	832.8662	$[Ru(O)Co_3(\mu_3\text{-}O)_4(OAc)_4(py)_3(H)]^+$, compound **1a**
816.7887	816.8712	$[RuCo_3(\mu_3\text{-}O)_4(OAc)_4(py)_3]\cdot H^+$
737.7300	737.8290	$[RuCo_3(\mu_3\text{-}O)_4(OAc)_4(py)_2]\cdot H^+$

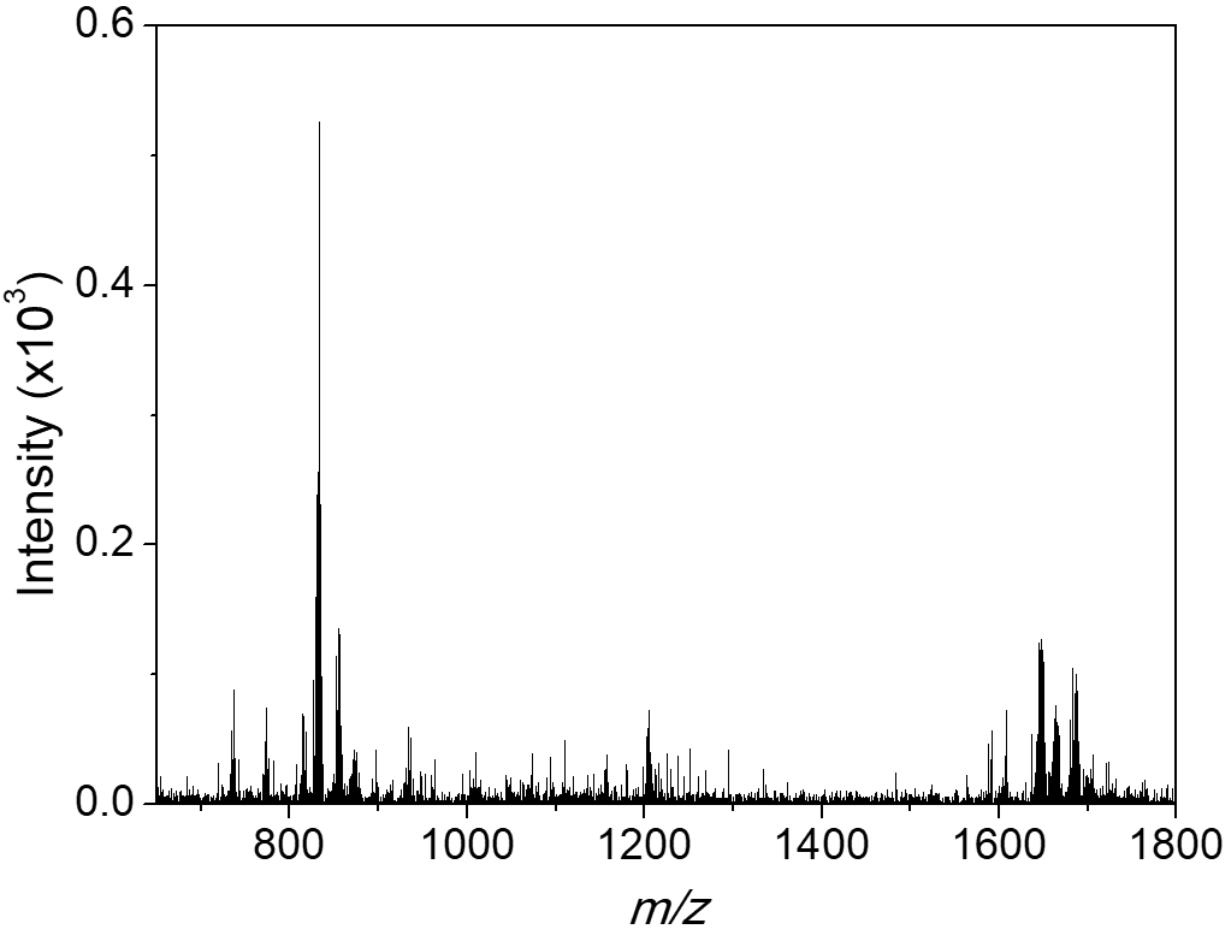

Figure S23. ESI spectrum of reaction mixture between compound **1a** and isopropyl alcohol in acetonitrile. An aliquot was taken from the reaction mixture and diluted with acetonitrile for ESI measurement.

Table S7. Products from reaction of compound **1a** and isopropyl alcohol identified by HR-ESI-MS in acetonitrile

Found *m/z*	Theoretical *m/z*	Assignment
1648.5568	1648.7295	$[(py)_3(OAc)_4Co_3(\mu_3\text{-}O)_4Ru]–O–[RuCo_3(\mu_3\text{-}O)_4(OAc)_4(py)_3]\cdot H^+$, compound **5**
854.7380	854.8481	$[Ru(O)Co_3(\mu_3\text{-}O)_4(OAc)_4(py)_3]\cdot Na^+$, compound **1a**
832.7776	832.8662	$[Ru(O)Co_3(\mu_3\text{-}O)_4(OAc)_4(py)_3]\cdot H^+$, compound **1a**

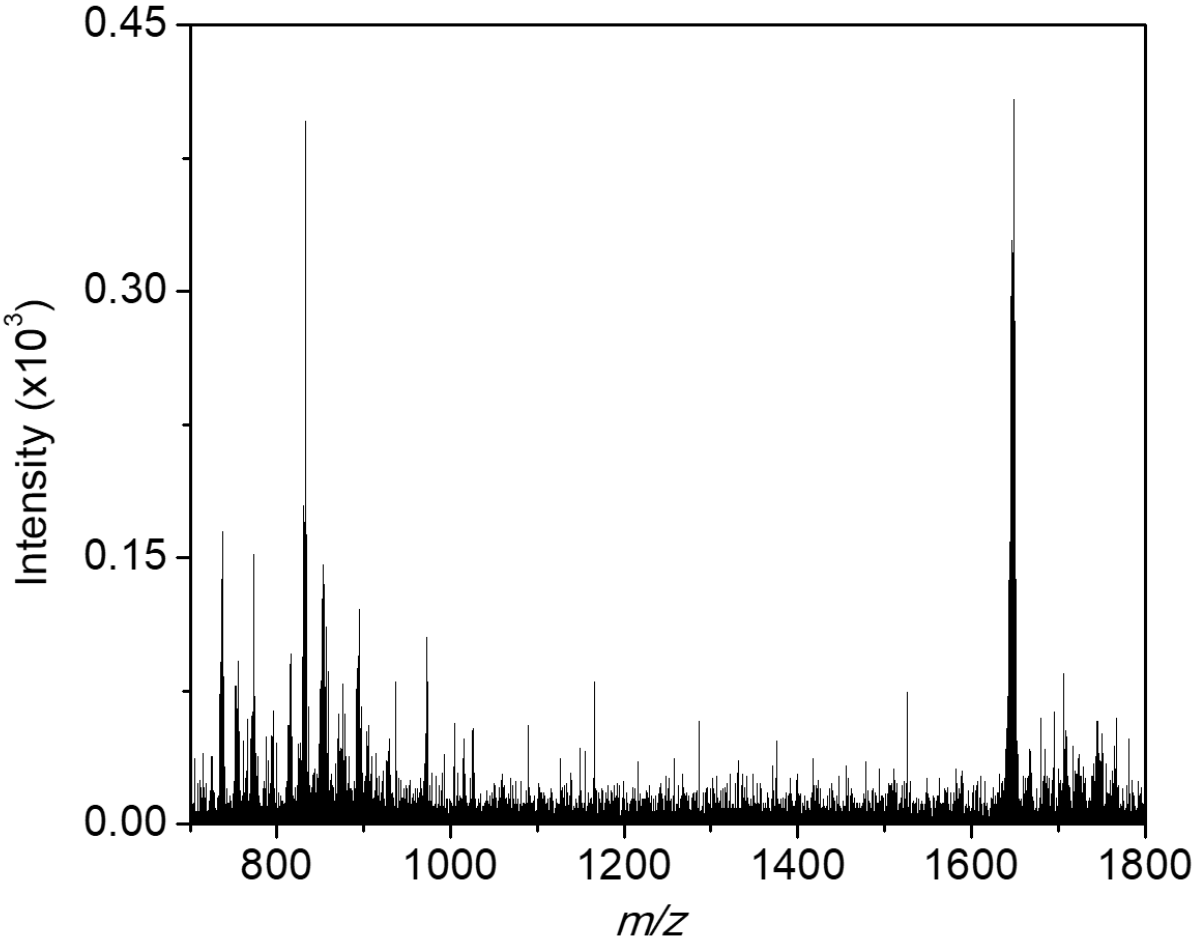

Figure S24. ESI spectrum of reaction mixture between compound **1a** and styrene in acetonitrile. An aliquot was taken from the reaction mixture and diluted with acetonitrile for ESI measurement.

Table S8. Products from reaction of compound **1a** and styrene identified by HR-ESI-MS in acetonitrile

Found *m/z*	Theoretical *m/z*	Assignment
1648.7379	1648.7295	$[(py)_3(OAc)_4Co_3(\mu_3\text{-}O)_4Ru]\text{–}O\text{–}[RuCo_3(\mu_3\text{-}O)_4(OAc)_4(py)_3]\cdot H^+$, compound **5**
895.9128	895.9134	$[Ru(py)Co_3(\mu_3\text{-}O)_4(OAc)_4(py)_3]\cdot H^+$
854.8638	854.8481	$[Ru(O)Co_3(\mu_3\text{-}O)_4(OAc)_4(py)_3]\cdot Na^+$, compound **1a**
832.8822	832.8662	$[Ru(O)Co_3(\mu_3\text{-}O)_4(OAc)_4(py)_3]\cdot H^+$, compound **1a**
737.8389	737.8290	$[RuCo_3(\mu_3\text{-}O)_4(OAc)_4(py)_2]\cdot H^+$

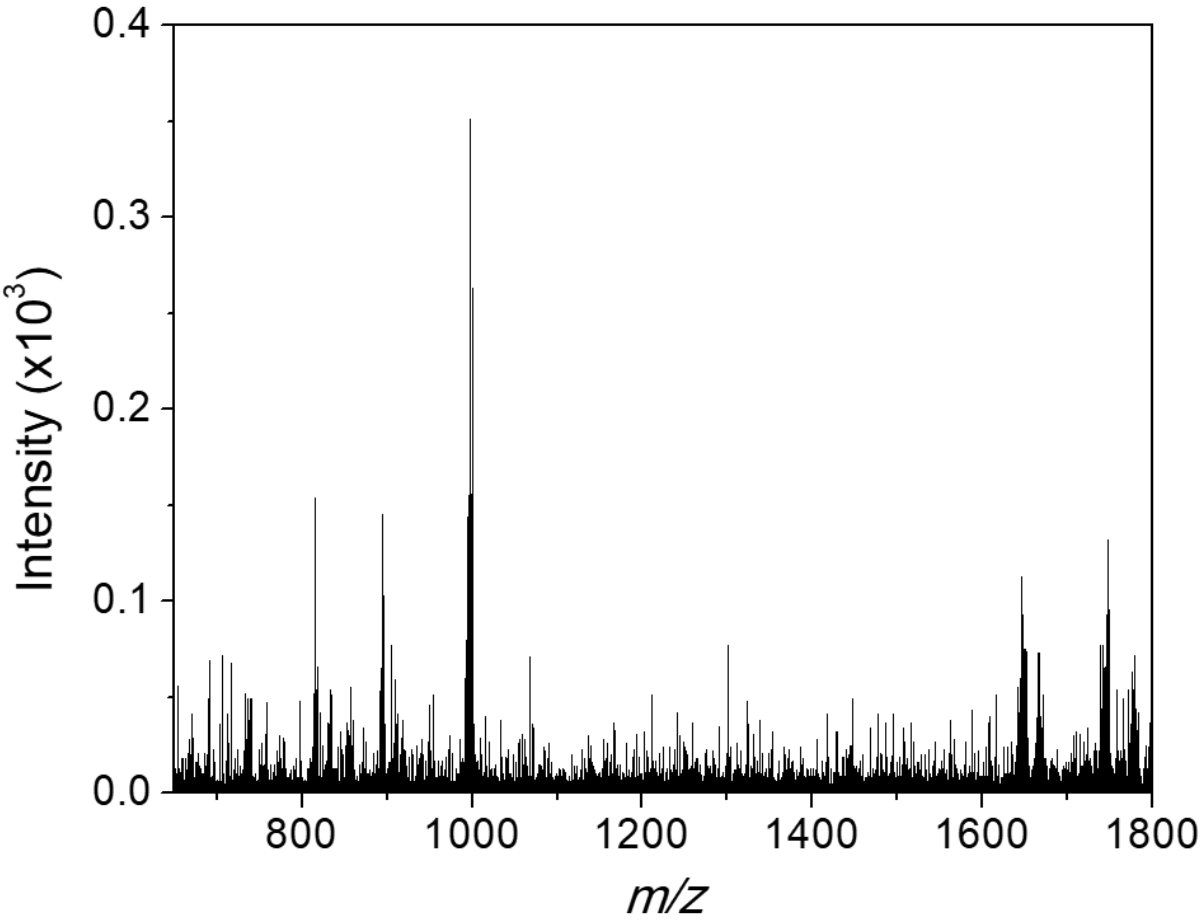

Figure S25. ESI spectrum of reaction mixture between compound **1a** and 1,2-diphenylhydrazine in acetonitrile. An aliquot was taken from the reaction mixture and diluted with acetonitrile for ESI measurement.

Table S9. Products from reaction of compound **1a** and 1,2-diphenylhydrazine identified by HR-ESI-MS in acetonitrile

Found *m/z*	Theoretical *m/z*	Assignment
1746.5958	1746.7901	$[RuCo_3(\mu_3\text{-}O)_4(OAc)_4(py)_3$ + $Ru(py)Co_3(\mu_3\text{-}O)_4(OAc)_4(py)_3 + (H_2O)_2]^+$
1648.5079	1648.7295	$[(py)_3(OAc)_4Co_3(\mu_3\text{-}O)_4Ru]\text{–}O\text{–}[RuCo_3(\mu_3\text{-}O)_4(OAc)_4(py)_3]\cdot H^+$, compound **5**
998.8025	998.9556	$[RuCo_3(\mu_3\text{-}O)_4(OAc)_4(py)_3 + C_{12}H_{10}N_2]\cdot H^+$
895.8786	895.9134	$[Ru(py)Co_3(\mu_3\text{-}O)_4(OAc)_4(py)_3]\cdot H^+$
816.7877	816.8712	$[RuCo_3(\mu_3\text{-}O)_4(OAc)_4(py)_3]\cdot H^+$

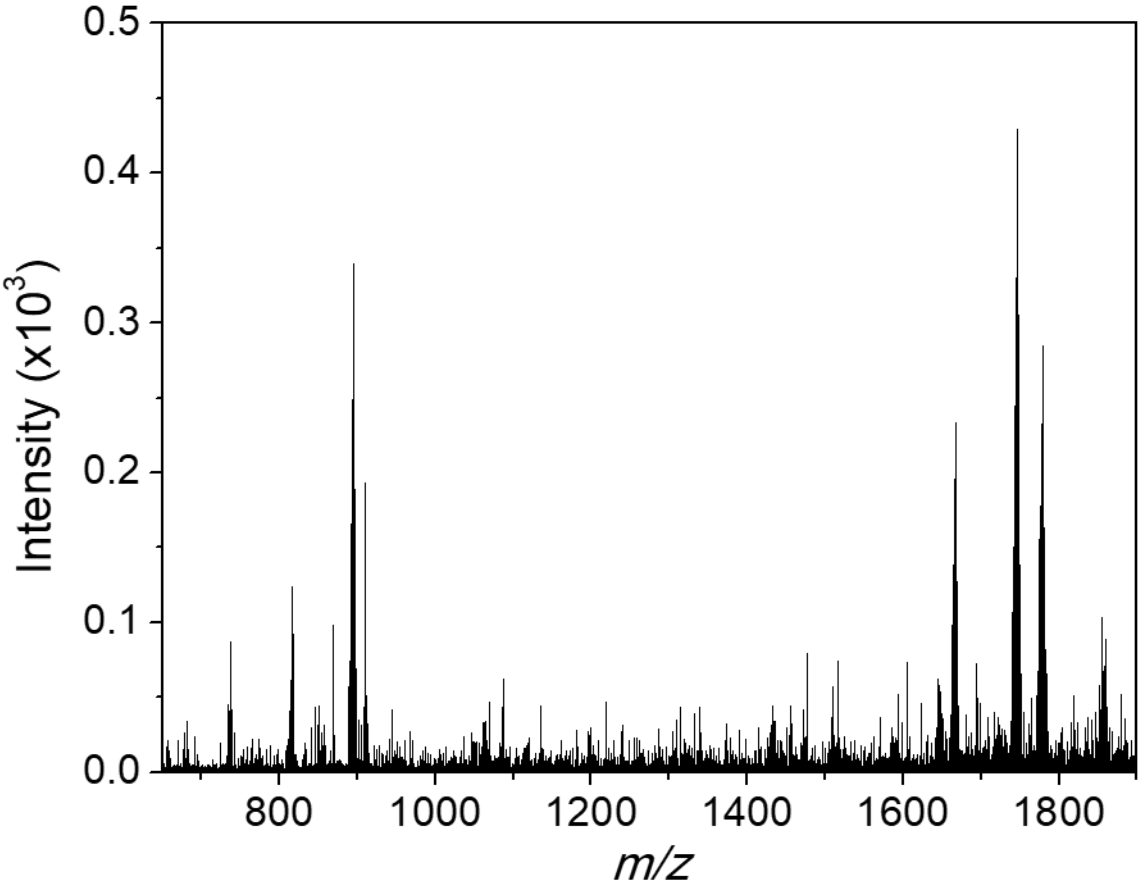

Figure S26. ESI spectrum of reaction mixture between compound **1a** and 1,4-cyclohexadiene in acetonitrile. An aliquot was taken from the reaction mixture and diluted with acetonitrile for ESI measurement.

Table S10. Products from reaction of compound **1a** and 1,4-cyclohexadiene identified by HR-ESI-MS in acetonitrile

Found *m/z*	Theoretical *m/z*	Assignment
1779.3987	-	Unidentifiable highly charged coordination polymer
1746.5484	1746.7901	$[RuCo_3(\mu_3\text{-}O)_4(OAc)_4(py)_3$ + $Ru(py)Co_3(\mu_3\text{-}O)_4(OAc)_4(py)_3 + (H_2O)_2]^+$
1648.5128	1648.7295	$[(py)_3(OAc)_4Co_3(\mu_3\text{-}O)_4Ru]\text{–}O\text{–}[RuCo_3(\mu_3\text{-}O)_4(OAc)_4(py)_3]\cdot H^+$, compound **5**
895.8286	895.9134	$[Ru(py)Co_3(\mu_3\text{-}O)_4(OAc)_4(py)_3]\cdot H^+$
816.7880	816.8712	$[RuCo_3(\mu_3\text{-}O)_4(OAc)_4(py)_3]\cdot H^+$
737.7246	737.8290	$[RuCo_3(\mu_3\text{-}O)_4(OAc)_4(py)_2]\cdot H^+$

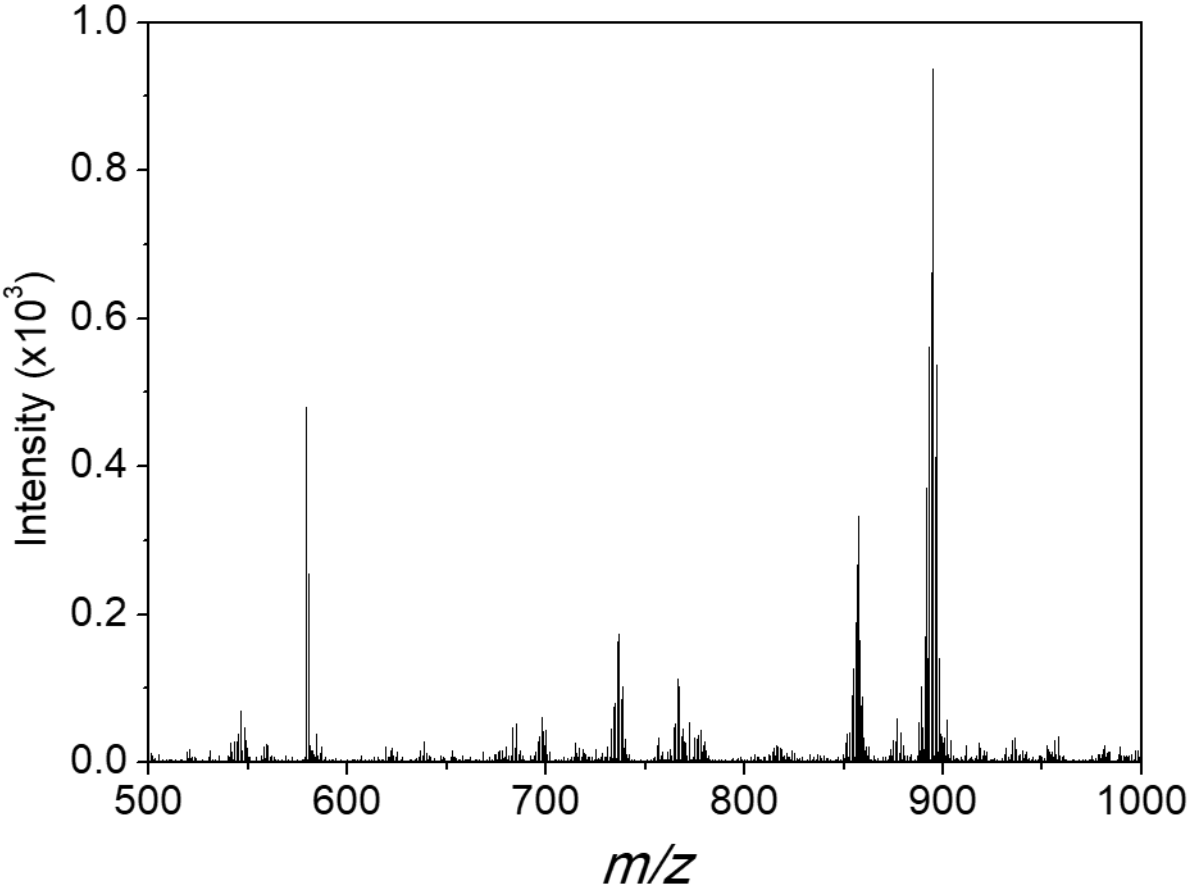

Figure S27. ESI spectrum of reaction mixture between compound **1a** and triphenylphosphine in acetonitrile. An aliquot was taken from the reaction mixture and diluted with acetonitrile for ESI measurement.

Table S11. Products from reaction of compound **1a** and triphenylphosphine identified by HR-MS-ESI in acetonitrile

Found *m/z*	Theoretical *m/z*	Assignment
895.8782	895.9134	$[Ru(py)Co_3(\mu_3\text{-}O)_4(OAc)_4(py)_3]\cdot H^+$
857.8328	857.8978	$[Ru(MeCN)Co_3(\mu_3\text{-}O)_4(OAc)_4(py)_3]\cdot H^+$
737.8080	737.8290	$[RuCo_3(\mu_3\text{-}O)_4(OAc)_4(py)_2]\cdot H^+$
579.1490	579.1619	$[OPPh_3]\cdot Na^+$

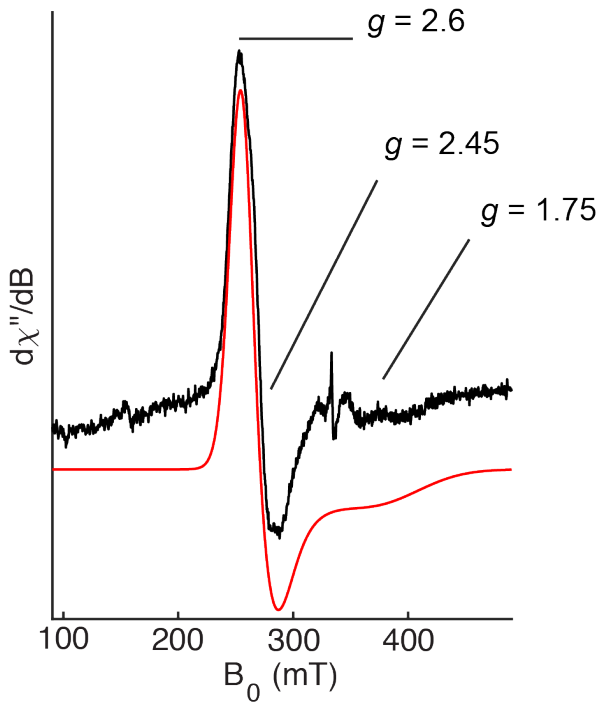

Figure S28. CW X-band (9.4 GHz) EPR spectrum (Black) of an aliquot of the product solution of the reaction between **1a** and triphenylphosphine with simulation of the data (Red) using *g*-values of [2.60, 2.45, 1.75]. Spectrum was collected at 20K, with 10 mW microwave power, and 5G modulation amplitude.

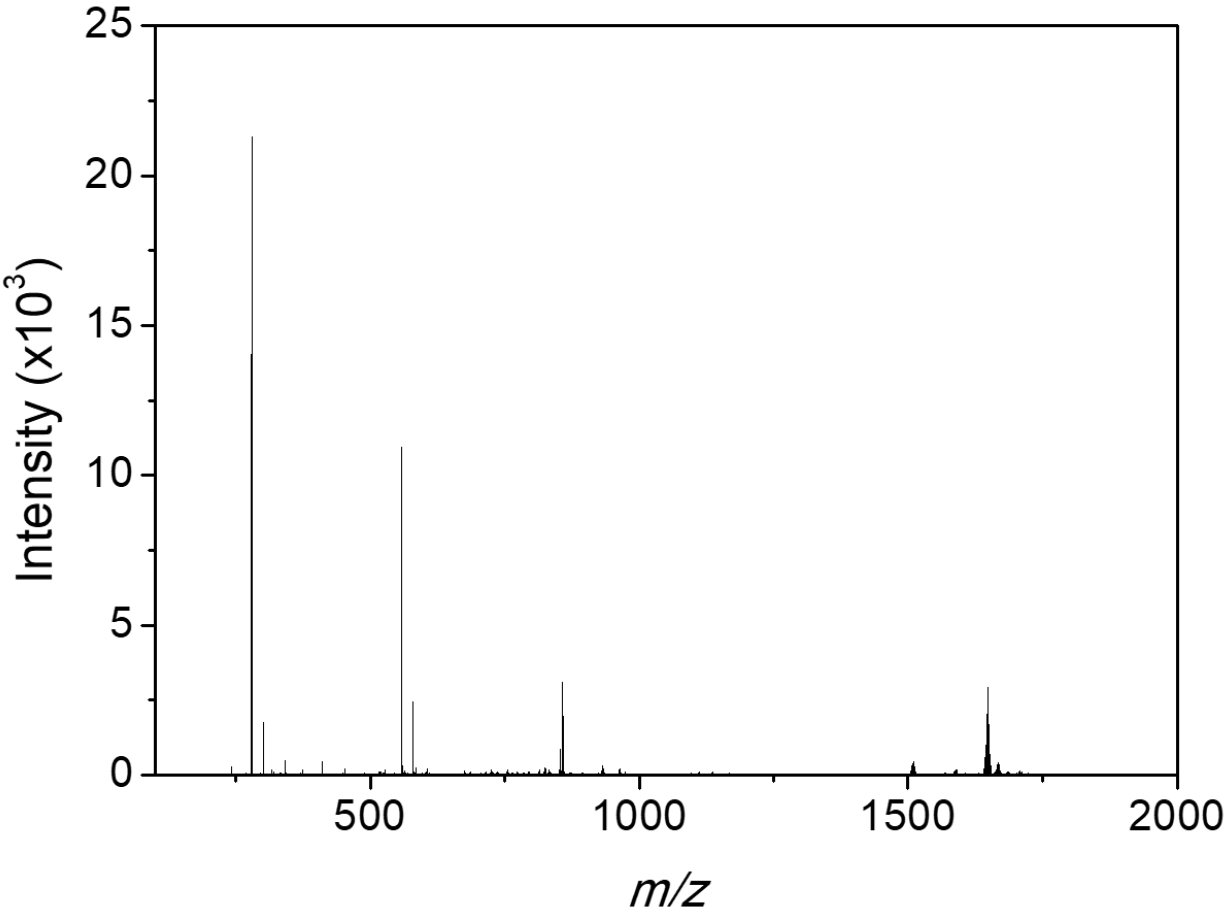

Figure S29. ESI spectrum of an aliquot of the product solution from the reaction of compound **1a** and 0.5 equiv of triphenylphosphine in acetonitrile.

Table S12. Products from reaction of compound **1a** and 0.5 equiv of triphenylphosphine identified by HR-ESI-MS in acetonitrile.

Found *m/z*	Theoretical *m/z*	Assignment
1648.7104	1648.7295	$[(py)_3(OAc)_4Co_3(\mu_3\text{-}O)_4Ru]\text{–}O\text{–}[RuCo_3(\mu_3\text{-}O)_4(OAc)_4(py)_3]\cdot H^+$, compound **5**
857.2695	857.2479	$[(OPPh_3)_3]\cdot Na^+$
557.1862	557.1799	$[(OPPh_3)_2]\cdot H^+$
279.0937	279.0939	$[OPPh_3]\cdot H^+$

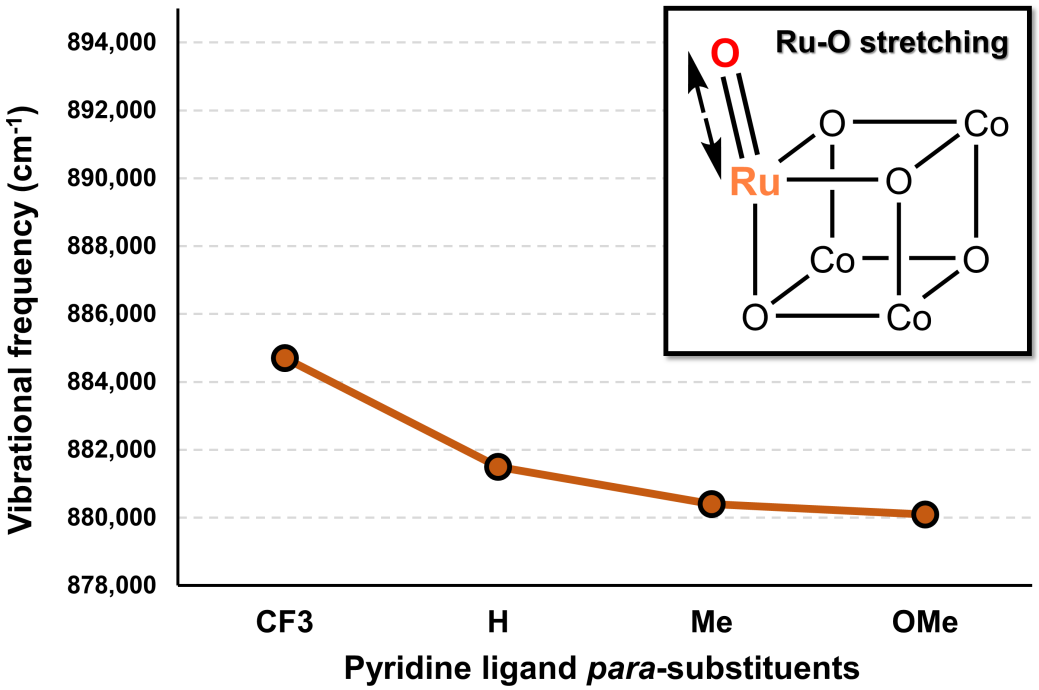

Figure S30. Ru^{V}–O stretching frequency dependence on the nature of the *para*-substituents of the pyridine ligands

References

(1) Moore, P. W.; Read, C. D. G.; Bernhardt, P. V.; Williams, C. M. ATP3 and MTP3: Easily Prepared Stable Perruthenate Salts for Oxidation Applications in Synthesis. *Chem. Eur. J.* **2018**, *24* (18), 4556–4561.

(2) Boduszek, B.; Shine, H. J. Preparation of Solid Thianthrene Cation Radical Tetrafluoroborate. *J. Org. Chem.* **1988**, *53* (21), 5142–5143.

(3) Manner, V. W.; Markle, T. F.; Freudenthal, J. H.; Roth, J. P.; Mayer, J. M. The First Crystal Structure of a Monomeric Phenoxyl Radical: 2,4,6-tri-*tert*-Butylphenoxyl Radical. *Chem. Commun.* **2008**, *246* (2), 256–258.

(4) Heurich, T.; Nesterov, V.; Schnakenburg, G.; Qu, Z. W.; Grimme, S.; Hazin, K.; Gates, D. P.; Engeser, M.; Streubel, R. Strong Evidence of a Phosphanoxyl Complex: Formation, Bonding, and Reactivity of Ligated Phosphorus Analogues of Nitroxides. *Angew. Chemie Int. Ed.* **2016**, *55* (46), 14439–14443.

(5) Evans, D. F. Paramagnetic Susceptibility, etc. 2003 400. The Determination of the Pararmagnetic Susceptibility. *J. Chem. Soc.* **1959**, 2003–2005.

(6) Flores, M.; Isaacson, R. A.; Calvo, R.; Feher, G.; Lubitz, W. Probing hydrogen bonding to quinone anion radicals by ^{1}H and ^{2}H ENDOR spectroscopy at 35 GHz. *Chem. Phys.* **2003**, *294* (3), 401–413.

(7) Schweiger, A.; Jeschke, G. *Principles of Pulse Electron Paramagnetic Resonance*; Oxford University Press: New York, 2001.

(8) Bruggemann, W.; Niklas, J. R. Stochastic ENDOR. *J. Magn. Reson. A* **1994**, *108* (1), 25–29.

(9) Stoll, S.; Schweiger, A. EasySpin, a comprehensive software package for spectral simulation and analysis in EPR. *J. Magn. Reson.* **2006**, *178* (1), 42–55.

(10) Bruker Analytical X-ray Systems, Inc., SAINT and APEX 2 Software for CCD Diffractometers. Bruker Analytical X-ray Systems, Inc.: Madison, WI, USA 2000.

(11) Sheldrick, G. M. TWINABS Version 2012/1. University of Gottingen 2012.

(12) Sheldrick, G. M. SADABS. Bruker Analytical X-ray Systems, Inc. 2014.

(13) Sheldrick, G. M. SHELXT - Integrated space-group and crystal-structure determination. *Acta Crystallogr. Sect. A Found. Crystallogr.* **2015**, *71* (1), 3–8.

(14) Sheldrick, G. M. Crystal structure refinement with SHELXL. *Acta Crystallogr. Sect. C Struct. Chem.* **2015**, *71* (Md), 3–8.

(15) Dolomanov, O. V.; Bourhis, L. J.; Gildea, R. J.; Howard, J. A. K.; Puschmann, H. OLEX2: A complete structure solution, refinement and analysis program. *J. Appl. Crystallogr.* **2009**, *42* (2), 339–341.

(16) Sheldrick, G. M. CELL NOW V2008/2. Bruker Analytical X-ray Systems, Inc. 2008.

(17) Tao, J.; Perdew, J. P.; Staroverov, V. N.; Scuseria, G. E. Climbing the density functional ladder: Nonempirical meta–generalized gradient approximation designed for molecules and solids. *Phys. Rev. Lett.* **2003**, *91* (14), 3–6.

(18) Frisch, M. J.; Trucks, G. W.; Schlegel, H. B.; Scuseria, G. E.; Robb, M. A.; Cheeseman, J. R.; Scalmani, G.; Barone, V.; Petersson, G. A.; Nakatsuji, H.; Li, X.; Caricato, M.; Marenich, A.; Bloino, J.; Janesko, B. G.; Gomperts, R.; Mennucci, B.; Hratchian, D. J. Gaussian 09, Revision D.01. Gaussian, Inc.: Wallingford, CT 2016.

(19) Weigend, F.; Ahlrichs, R. Balanced basis sets of split valence, triple zeta valence and quadruple zeta valence quality for H to Rn: Design and assessment of accuracy. *Phys. Chem. Chem. Phys.* **2005**, *7* (18), 3297–3305.

(20) Nguyen, A. I.; Darago, L. E.; Balcells, D.; Tilley, T. D. Influence of a “dangling” Co(II) Ion Bound to a [$MnCo_3O_4$] Oxo Cubane. *J. Am. Chem. Soc.* **2018**, *140* (29), 9030–9033.

(21) Computational Chemistry Comparison and Benchmark Data Base Release 19. Standard Reference Database 101. National Institute of Standards and Technology.

(22) Goerigk, L.; Grimme, S. A thorough benchmark of density functional methods for general main group thermochemistry, kinetics, and noncovalent interactions. *Phys. Chem. Chem. Phys.* **2011**, *13* (14), 6670–6688.

(23) Bauernschmitt, R.; Ahlrichs, R. Stability analysis for solutions of the closed shell Kohn-Sham equation. *J. Chem. Phys.* **1996**, *104* (22), 9047–9052.

(24) Cossi, M.; Rega, N.; Scalmani, G.; Barone, V. Energies, structures, and electronic properties of molecules in solution with the C-PCM solvation model. *J. Comput. Chem.* **2003**, *24* (6), 669–681.

(25) Chai, J. Da; Head-Gordon, M. Long-range corrected hybrid density functionals with damped atom-atom dispersion corrections. *Phys. Chem. Chem. Phys.* **2008**, *10* (44), 6615–6620.

(26) Glendening, E. D.; Landis, C. R.; Weinhold, F. NBO 6.0: Natural bond orbital analysis program. *J. Comput. Chem.* **2013**, *34* (16), 1429–1437.

(27) Chakrabarty, R.; Bora, S. J.; Das, B. K. Synthesis, structure, spectral and electrochemical properties, and catalytic use of cobalt(III)-oxo cubane clusters. *Inorg. Chem.* **2007**, *46* (22), 9450–9462.

(28) Nguyen, A. I.; Suess, D. L. M.; Darago, L. E.; Oyala, P. H.; Levine, D. S.; Ziegler, M. S.; Britt, R. D.; Tilley, T.

D. Manganese-Cobalt Oxido Cubanes Relevant to Manganese-Doped Water Oxidation Catalysts. *J. Am. Chem. Soc.* **2017**, *139* (15), 5579–5587.

(29) Reichardt, C. Solvatochromic Dyes as Solvent Polarity Indicators. *Chem. Rev.* **1994**, *94* (8), 2319–2358.

(30) Reichardt, C. Empirical Parameters of Solvent Polarity as Linear Free-Energy Relationships. *Angew. Chemie Int. Ed. Engl.* **1979**, *18* (2), 98–110.

(31) Kamlet, M. J.; Abboud, J. L. M.; Taft, R. W. An Examination of Linear Solvation Energy Relationships. *Prog. Phys. Org. Chem.* **1981**, *13*, 485–630.